

2014

FATE AND REMOVAL OF CONTAMINANTS IN URBAN ENVIRONMENT

Varun K. Kasaraneni
University of Rhode Island, vkasaraneni@my.uri.edu

Follow this and additional works at: https://digitalcommons.uri.edu/oa_diss

Terms of Use

All rights reserved under copyright.

Recommended Citation

Kasaraneni, Varun K., "FATE AND REMOVAL OF CONTAMINANTS IN URBAN ENVIRONMENT" (2014).
Open Access Dissertations. Paper 288.
https://digitalcommons.uri.edu/oa_diss/288

This Dissertation is brought to you by the University of Rhode Island. It has been accepted for inclusion in Open Access Dissertations by an authorized administrator of DigitalCommons@URI. For more information, please contact digitalcommons-group@uri.edu. For permission to reuse copyrighted content, contact the author directly.

FATE AND REMOVAL OF CONTAMINANTS IN URBAN ENVIRONMENT

BY

VARUN K. KASARANENI

A DISSERTATION SUBMITTED IN PARTIAL FULFILLMENT OF THE

REQUIREMENTS FOR THE DEGREE OF

DOCTOR OF PHILOSOPHY

IN

CIVIL AND ENVIRONMENTAL ENGINEERING

UNIVERSITY OF RHODE ISLAND

2014

DOCTOR OF PHILOSOPHY
IN
CIVIL AND ENVIRONMENTAL ENGINEERING
OF
VARUN K KASARANENI

APPROVED:

Thesis Committee:

Major Professor Vinka Craver

Thomas B. Boving

Jose Amador

Nasser H. Zawia
DEAN OF THE GRADUATE SCHOOL

UNIVERSITY OF RHODE ISLAND

2014

ABSTRACT

Stormwater runoff from impermeable surfaces, such as roads, roof tops, and parking lots, is a cause of non-point source pollution problem. Sources such as fossil fuel combustion, automobiles, and other human and animal activities introduce high concentration of organic, inorganic and pathogenic contaminants in to environment. Stormwater runoff carrying these contaminants when untreated has the potential to impair water quality in the receiving water bodies such as surface and ground waters. The existing treatment systems are not reliable and needed improvements in order to meet water quality standards. Determining the levels and sources of contamination in an environment can help mitigate the pollutant and reduce risk to humans. In here we have developed materials for use in stromwater treatment and applied source apportionment techniques to determine the sources of polycyclic aromatic hydrocarbons in surface soils of San Mateo Ixtatán, Guatemala. In chapter 2 of this dissertation, we evaluated the pollutant removal capacity of pervious concrete pavement systems and propose a methodology to enhance the containment of polycyclic aromatic hydrocarbons (PAHs) through organic modification of Rhode Island soils. In chapter 3 we have proposed using nano and polymer based materials for treatment of stormwater runoff contaminants such as pathogens, organic and inorganic contaminants. The modification materials had successfully increased the contaminant removal capacities of the materials. These proposed materials can find applications in Best management practices such as tree filters. In chapter 4 we have provide the levels, sources of PAHs in surface soils of San Mateo Ixtatán, Guatemala. In addition cancer risk assessment due to exposure to surface soil was performed.

ACKNOWLEDGMENTS

I would like to take this opportunity to acknowledge and thank people who have been instrumental in making this thesis possible. First I would like to express my sincere gratitude to my advisor Dr. Vinka Oyanedel-Craver for her excellent guidance, caring and support. Throughout this journey she was incredibly patient and has provided encouragement all along.

I would also like to express my special thanks to Dr. Thomas Boving for his useful suggestions, constructive and timely advices. I thank my dissertation committee members Dr. Jose Amador, Dr. Leon Thiem and Dr. Arijit Bose for their valuable inputs.

I would like to thank my friends and colleagues at URI for their support and cheering during hard times. My research would not have been possible without their help.

I am grateful to my family and friends for their love, encouragement and for standing by me during good and bad times.

PREFACE

This dissertation is in manuscript format. The chapter is an introduction. The second chapter titled “Enhanced containment of polycyclic aromatic hydrocarbons through organic modification of soils” 33.1 (2014): 47-54 was originally published in Journal of Environmental Progress and Sustainable Energy. Chapter 3 titled “Enhancement of Surface Runoff Quality Using Modified Sorbents” 2.7 (2014): 1609-1615 has been published in ACS Sustainable Chemistry and Engineering. Supporting information for this manuscript is provided at the end of the chapter. Chapter 4 is a manuscript “Levels, sources and risk assessment of polycyclic aromatic hydrocarbons (PAH) in San Mateo Ixtatán, Guatemala” is prepared for submission to Journal of Hazardous Materials. In addition a manuscript titled “Selecting an antimicrobial filter media for improved stormwater best management practices” prepared for submission for Journal Water Research is added to appendices.

TABLE OF CONTENTS

ABSTRACT.....	III
ACKNOWLEDGMENTS	III
PREFACE.....	IV
TABLE OF CONTENTS.....	V
LIST OF TABLES.....	VIII
LIST OF FIGURES	X
CHAPTER 1	1
INTRODUCTION	1
REFERENCES	4
CHAPTER 2	6
ENHANCED CONTAINMENT OF POLYCYCLIC AROMATIC HYDROCARBONS (PAHS) THROUGH ORGANIC MODIFICATION OF SOILS	6
ABSTRACT	7
1. INTRODUCTION	8
2. METHODS AND MATERIALS	10
2.1 Overview of Experimental Methodology.....	10
2.2 Materials.....	10
2.3 Synthesis and Characterization of Organically Modified Soil Amendments.....	11
2.4 Sorption Isotherms	13
2.5 Column Experiments.....	13
2.6 HYDRUS 1D	14
3. RESULTS AND DISCUSSION	15
3.1 Evaluation of the effectiveness of the organic modification in Rhode Island soil	15
3.1.1 Synthesis and characterization of organically modified soil amendments	15
3.1.2 Sorption Isotherms	16
3.1.3 Column experiments with unmodified, organically modified, and blended Rhode Island glacial outwash soils	18
3.2 Performance of convention and organically modified pervious concrete pavements	21
4. CONCLUSIONS	24

REFERENCES	25
CHAPTER 3	29
ENHANCEMENT OF SURFACE RUNOFF QUALITY USING MODIFIED SORBENTS.....	29
ABSTRACT	30
1. INTRODUCTION	31
2. METHODS	33
2.1 Materials.....	33
2.2 Material Characterization	34
2.3 Laboratory Analysis	34
2.4 Experimental Methodology.....	35
2.4.1 Phase I: Nanoparticle and Polymer Loading Capacity of Sorbents	35
2.4.2 Phase II: Organic and Inorganic Contaminant Removal Efficiency of Modified Sorbents	36
2.5 Cost Analysis and Limitations	37
3. RESULTS AND DISCUSSION	38
3.1 Material Characterization.....	38
3.2 Phase I: Nanoparticle and Polymer Loading Capacity of Sorbents	38
3.3 Phase II: Organic and Inorganic Contaminant Removal Efficiency of Modified Sorbents	40
3.4 Cost Analysis and Limitations	43
REFERENCES	49
SUPPORTING INFORMATION.....	52
CHAPTER 4	64
LEVELS, SOURCES AND RISK ASSESSMENT OF POLYCYCLIC AROMATIC HYDROCARBONS (PAH) IN SAN MATEO IXTATÁN, GUATEMALA.	64
ABSTRACT.....	65
1. INTRODUCTION	66
2. MATERIALS AND METHODS	68
2.1 Description of study area and sampling sites	68
2.2 Sample preparation, extraction, cleanup and analysis.....	68
2.3 Quality assurance/quality control (QA/QC) and statistical analysis	68
2.4 Soil toxicity	69

2.5 Estimation of PAH accumulation in corn grains and dietary intake	69
2.6 Cancer health risk assessment	71
3. RESULTS AND DISCUSSION	72
3.1 Levels and composition profiles of PAHs in surface soil samples	72
3.2 Correlation among individual PAHs and with soil organic carbon (TOC)	72
3.3 PAH Source identification and estimation	74
3.3.1 Isomer ratios of PAHs.....	74
3.3.2 Principal component analysis/Multiple linear regression	74
3.4 Soil toxicity	74
3.5 Estimation of PAH accumulation in corn grains and dietary intake	76
3.6 Risk assessment.....	76
3.7 Contamination of river sediments	77
4 CONCLUSIONS	79
REFERENCES	95
APPENDICES	100
SELECTING AN ANTIMICROBIAL FILTER MEDIA FOR IMPROVED STORMWATER BEST MANAGEMENT PRACTICES	100

List of Tables

Table	Page
Table 2-1: Soil Organic Carbon, Particle Size, And Hydraulic Conductivity Properties.....	15
Table 2-2: Freundlich Sorption Parameters From Batch And Column Studies Of Modified Soils.....	18
Table 2-3: Column Intrinsic Parameters And Naphthalene Retardation.....	21
Table 2-4: Column Intrinsic Parameters And Retardation Factors	23
Table 3-1: Amendment Loadings Achieved By Exposing Red Cedar To Aqueous Solutions Of Either Tpa Or Agnps.....	45
Table 3-2: Langmuir Maximum Sorption Capacity (Q) For Pahs And Metals For All Sorbents.....	45
Table 3-S1: Equilibrium Times Of Batch Isotherms For Tpa And Agnps Modifications Of Red Cedar And Shale.....	59
Table 3-S2: Fraction Of Agnps And Ag Ions Desorbed During Desorption Study.	59
Table 3-S3: Composition Of The Synthetic Runoff Stock Solution. Five Dilutions Were Prepared From This Solution To Cover 3 Orders Of Magnitude For Each Compound Of Interest.....	59
Table 3-S4: N ₂ Bet Specific Surface Areas And Contact Angle Measurements For All Sorbent Materials.....	60
Table 3-S5: Isotherm Parameters For Pahs And Metals For All Sorbents.....	60
Table 3-S6: Speciation Data For Metals At Ph 5.5.....	61
Table 3-S7: Cost Of Modification Of Red Cedar Wood Chips Using Tpa And Agnps At Various Loadings.....	62
Table 3-S8: Toxicity Data Of AgNps And TPA.....	62
Table 4-1: List Of Pahs Analyzed, Molecular Weight, Number Of Rings And Bap Toxicity Equivalent Factors.....	80
Table 4-2: Soil, Corn Plant And Grain Physical–Chemical Parameters Applied To The Model To Estimate The Polycyclic Aromatic Hydrocarbons (Pah) Accumulation In Corn Grains.....	81
Table 4-3: Exposure Parameter Values.....	82

Table 4-4: Concentrations Of Pahs ($\mu\text{g}/\text{Kg}$ Dry Weight) In Soils From Different Functional Areas In San Mateo Ixtatán, Guatemala.....	83
Table 4-5a: Pearson Correlation Coefficients For Toc And 17 Individual Pahs At Town Sites.....	84
Table 4-5b: Pearson Correlation Coefficients For Toc And 17 Individual Pahs At Agricultural Sites.....	85
Table 4-6: Factor Loadings And Source Contribution Obtained From Pca/Mlr.....	86
Table 4-7: Concentration Of Individual Pahs (Ug/Kg Of Corn) And Bap Equivalent Concentrations Estimated In Corn Grain Cultivated At Agricultural Sites	87
Table 4-8: Dietary Uptake Of $\sum 16\text{pah}$ ($\mu\text{g}/\text{Day}$).....	87
Table 4-9: Concentrations Of $\sum 17\text{pah}$ And $\sum 7\text{carpah}$ In Sediments And The Isomer Pair Ratios.	88

List of figures

Figure	Page
figure 2-1: Sorption Isotherms For The Sorption Of Naphthalene	17
Figure 2-2: Observed And Predicted Btcs Of Naphthalene For A) Ri Glacial Outwash B) Hdtma Modified Soil C) Bhdh Modified Soil D) Blended Modified Soil.....	19
Figure 2-3: Btcs Of Acenaphthene And Flourene In Column Experiments For A) Concrete B) Aggregate C) Ri Glacial Outwash Soil D) Blend Of Organo Clay-Glacial Outwash Soil.	22
Figure 3-1: Polymer And Nanoparticle Loading Capacity Of Sorbents	46
Figure 3-2: Langmuir Maximum Sorption Coefficient Q Of A) Pahs And B) Heavy Metals.....	47
Figure 3-3: Deactivation Of E. Coli At Increasing Concentrations Using Unmodified And Modified Materials.....	48
Figure 3-S1: Sorption Isotherm For Red Cedar And Expanded Shale For A) Tpa And B) Agnp.56	
Figure 3-S2: Tem Image Of Agnps.....	57
Figure 3-S3: Batch Isotherm Results Of A) Acenaphthene, B) Fluorene, C) Lead, D) Cadmium, E) Zinc, F) Nickel, And G) Copper	58
Figure 4-1: Location Of San Mateo Ixtatán And The Sampling Sites	89
Figure 4-2: Spatial Distribution Of Pah In Surface Soils Of San Mateo Ixtatán, Guatemala. Concentrations In $\mu\text{g}/\text{Kg}$ Of Dry Weight.....	90
Figure 4-3: Percent Contribution Of 2, 3, 4, 5, 6-Ring Pahs In Surface Soils Of San Mateo Ixtatán.	91
Figure 4-4: Cross Plot Of The Isometric Ratios Of (A) $\text{Ant}/(\text{Ant}+\text{Phn})$ Vs $\text{Fln}/(\text{Fln}+\text{Pyr})$, And (B) $\text{Baa}/(\text{Baa}+\text{Chr})$ Vs $\text{Ip}/(\text{Ip}+\text{Bgp})$ In Surface Soil Samples Of San Mateo Ixtatán.	92
Figure 4-5: Graph Showing The Soil Toxicity At Various Sampling Sites Expressed In Terms Of Benzo[A]Pyrene Equivalent Concentrations.	93
Figure 4-6: The Estimated Incremental Lifetime Cancer Risk Due To Ingestion Of Soil, Through Dermal Contact And Dietary Uptake Of Pah Through Corn.....	94

CHAPTER 1

Introduction

Rapid growth of urban and industrial areas has resulted in an increase of the land area covered by impermeable surfaces such as roofs, roadways and paved surfaces. This continuous expansion and infilling of urban and industrial land use is increasing the burden on existing drainage networks and urban watercourses. During periods of high intensity rain, large volumes of stormwater runoff can exceed the capacity of collection systems, resulting in flooding of roads, property damage, and human health hazards. In addition, pollutants deposited on impermeable surfaces are mobilized by storm runoff to collection systems, and discharged to aquatic ecosystems with little or no treatment [1,2,3] including discharges to groundwater.

The pollutants in stormwater include organic contaminants such as polycyclic aromatic hydrocarbons (PAH), inorganic contaminants such as heavy metals, nutrients such as nitrates and pathogens such as bacteria [1,3,4]. Most of the pollutants present in urban stormwater runoff originate from nonpoint or diffuse sources. These are notoriously difficult to locate and quantify and include wet and dry atmospheric deposition from industrial and domestic properties; traffic emissions; decomposed litter; de-icing salts; vegetative residues; pet feces; soil losses, among others[4–6]. The concentrations of these contaminants are often order of magnitude above the maximum contaminant level (MCL)for drinking water standards [1,3,4][7] which can impair the water bodies. Some of the contaminants of concern are PAHs, heavy metals and pathogens.

The fate and transport of some of these contaminants was studied herein, including PAHs, heavy metals and pathogens. Polycyclic aromatic hydrocarbons are class of compounds originating from the incomplete combustion of organic materials, including petroleum products and biomass. The US Environmental protection agency (US EPA) has listed 16 PAHs as priority pollutants of which seven PAHs are listed as probable human carcinogens or mutagens. PAHs are toxic, carcinogenic and mutagenic compounds with drinking water MCL for PAHs is of 0.2 µg/l [7].

Heavy metals are other group of contaminants found in urban runoff, this group includes but not limited to metals such as cadmium, lead, zinc, nickel and copper. The primary sources of these metals in urban runoff are automobiles, tires, and abrasion of road surfaces. The pathogens present in urban stormwater runoff are related to elevated waterborne illnesses after storm events. *Escherichia coli* (*E. coli*) is bacterium that is commonly monitored in surface and drinking water as an indicator for pathogenic contamination. The concentration of *E. coli* in stormwater runoff often exceeds 10^4 colony forming units (CFU) /100ml [3]. The high microbial concentration in stormwater not only has negative impact on human health, but also is resulting in local economic impact through beach closing and fishing bans.

In order to reduce the volume and pollutant loads of stormwater runoff structural best management practices (BMPs) were adapted by agencies such as EPA, Department of environmental management (DEM) and Department of Transportation (DOT). Examples of these BMPs include pervious pavements, retention/detention ponds, tree filters, bio-swales and infiltration trenches. Previous research demonstrated that the installation of these BMPs has resulted in reduction of runoff volume and lower pollutant concentrations. Although BMPs such as porous pavements and tree filters have shown to remove total suspended solids and heavy metals the long term performance of these systems is unreliable [8–10]. Further the removal of contaminants such as PAHs and pathogens has not been fully tested. Modification of materials with quaternary ammonium compounds, or nanoparticles, for example have shown to significantly increase the contaminant removal of filter media [11–13] and therefore carry promise as amendments to existing BMP or to be the basis of an entirely new line of BMPs.

In urban and suburban environment PAHs are released to environment mainly due to anthropogenic sources such as oil spills, vehicle exhaust, industrial smoke stack emissions, combustion of fossil fuels and biomass burning (such as wood) [14–16]. PAHs emitted in to atmosphere through these sources can contaminate surface soil and water systems. Several studies

have reported high concentrations of PAH in surface soils and sediment around the world. [4, 14–18] In developing countries nearly 90% of households living in rural areas rely on biomass for their energy needs.[19] Identification of PAH contamination and source apportionment therefore important for pollution control, remediation to minimize risk of exposure and can help plan intervention studies.

The objectives of this dissertation work were 1) to develop a methodology to enhance the organic contaminant removal capacity of Rhode Island soils and test the contaminant removal capacity of porous concrete pavement systems; 2) to develop a filter media amended with nanoparticles or quaternary ammonium polymer to enhance the simultaneous removal of PAHs, metals, and pathogens from stormwater runoff and, 3) to determine the concentration and sources of PAHs in surface soils in San Mateo Ixtatán, Guatemala, and perform a risk assessment

References

- [1] P. Göbel, C. Dierkes, W.G. Coldewey, Storm water runoff concentration matrix for urban areas, *J. Contam. Hydrol.* 91 (2007) 26–42. doi:10.1016/j.jconhyd.2006.08.008.
- [2] E. Manoli, C. Samara, Polycyclic aromatic hydrocarbons in natural waters: sources, occurrence and analysis, *TrAC Trends Anal. Chem.* 18 (1999) 417–428. doi:10.1016/S0165-9936(99)00111-9.
- [3] T.R. Schueler, H. Holland, Microbes and urban watersheds: concentrations, sources, and pathways, *Pract. Watershed Prot.* (2000) 74–84.
- [4] R. Pitt, R. Field, M. Lalor, M. Brown, Urban stormwater toxic pollutants: assessment, sources, and treatability, *Water Environ. Res.* 67 (1995) 260–275. doi:10.2175/106143095X131466.
- [5] P.L. Brezonik, T.H. Stadelmann, Analysis and predictive models of stormwater runoff volumes, loads, and pollutant concentrations from watersheds in the Twin Cities metropolitan area, Minnesota, USA, *Water Res.* 36 (2002) 1743–1757. doi:10.1016/S0043-1354(01)00375-X.
- [6] I. Gnecco, C. Berretta, L.G. Lanza, P. La Barbera, Storm water pollution in the urban environment of Genoa, Italy, *Atmospheric Res.* 77 (2005) 60–73. doi:10.1016/j.atmosres.2004.10.017.
- [7] O. US EPA, Drinking Water Contaminants, (n.d.). <http://water.epa.gov/drink/contaminants/> (accessed November 1, 2014).
- [8] F.K.F. Geronimo, M.C. Maniquiz-Redillas, L.-H. Kim, Treatment of parking lot runoff by a tree box filter, *Desalination Water Treat.* 51 (2013) 4044–4049. doi:10.1080/19443994.2013.781099.
- [9] J.D. Luck, S.R. Workman, M.S. Coyne, S.F. Higgins, Solid material retention and nutrient reduction properties of pervious concrete mixtures, *Biosyst. Eng.* 100 (2008) 401–408. doi:10.1016/j.biosystemseng.2008.03.011.
- [10] B.O. Brattebo, D.B. Booth, Long-term stormwater quantity and quality performance of permeable pavement systems, *Water Res.* 37 (2003) 4369–4376. doi:10.1016/S0043-1354(03)00410-X.

- [11] V.A. Oyanedel-Craver, M. Fuller, J.A. Smith, Simultaneous sorption of benzene and heavy metals onto two organoclays, *J. Colloid Interface Sci.* 309 (2007) 485–492. doi:10.1016/j.jcis.2006.10.001.
- [12] V.A. Oyanedel-Craver, J.A. Smith, Effect of quaternary ammonium cation loading and pH on heavy metal sorption to Ca bentonite and two organobentonites, *J. Hazard. Mater.* 137 (2006) 1102–1114. doi:10.1016/j.jhazmat.2006.03.051.
- [13] J. Rayner, H. Zhang, J. Schubert, P. Lennon, D. Lantagne, V. Oyanedel-Craver, Laboratory Investigation into the Effect of Silver Application on the Bacterial Removal Efficacy of Filter Material for Use on Locally Produced Ceramic Water Filters for Household Drinking Water Treatment, *ACS Sustain. Chem. Eng.* 1 (2013) 737–745. doi:10.1021/sc400068p.
- [14] T. Agarwal, P.S. Khillare, V. Shridhar, S. Ray, Pattern, sources and toxic potential of PAHs in the agricultural soils of Delhi, India, *J. Hazard. Mater.* 163 (2009) 1033–1039. doi:10.1016/j.jhazmat.2008.07.058.
- [15] Y.-F. Jiang, X.-T. Wang, F. Wang, Y. Jia, M.-H. Wu, G.-Y. Sheng, et al., Levels, composition profiles and sources of polycyclic aromatic hydrocarbons in urban soil of Shanghai, China, *Chemosphere.* 75 (2009) 1112–1118. doi:10.1016/j.chemosphere.2009.01.027.
- [16] R. Xiao, J. Bai, J. Wang, Q. Lu, Q. Zhao, B. Cui, et al., Polycyclic aromatic hydrocarbons (PAHs) in wetland soils under different land uses in a coastal estuary: Toxic levels, sources and relationships with soil organic matter and water-stable aggregates, *Chemosphere.* 110 (2014) 8–16. doi:10.1016/j.chemosphere.2014.03.001.
- [17] M. Nadal, M. Schuhmacher, J.L. Domingo, Levels of PAHs in soil and vegetation samples from Tarragona County, Spain, *Environ. Pollut.* 132 (2004) 1–11. doi:10.1016/j.envpol.2004.04.003.
- [18] S. Orecchio, Assessment of polycyclic aromatic hydrocarbons (PAHs) in soil of a Natural Reserve (Isola delle Femmine) (Italy) located in front of a plant for the production of cement, *J. Hazard. Mater.* 173 (2010) 358–368. doi:10.1016/j.jhazmat.2009.08.088.
- [19] WHO. *Bulletin of the World Health Organization*, (2000).

Chapter 2

Enhanced Containment of Polycyclic Aromatic Hydrocarbons (PAHs) Through

Organic Modification of Soils

By

Varun Kasaraneni¹, Steven E. Khom¹, Dylan Eberle², Thomas Boving^{1,2}, Vinka Oyanedel-Craver¹

Is published in Journal of Environmental Progress and Sustainable Energy

¹ Department of Civil and Environmental Engineering, University of Rhode Island, Bliss Hall
213, Kingston, RI 02881, USA

² Department of Geosciences, University of Rhode Island, Woodward Hall 315, Kingston, RI
02881, USA

Abstract

A methodology to enhance the containment of polycyclic aromatic hydrocarbons (PAHs) in pervious pavement systems was developed through the chemical modification of a typical Rhode Island glacial outwash soil. In addition, the PAH-retaining capacity of different structural components of pervious pavements was evaluated using column experiments in terms of PAH retention. Two methods were used for soil amendments. The first method was a direct modification of the porous matrix using quaternary ammonium cations through an ion exchange process. The second method involved blending the soil with a commercial organoclay (PM-199; CETCO Oil Field Services). These amendments successfully increased the soil's fraction of organic carbon (f_{oc}) by at least 70%. To quantify the efficiency of these amended soils to sorb PAHs, a series of batch isotherms and column experiments were conducted on unmodified and modified soils. These studies demonstrated that, through the synthetic modification, the sorption of PAH was increased by up to 20-fold. The Langmuir (α , β) and Freundlich (K_F , n) isotherm coefficients calculated from batch studies were higher when compared with column experiments. Overall, the organoclay-glacial outwash blend exhibited the greatest K_F value of 114.2. Breakthrough curves obtained using HYDRUS 1D were compared with measured data. The column experiments conducted on porous concrete and aggregate demonstrated that these materials have a minimal contribution to the overall containment of PAH in pervious pavement systems.

1. Introduction

Impermeable surfaces such as conventional concrete and asphalt have the potential to generate large volumes of contaminated storm-water runoff during precipitation events. Storm-water runoff is a source of organic and inorganic contaminants that can end up polluting natural bodies of water [1]. Of particular concern are polycyclic aromatic hydrocarbons (PAHs), which are a family of organic compounds containing two or more benzene rings.

PAHs are ubiquitous in the environment and present in the soil, water, and air. Most PAHs are acutely toxic and suspected human carcinogens [2]. The Safe Drinking Water Act enforces a maximum contaminant level of 0.0002 mg/L for PAHs [3]. Acute oral toxicity of PAHs range from 50 to 2000 mg/kg of body weight depending on the specific compound [2]. One of the main characteristics of PAH is that, as the number of benzene rings increases, the solubility in aqueous solutions decreases. Due to the hydrophobic properties of these compounds, PAHs are rapidly sorbed onto sediment particles and subsequently deposited. As previously demonstrated, the re-release of PAHs into clean or less contaminated waters is possible [4, 5]. After a rainfall event, PAHs are carried into the drainage infrastructure and are eventually transported into ground and surface waters. Hoffman et al. [4] reported that urban runoff entering Narragansett Bay was responsible for 71% percent of the total inputs of higher molecular weight PAHs and 36% of total PAHs. Another study, spanning from 1993 to 2001, showed that storm-water runoff contributes about 51% of all PAHs to the San Francisco Bay [6].

As vehicles produce the greatest concentration of PAHs during ignition and acceleration [7], roads and parking lots are ideal locations for containing the transport of these contaminants before they are discharged into natural ecosystems. In most major American cities, parking lots account for 10% to 15% of the total impervious area [8], and impervious areas in urban and suburban settings are expected to increase in the future. In addition to automotive-related

releases, coats of pavement sealants and oil leakages are also important sources of PAHs [4, 9-11].

Engineered systems can mitigate the discharge of PAHs from parking lots, thereby drastically reducing the influx of contaminants into water resources. For example, pervious pavement has been used to reduce both the volume and contaminant load in storm runoff [12-15]. In addition, pervious concrete pavements can elevate pH of runoff from acidic nature [16]. However, conventional pervious pavements systems have a limited contaminant removal capacity [17]. The pollutant removal performance of the pervious pavement systems is not consistent over time and also depends on location [17].

Previous studies have demonstrated that, by increasing the fraction of carbon (f_{oc}) of a sorbent, the sorption of PAHs increases [18-20]. Several approaches have been suggested to increase the f_{oc} of soils or other engineered materials [18, 21], such as activated carbon [22, 23], which can be expensive, can be labor intensive, and may require frequent maintenance.

The purpose of this study was to design and test a porous medium that can potentially be applied in pervious pavement systems. The principle goals were to identify a material capable of enhancing the PAH sorption capacity, thereby mitigating the influx of PAHs into the deeper subsurface. The necessary laboratory studies were performed in three phases: (i) synthesis of organically modified soils; (ii) testing of the effectiveness of the organic amendments to Rhode Island glacial outwash soil and organoclay to sorb the PAH compound naphthalene; and (iii) determination of whether any of the conventional construction components of pervious pavement systems (i.e., porous concrete, aggregate, including unmodified soil) contribute to PAH removal. The PAH compounds acenaphthene and flourene were used for the second part of the study.

2. Methods and Materials

2.1 Overview of Experimental Methodology

The experiment was divided into three phases. The first phase involved the synthesis and characterization of the organically modified soil amendments. Second, the performance of the modified soil in terms of PAH sorption was assessed using naphthalene as the model PAH. This phase involved both batch isotherms and column experiments. Naphthalene was chosen due to its high aqueous solubility. The third phase focused on the assessment of PAH-retaining capabilities of conventional and organically modified pervious pavement elements. In these column experiments, acenaphthene and fluorene were used as model PAHs. These PAHs were selected as they have high aqueous solubility, have higher molecular weight, and are commonly found at contaminated sites.

2.2 Materials

Naphthalene, fluorine, and acenaphthene (purity grade of 98% or higher) were obtained from Aldrich. Analytical grade solvents (dichloromethane and methanol) were obtained from Fisher Scientific. Aqueous solutions were prepared in deionized water free of detectable traces of PAH and with a pH near neutral. PAH are nonionic compounds, there is no influence of pH on the characteristics of PAH in the aqueous phase. Furthermore, the pH of runoff originating from traffic areas ranges between 6.4 and 7.9 [1]. The pH used for our experiments is 7.0, which is well within the narrow range of natural conditions. A gas chromatograph with flame ionization detector (Shimadzu GC-17 A/FID) and a gas chromatograph/mass spectrometer (Shimadzu GC-MS QP2010) were used to quantify PAH compounds. Only glass vessels were used, and care was taken to prevent PAH photo degradation. Hexadecyltrimethyl ammonium chloride (HDTMA) and benzyldimethylhexadecyl ammonium chloride (BHDH) were obtained from sigma Aldrich, with a purity of 99%; they were used as received.

The PAH-saturated solutions were prepared following a method described by Wang et al. [24]. In brief, PAHs were dissolved in 1 mL of dichloromethane in a 4 L Erlenmeyer flask. As the solvent volatilized, a thin film of PAH formed on the glass. The flask was then filled with deionized water, which was allowed to saturate and equilibrate with the PAH over the course of 1 week. The initial concentration (C_0) of all three target PAHs in the aqueous phase was determined using the gas chromatograph-mass spectrometry.

A bulk sample (20 kg) of Rhode Island glacial outwash soil was collected at the Peckham farm research site near the University of Rhode Island campus. The soil was fully dried and sieved through a number 10 sieve (2.0 mm). The fraction of soil passing through the sieve was sterilized in an autoclave. Aggregate material was obtained from the Cherenzia Excavation site in Rhode Island. The aggregates confirmed to ASTM C 33, Size No. 67 (3/4 in. to No. 4). In addition, Portland Type II cement was obtained from the Home Depot in Middletown, RI. Pervious concrete was prepared following one of the compaction techniques described in Putman and Neptune [25]. Briefly, concrete was mixed and placed in 2-inch layers by compacting using a 15.9 mm diameter steel rod, rodding it 15 times. The pervious concrete had a void content of 15% to 18%, which is typical for this type of material [26]. The porosity (Eq. (1)) of the materials was determined using the volume of voids which was determined by identifying the difference in weight between the dry sample and a water-saturated sample.

$$\phi = \frac{V_v}{V_T} \quad \text{Equation (1)}$$

2.3 Synthesis and Characterization of Organically Modified Soil Amendments

The cation exchange capacity (CEC) of the soil was determined by the Soil, Water, and Plant Testing Laboratory at Colorado State University. A characterization of the soil particle size distribution was conducted on all modified and unmodified soils through sieve and hydrometer analysis using ASTM 136 and 152 H methods [27]. The hydraulic conductivity of the concrete,

aggregate and soils was determined using the falling head permeameter method [28]. HDTMA and BHDH are long-chained cations with relatively high carbon content; therefore, they are considered to be an attractive choice for increasing the f_{oc} of the porous matrices. Equation (2) was developed by Boyd et al. [29] to determine the mass of quaternary ammonium cation (QAC) with respect to the mass of soil and CEC.

$$f = M_{\text{cation}} / (\text{CEC} * M_{\text{soil}} * \text{GMW}_{\text{cation}} * z) \quad (2)$$

where CEC is the cation exchange capacity in milli-equivalents per gram of soil, f is the fraction of CEC exchanged, M_{cation} is the mass of cation used in grams, M_{soil} is the mass of soil in grams, $\text{GMW}_{\text{cation}}$ is the formula weight of cation in grams per mole, and z represents the moles of charge per equivalent moles per milli-equivalent of exchange capacity.

The wet method developed by Breakwell et al. [30] was used to modify the soils. Briefly, the amount of QAC necessary to produce 100 g of 100% CEC modified soil was calculated using Boyd's equation. The QAC was dissolved into 400 ml of deionized water using a stir bar and a glass beaker. Soil was mixed into the QAC solution and agitated for 3 days at 150 rpm in an incubator at 20°C. The contents of the glass beaker were carefully decanted after settling, and the soil was placed into the oven for 6 h at 100°C to dry. The residual chloride ions were removed by rinsing with deionized water until electrical conductivities were below 1 $\mu\text{s}/\text{cm}$. Once dried, the modified soils were analyzed using a Carlo Erba EA1108 Carbon Hydrogen and Nitrogen analyzer to quantify the amount of carbon.

The second approach for introducing f_{oc} involved mixing the glacial outwash soil with commercial organoclay (PM-199; CETCO Oil Field Services). To maintain a point of reference in isotherm and column experiments, the mass of the total organic carbon in the blend was calculated to match the mass of total organic carbon in the BHDH-modified soil. This resulted in a 1:18 ratio of commercial organoclay and Rhode Island glacial outwash.

2.4 Sorption Isotherms

A series of batch isotherms were performed for all sorbents to study the static interaction between sorbent and aqueous PAH. A constant mass (different for each soil) of the particular sorbent was exposed to increasing concentrations (ranging from 2 to 22 mg/L) of the aqueous naphthalene solution. Kinetic investigation showed that it took 30 h to reach equilibrium between the aqueous phase and the sorbent. Based on this finding, the isotherms tests were performed for at least 48 h at 20°C. Afterward, all samples were centrifuged for 10 min at 2500 rpm to remove any particulates from the aqueous phase. After the liquid–liquid extraction with dichloromethane following EPA method 610, the naphthalene concentration was determined using gas chromatography-mass spectrometry (GS-MS). The Langmuir equation (Eq. (3)) was used to model sorption data for the glacial outwash material, while the Freundlich equation (Eq. (4)) was used to model the sorption of all other materials.

$$\frac{C_s}{C_e} = \frac{1}{\alpha\beta} + \frac{C_s}{\beta} \quad (3)$$

$$C_s = K_f C_e^n \quad (4)$$

where C_e is the concentration of naphthalene in solution at equilibrium [M/L³], C_s is the mass of naphthalene sorbed per dry unit weight of sorbent [M/M], α is a Langmuir adsorption constant and β is the Langmuir maximum amount of naphthalene that can be absorbed by the sorbent, n is the unitless Freundlich exponent, and K_f is the Freundlich sorption coefficient [L³/(M-M (1-N))].

2.5 Column Experiments

Column experiments were conducted to study the sorption and desorption of PAHs under dynamic, flow-through conditions. For the concrete and aggregate materials, larger glass columns (length: 15.0 cm, ID: 8.5 cm) were used, whereas smaller ones (length: 5.0 cm, ID: 2.5 cm) were used for soil. Columns filled with porous concrete and aggregate were connected to a Masterflex L/S pump with Teflon tubing. The columns packed with soil were connected to an Accuject

Series I injector pump with Teflon tubing. Conservative tracer tests with sodium chloride (NaCl) were performed to determine pore velocity and dispersion coefficient. After determining the column intrinsic parameters, an aqueous solution saturated with the target PAH was pumped through the columns. Effluent samples were collected until breakthrough, which defined as C/C_0 equaling one (i.e., the effluent concentration is equal to the influent concentration). The flow velocities were held constant at 2 mL/min for soil columns and 20 mL/min for concrete and aggregate columns. After breakthrough, the influent was switched to deionized water to study desorption. The pumping of deionized water continued until at least 90% of the PAH was recovered. This same procedure was repeated for concrete, aggregate, and all other soil media.

2.6 HYDRUS 1D

HYDRUS-1D (version 4.14) software was used to stimulate solute transport through unmodified and modified soils. Parameters obtained from sorption isotherms, soil characterization, and column experiments were used to predict the breakthrough curves (BTCs) for naphthalene in unmodified and modified soils. Langmuir and Freundlich isotherm coefficients were obtained from isotherm experiments. Dispersion coefficient and bulk densities were obtained from column tracer experiments. Hydraulic conductivities were obtained from falling head permeameter tests. HYDRUS-1D was also used to estimate the adsorption coefficient from column experiments using the inverse solution to the Levenberg–Marquardt nonlinear parameter optimization method.

3. Results and Discussion

3.1 Evaluation of the effectiveness of the organic modification in Rhode Island soil

3.1.1 Synthesis and characterization of organically modified soil amendments

A CEC of 5.6 milli-equivalents of exchangeable cations per 100 g of glacial outwash soil (meq/100 g) was measured. These results were consistent with the CEC values determined by Wright and Sautter [31]. The results from soil modification, particle size analysis, and hydraulic conductivity measurements are summarized in Table 2-1. Also shown are the initial f_{oc} and the percentage of f_{oc} increase resulting from the soil modification.

Table 2-1: Soil Organic Carbon, Particle Size, and Hydraulic Conductivity Properties

Soil Type	f_{oc} [%]	f_{oc} Increase [%]	D_{10} [mm]	Uniformity Index (U) [-]	n [-]	K [cm/s]
Unmodified Glacial Outwash	1.70	--	0.070	9.286	0.54	1.53E-03
HDTMA	2.90	70.6	0.030	13.333	0.504	6.73E-04
BHDH	2.94	72.9	0.040	12.500	0.56	9.33E-04
Blend	2.94	72.9	0.090	6.667	0.52	2.93E-03

f_{oc} = Fraction of Organic Carbon; D_{10} =effective grain size; n is porosity, K is hydraulic conductivity, Blend is 1:18 mix of organoclay and glacial outwash soil.

QACs HDTMA and BHDH increased the fraction of organic carbon in the Rhode Island glacial outwash soil by 70.6% and 72.9%, respectively. The f_{oc} increase in the blend was calculated to match the organic carbon in the BHDH-modified soil. This resulted in mix of 1:18 commercial organoclay and glacial outwash. The hydraulic conductivities of the modified soils were an order of magnitude smaller than the unmodified soil. Decreases in effective grain size (D_{10}) and porosity were also observed, although the reasons for these decreases were not investigated. Conversely, adding the PM-199 organoclay to the unmodified soil increased the effective grain

size D_{10} of the blend while decreasing the uniformity coefficient and increasing the hydraulic conductivity. Thus, a material with increased hydraulic conductivity, such as this organoclay-glacial outwash blend, will be best suited for application below permeable pavement because it will aid in faster drainage of storm water.

3.1.2 Sorption Isotherms

Kinetic investigation revealed an equilibrium time of 30 h (data not shown) between the soils and naphthalene, which is consistent with prior research [32, 33]. The sorption isotherm results for the glacial outwash fit the Langmuir model, in which a limited number of sorption sites are available that can be fully saturated during isotherm experimentation. The use of the Langmuir model for glacial outwash materials is consistent with the results of Appert-Collin et al. [34], who exposed saturated aqueous naphthalene solutions to soils with low organic carbon material. Correlation coefficients values, R^2 , of the glacial outwash Langmuir fit were 0.997. Figure 2-1 shows the results of the naphthalene-soil isotherm experiments for glacial outwash. The maximum amount of naphthalene that can be sorbed by the glacial outwash, β , was determined to be 0.48 mg naphthalene per gram of soil. The adsorption constant related to binding energy, α , was 0.24 L/g. The predicted α from column experiments was 0.18 L/g.

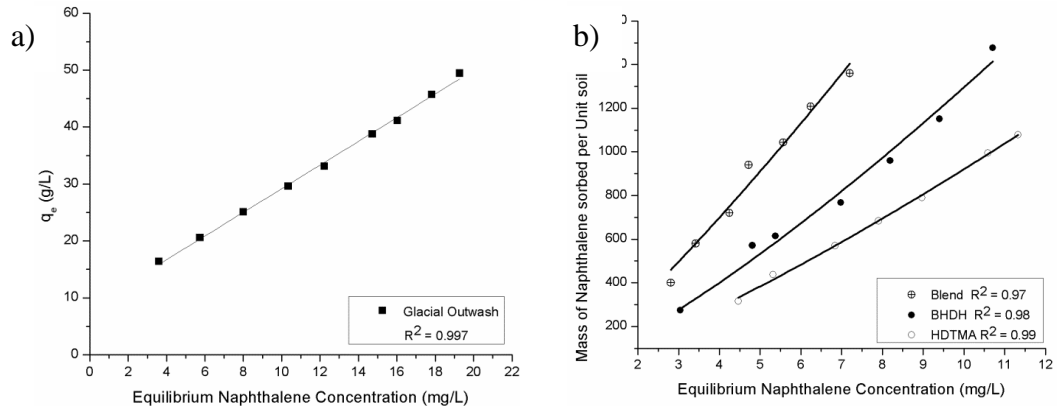


Figure 2-1: Sorption isotherms for the sorption of naphthalene on (a) Glacial Outwash Soil (Linearized Langmuir model). q_e is aqueous naphthalene / mass of naphthalene sorbed per unit mass of soil (b) Modified soils (HDTMA, BHDH and blend) Freundlich model. Origin data analysis software was used for fitting. Freundlich Model power fit was used to obtain Freundlich Isotherm constants.

In contrast to the unmodified soil (Figure 2-1a), the isotherms experiments on the modified soils and naphthalene demonstrated that sorption sites were not exhausted within the range of PAH concentrations tested. For this reason, the isotherm data for the modified soil were fitted with the Freundlich isotherm model ($R^2 = 0.98$). As expected, Freundlich constants (K_F ; Table 2-2) increased with increasing organic carbon content of the soils, leading to increased naphthalene sorption. Of the modified soils, the organoclay-glacial outwash blend (1:18 ratio) exhibited the greatest K_F value (114.2). Although the Freundlich model suggested that no upper limit exists for sorption in the experimental concentration range, in reality one is likely to exist, although it remains to be determined what this limit is.

Table 2-2: Freundlich sorption parameters from batch and column studies of modified Soils

Soil	Batch Isotherm			Column study	
	K_F	N	R^2	K_F	N
HDTMA	36.90	1.23	0.99	5.50	1.58
BHDH	54.30	1.28	0.98	19.3	1.04
Blend	114.20	1.18	0.97	89.9	1.12

N is the unitless Freundlich linearity exponent; K_F is the Freundlich sorption coefficient and R^2 is the correlation coefficient.

3.1.3 Column experiments with unmodified, organically modified, and blended Rhode Island glacial outwash soils

Parameters for the four column experiments, including pore volume, pore water velocity, and dispersion coefficients, are shown in Table 2-3. Observed and predicted naphthalene BTCs for all soils are plotted in dimensionless terms of relative concentration (C/C_0) and pore volumes (Figure 2-2). Column experiments supported the results obtained from the batch isotherms. Unmodified glacial outwash soil had the fastest breakthrough and the lowest retardation factor of 54.3. These results are consistent with the outwash having the lowest f_{oc} . Of the modified soils fitted with the Freundlich isotherm model, the HDTMA soil had the lowest retardation factor $R = 76$ and the lowest $K_F = 36.9$, versus $R = 304$ and $K_F = 54.3$ for BHDH-modified soil. Although the HDTMA and BHDH soils had very similar f_{oc} values (2.90% and 2.94%, respectively), their Freundlich sorption coefficients differed (Table 2-2) which may be due to the presence of the benzyl group in the BHDH. Naphthalene is composed of two fused benzene rings, and the similar structure between the sorbent and solute can facilitate and greatly increase sorption. This would be consistent with the findings in other studies focusing on QAC-modified sorbents containing benzyl groups [35]. The column that exhibited the greatest retardation of naphthalene was the blended commercial organoclay-glacial outwash material. This sorbent retarded naphthalene by $R = 438$, which correlates with the blended material having the largest K_F of 114.2 and $f_{oc} = 2.94$. Although the BHDH and Blended soils had very similar f_{oc} values (2.94%), there is higher

sorption of naphthalene by the blended material. This due to the quaternary ammonium cation (QAC) used in preparation of organoclay PM-199 which is dialkyldimethyl ammonium chloride. The proprietary alkyl groups are shown are not revealed. The higher sorption of naphthalene by blend can be attributed to the hydrophobicity of the hydrocarbon chain in the ammonium salt used to produce PM-199 [33].

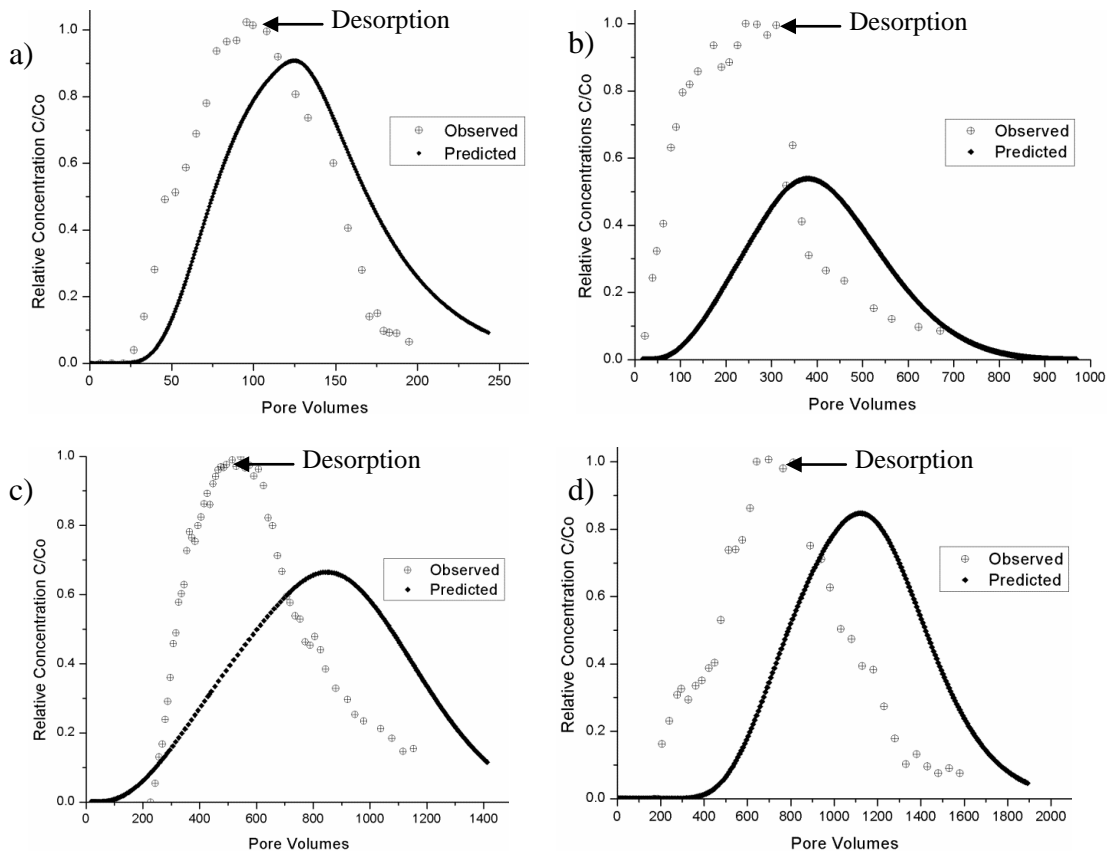


Figure 2-2: Observed and predicted BTCs of naphthalene for a) RI glacial outwash b) HDTMA modified soil c) BHDH modified soil d) Blended modified soil. The injected naphthalene concentrations were 30 ± 2 mg/l and flow rates were maintained at 2 ml/min. Desorption experiment started once the relative concentration reached 1.

The CXT fit model [36] was used to determine column intrinsic parameters and the retardation factors for naphthalene. CXT fit allows for inverse estimation of transport parameters from a laboratory study. The program uses convection dispersion equation with a data set, using the nonlinear least-squares parameter optimization method. Together with experimental data,

including hydraulic conductivity, bulk density, and isotherm coefficients from sorption studies, parameters determined with CXT fit were used as inputs to predict BTCs with HYDRUS. The predicted BTC (Figure 2-2) compared poorly with the measured batch experimental data. Similarly, the predicted adsorption isotherm coefficients (Table 2-2) for column experiment data were lower than the values from batch experiments. Maraqa et al. [37] also reported that their batch study overestimated adsorption coefficients of benzene and dimethylphthalate compared with the results from the column study. Similarly, Lee et al. [38] reported a poor match of their predicted BTCs relative to the ones measured for naphthalene. However, the Langmuir coefficients predicted from column experiments for glacial outwash are in close agreement with isotherm coefficients. The fraction of Type 1 adsorption sites at which sorption is assumed to be instantaneous was set to one, and the first-order rate constant was set to zero for the calculation of BTCs and the inverse solution. HYDRUS permits chemical nonequilibrium (adsorption–desorption process) and physical nonequilibrium (possible heterogeneity of soil). As none of these processes were considered in the modeling of the results, this could be a reason for the poor prediction of BTCs. Additional experiments are required to obtain the parameters needed to include chemical and physical nonequilibrium processes. The HYDRUS modeling was test if the results can be replicated using this computational tool. The results suggest that HYDRUS and these results will support a more thorough future modeling study regarding determining the life time and optimizing the ratio of organoclay to glacial outwash. More data and modeling effort is needed to obtain an optimal fit. The BTCs obtained using the isotherm data was used to compare the experimental data and modeling data. This allowed us to determine how effective the modeling data is when compared to laboratory scale/field scale results.

Table 2-3: Column Intrinsic Parameters and Naphthalene Retardation

Soil	Pore Volume [-]	Bulk Density [g/cm³]	Velocity [cm/min]	Dispersion [cm²/min]	Retardation factor CXT fit
G. O*	13.23	1.43	0.75	0.60	54.3
HDTMA	12.37	1.58	0.96	0.77	76
BHDH	12.75	1.45	0.82	0.73	304
Blend	13.75	1.15	0.76	0.26	438

Retardation factor obtained from breakthrough curve plotted in the unitless terms of relative concentration (C/C_0) and pore volumes (PV). * G.O unmodified glacial outwash

3.2 Performance of convention and organically modified pervious concrete pavements

As potential parts of a pervious pavement system, the capacities of porous concrete and aggregate for retaining PAH of different molecular weights were determined through column experiments (Table 2-4). The sorption and desorption results for acenaphthene and flourene are shown in Figures 3a and 3b. The PAH retardation factor for concrete was $R_f = 1$, indicating that this material has no PAH sorption capacity. For the aggregate, the retardation factor is $R_f = 11$ and $R_f = 7$ for acenaphthene and flourene, respectively. Due to the very low organic matter, the retardation of PAHs in concrete and aggregate is significantly lower compared to in soils [18-20]. Similarly, low retardation was found in the case of the glacial outwash soil ($R_f = 16.5$; Figure 2-3c).

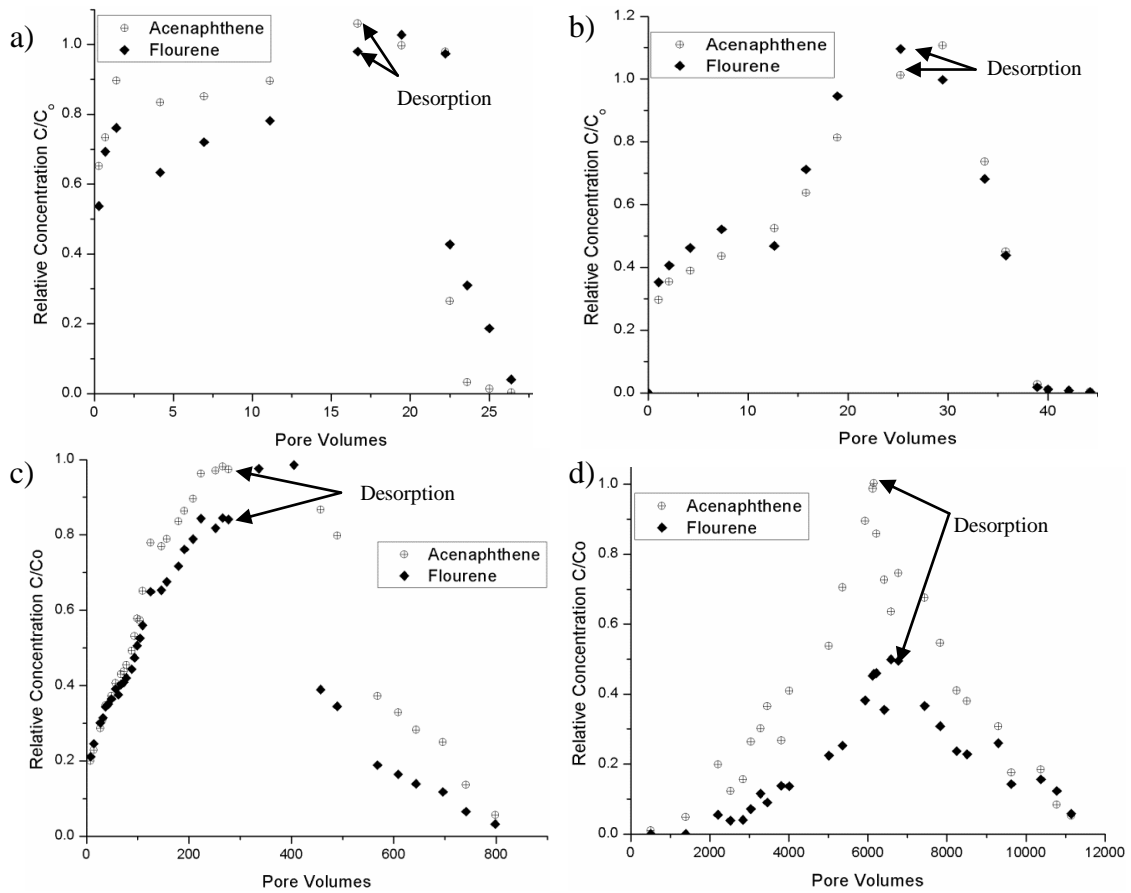


Figure 2-3: BTCs of acenaphthene and fluorene in column experiments for a) concrete b) aggregate c) RI glacial outwash soil d) blend of organo clay-glacial outwash soil. Desorption experiment started once the relative concentration reached 1.0. The influent concentrations of acenaphthene and fluorene were $1.6 \pm 0.2 \text{ mg/l}$ and $0.6 \pm 0.2 \text{ mg/l}$ respectively.

By far, the greatest retardation ($R = 4125.6$ for acenaphthene) was achieved with the blend of organoclay-glacial outwash, which reinforces that increasing foc leads to an increase in PAH sorption capacity. Retardation of fluorene for the organoclay-glacial outwash blend column was not calculated because $C/C_0 = 1$ was not reached during this experiment.

Table 2-4: Column Intrinsic Parameters and Retardation factors

	ρ [g/cm ³]	PV [cm ³]	Porosity [-]	Dispersion [cm ² /min]	Ace R _f [-]	Flu R _f [-]	K [cm/s]
Concrete*	2.4	190	0.17	47.6	1	1	9 E-02
Aggregate*	1.8	380	0.45	10.3	11	7	11.7 E-02
Glacial** outwash	1.82	11.43	0.46	0.72	16.5	18.2	1.93E-03
Blend**	1.86	10.18	0.41	0.31	4125.6	-	2.87E-03

ρ is bulk density, PV is pore volume, Ace is Acenaphthene, Flu is Fluorene, R_f is Retardation factor * The column volume of concrete and aggregate columns were 850 cm³ ** Column volume is 24.5 cm³

Commercial organoclay ranges in cost between one to two dollars per pound. If the organoclay–glacial outwash blending ratio and bulk density used in the study was kept constant, the cost of the organoclay material would average about \$200.00 per cubic meter. However, the thickness of the modified section could be reduced to decrease the cost. Also, the QAC loading on the soil could be optimized to further reduce prices. The cost–benefit analysis and optimization of the enhanced sorption section is beyond the context of this study but will be a subject of our future studies.

4. Conclusions

The adverse effects of contaminants commonly present in storm-water runoff can be minimized using BMPs, such as pervious pavement systems. The results of this study demonstrated that conventional pervious pavement components, such as porous concrete, aggregate, and unmodified soil, have little capacity to retain PAHs from the aqueous phase. The modification of glacial outwash using QAC increased the fraction of organic carbon in the soil and greatly enhanced the PAH sorption capacity of the soils. After flushing several 100 pore volumes of PAH saturated water, the modified soil media removed up to 74% of PAHs (i.e., irreversible sorption). Thus, modified soil media, such as a blend of organoclay and glacial outwash, could find applications in BMPs to reduce contaminant flux into surface water or groundwater. These modified organoclay–glacial outwash blends can potentially be incorporated as a layer beneath pervious pavement. In addition to retaining PAHs, their higher hydraulic conductivity relative to the unmodified soil is an added advantage. However, cost is an important factor when incorporating modified materials into permeable pavement design. Currently, the cost of commercial organoclay ranges from 1 to 2 dollars per pound, which may prevent the widespread application of this promising amendment.

Acknowledgments

The authors would like to thank the University of Rhode Island Transportation Center, Rhode Island Department of Transportation and the Rhode Island Water Resource Center for the support provided to perform this work.

References

- 1) Göbel, P., Dierkes, C., Coldewey, W.G., 2007. Storm water runoff concentration matrix for urban areas. *J. Contam. Hydrol.* 91, 26–42.
- 2) Eisler, R. (1987). Polycyclic aromatic hydrocarbon hazard to fish, wildlife, and invertebrates: A synoptic review, Patuxent Wildlife Research Center Contaminant Hazard Reviews, 1, 1–55.
- 3) EPA (2009). United States Environmental Protection Agency. Technical Fact Sheet on Polycyclic Aromatic Hydrocarbons, EPA Safewater, Washington, D.C.
- 4) Hoffman, E.J., Mills, G.L., Latimer, J.S., Quinn, J.G., 1984. Urban runoff as a source of polycyclic aromatic hydrocarbons to coastal waters. *Environ. Sci. Technol.* 18, 580–587.
- 5) Neary, K., Boving, T.B., 2011. The fate of the aqueous phase polycyclic aromatic hydrocarbon fraction in a detention pond system. *Environ. Pollut.* 159, 2882–2890. doi:10.1016/j.envpol.2011.04.046
- 6) Oros, D.R., Ross, J.R.M., Spies, R.B., Mumley, T., 2007. Polycyclic aromatic hydrocarbon (PAH) contamination in San Francisco Bay: A 10-year retrospective of monitoring in an urbanized estuary. *Environ. Res., Pollutants in the San Francisco Bay Estuary* 105, 101–118.
- 7) Joneck, M., & Prinz, R. (1996). Organic and Inorganic pollutants in roadside soils from streets with different traffic densities in Bavaria (Berlin), *Wasser und Boden*, 48, 49–54.
- 8) Wong, E. (2005). Cool pavements. Reducing urban heat islands: Compendium of strategies. EPA, Washington, D.C.
- 9) Jiries, A.G., Hussein, H.H., Lintelmann, J., 2003. Polycyclic aromatic hydrocarbon in rain and street runoff in Amman, Jordan. *J. Environ. Sci. China* 15, 848–853.
- 10) Mahler, B.J., Van Metre, P.C., Bashara, T.J., Wilson, J.T., Johns, D.A., 2005. Parking Lot Sealcoat: An Unrecognized Source of Urban Polycyclic Aromatic Hydrocarbons. *Environ. Sci. Technol.*
- 11) Legret, M., Odie, L., Demare, D., Jullien, A., 2005. Leaching of heavy metals and polycyclic aromatic hydrocarbons from reclaimed asphalt pavement. *Water Res.* 39, 3675–3685. doi:10.1016/j.watres.2005.06.017
- 12) Kadurupokune, N., Jayasuriya, N., 2009. Pollutant load removal efficiency of pervious pavements: is clogging an issue? *Water Sci. Technol.* 60, 1787. doi:10.2166/wst.2009.571

- 13) Luck, J.D., Workman, S.R., Coyne, M.S., Higgins, S.F., 2008. Solid material retention and nutrient reduction properties of pervious concrete mixtures. *Biosyst. Eng.* 100, 401–408.
- 14) Luck, J.D., Workman, S.R., Coyne, M.S., Higgins, S.F., 2009. Consequences of manure filtration through pervious concrete during simulated rainfall events. *Biosyst. Eng.* 102, 417–423.
- 15) Kuang, X., Fu, Y., 2013. Coupled infiltration and filtration behaviours of concrete porous pavement for stormwater management. *Hydrol. Process.* 27, 532–540.
doi:10.1002/hyp.9279
- 16) Kuang, X., Sansalone, J., 2011. Cementitious porous pavement in stormwater quality control: pH and alkalinity elevation. *Water Sci. Technol.* 63, 2992.
doi:10.2166/wst.2011.505
- 17) Brattebo, B.O., Booth, D.B., 2003. Long-term stormwater quantity and quality performance of permeable pavement systems. *Water Res.* 37, 4369–4376.
- 18) Jonker, M.T.O., Koelmans, A.A., 2002. Sorption of Polycyclic Aromatic Hydrocarbons and Polychlorinated Biphenyls to Soot and Soot-like Materials in the Aqueous Environment: Mechanistic Considerations. *Environ. Sci. Technol.* 36, 3725–3734.
- 19) Cornelissen, G., Breedveld, G.D., Kalaitzidis, S., Christanis, K., Kibsgaard, A., Oen, A.M.P., 2006. Strong Sorption of Native PAHs to Pyrogenic and Unburned Carbonaceous Geosorbents in Sediments. *Environ. Sci. Technol.* 40, 1197–1203.
doi:10.1021/es0520722
- 20) Brändli, R.C., Hartnik, T., Henriksen, T., Cornelissen, G., 2008. Sorption of native polyaromatic hydrocarbons (PAH) to black carbon and amended activated carbon in soil. *Chemosphere* 73, 1805–1810. doi:10.1016/j.chemosphere.2008.08.034
- 21) Li, R., Wen, B., Zhang, S., Pei, Z., Shan, X., 2009. Influence of organic amendments on the sorption of pentachlorophenol on soils. *J. Environ. Sci.* 21, 474–480.
- 22) Zimmerman, J.R., Ghosh, U., Millward, R.N., Bridges, T.S., Luthy, R.G., 2004. Addition of Carbon Sorbents to Reduce PCB and PAH Bioavailability in Marine Sediments: Physicochemical Tests. *Environ. Sci. Technol.* 38, 5458–5464.
- 23) Millward, R.N., Bridges, T.S., Ghosh, U., Zimmerman, J.R., Luthy, R.G., 2005. Addition of Activated Carbon to Sediments to Reduce PCB Bioaccumulation by a Polychaete (*Neanthes arenaceodentata*) and an Amphipod (*Leptocheirus plumulosus*). *Environ. Sci. Technol.* 39, 2880–2887.

- 24) Wang, J.-M., Maier, R.M., Brusseau, M.L., 2005. Influence of hydroxypropyl- β -cyclodextrin (HPCD) on the bioavailability and biodegradation of pyrene. *Chemosphere* 60, 725–728. doi:10.1016/j.chemosphere.2005.03.031
- 25) Putman, B.J., Neptune, A.I., 2011. Comparison of test specimen preparation techniques for pervious concrete pavements. *Constr. Build. Mater.* 25, 3480–3485. doi:10.1016/j.conbuildmat.2011.03.039
- 26) Tennis, P.D., Leming, M.L., & Akers, D.J. (2004). *Pervious Concrete Pavements, EB302.02*. Portland cement association, skokie, illinois, and national ready mixed concrete association, Maryland, USA: Silver Spring.
- 27) Das, B.M. (2009). *Soil mechanics laboratory manual (7th Edition)*, New York: Oxford University Press, pp. 17–36.
- 28) NAVFAC. (1986). *NAVFAC Soil Mechanics, Design Manual 7.01*, Naval Facilities Engineering Command, Alexandria, USA.
- 29) Boyd, S.A., Mortland, M.M., Chiou, C.T., 1988. Sorption Characteristics of Organic Compounds on hexadecyltrimethylammonium-Smectite. *Soil Sci Soc Am J* 52, 652–657.
- 30) Breakwell, I.K., Homer, J., Lawrence, M.A.M., McWhinnie, W.R., 1995. Studies of organophilic clays: the distribution of quaternary ammonium compounds on clay surfaces and the role of impurities. *Polyhedron* 14, 2511–2518.
- 31) Wright, W., & Sautter, E. (1988). *Soils of Rhode Island landscapes*, Agricultural Experiment Station Bulletin, 492.
- 32) Bayard, R., Barna, L., & Mahjoub, B. (2000). Influence of the presence of PAHs and coal tar on naphthalene sorption in soils, *Journal of Contaminant Hydrology*, 46, 61–80.
- 33) Reible, D.D., Lu, X., Jasmine, G., & Qi, Y. (2010). *CETCO Oilfield Services, PM-199 Sorbent Technical Fact Sheet*, Covington, Louisiana.
- 34) Appert-Collin, J.C., Driri-Dhaouadi, S., Simonnot, M.O., & Sardin, M. (1999). Nonlinear sorption of naphthalene and phenanthrene during saturated transport in porous media, *Physics and Chemistry of the Earth*, 24, 543–548.
- 35) Smith, J.A., Jaffe, P.R., Chiou, C.T., 1990. Effect of ten quaternary ammonium cations on tetrachloromethane sorption to clay from water. *Environ. Sci. Technol.* 24, 1167–1172.
- 36) Toride, N., Leij, F.J., & van Genuchten, M.T. (1995). *The CXTFIT code for estimating transport parameters from laboratory or field tracer experiments, Version 2.0*, Research Report No. 137, U.S. Salinity Laboratory, USDA, ARS, Riverside, CA.

- 37) Maraqa, M.A., Zhao, X., Wallace, R.B., Voice, T.C., 1998. Retardation Coefficients of Nonionic Organic Compounds Determined by Batch and Column Techniques. *Soil Sci Soc Am J* 62, 142–152.
- 38) Lee, J., Hundal, L.S., Horton, R., Thompson, M.L., 2002. Sorption and Transport Behavior of Naphthalene in an Aggregated Soil. *J Env. Qual* 31, 1716–1721.

Chapter 3

Enhancement of Surface Runoff Quality Using Modified Sorbents

By

¹Kasaraneni, Varun K; ²Schifman, Laura A.; ^{1,2}Boving, Thomas B; ¹Oyanedel-Craver, Vinka

Is published in ACS Sustainable Chemistry & Engineering

¹Department of Civil and Environmental Engineering, University of Rhode Island, 1 Lippitt Rd,
Kingston, RI USA 02881

²Department of Geosciences, University of Rhode Island, 9 E. Alumni Ave, Kingston, RI USA
02881.

Abstract

The objective of this study was to develop and test nanoparticle and polymer based bioactive amended sorbents to enhance stormwater runoff treatment in best management practices (BMPs). Red cedar wood and expanded shale were the sorbents tested. Red cedar wood chips (RC) were modified with 3-(trihydroxysilyl) propyldimethyloctadecyl ammonium chloride (TPA) and silver nanoparticles (AgNPs) at different mass loadings (3.6 mg/g, 6.7 mg/g and 9.3 mg/g for TPA and 0.33 mg/g and 0.68 mg/g for AgNPs) to simultaneously improve the sorption of organic and inorganic contaminants and pathogenic deactivation in BMPs treating stormwater runoff. Unmodified expanded shale is often used as a filter material for stormwater treatment and was used as a base comparison. The results showed that TPA and AgNP loading onto red cedar increased the Langmuir maximum sorption coefficient (Q) for polycyclic aromatic hydrocarbons, up to 35 fold and 29 fold, respectively compared to unmodified red cedar. In case of heavy metals, Q for lead increased with increased loading of TPA and AgNPs, whereas no significant change in the Q value for cadmium was observed, while zinc and nickel sorption slightly decreased. The Langmuir maximum sorption coefficient of copper was higher for modified red cedar, however no correlation was observed with TPA or AgNP loadings. The log reduction value (LRV) for *Escherichia coli* using unmodified red cedar was <1 log, while modified red cedar exhibited LRV up to 2.90 ± 0.50 log for 6.7 mg/g TPA-RC and up to 2.10 ± 0.90 log for 0.68 mg/g AgNP-RC. Although AgNP modified red cedar shows a comparable performance to TPA-RC, the high cost of production may limit the use of AgNP amended materials. While TPA modified red cedar has advantages of lower cost and lower toxicity, the fate, transport and environmental implications of TPA in natural environments has not been fully evaluated. The findings from this study show that if BMPs were to incorporate the modified red cedar, stormwater treatment of PAH and *E.coli* could be enhanced and the quality of the treated water will improve.

1. Introduction

Stormwater runoff contains polycyclic aromatic hydrocarbons (PAH), heavy metals, and pathogens that are discharged into natural surface and groundwater bodies, impairing ecosystems and compromising human health¹⁻³. During and after precipitation events, these contaminants commonly exceed the maximum contaminant level (MCL) standards in runoff and receiving water bodies^{1, 4, 5}. High concentrations of heavy metals and petroleum hydrocarbons, such as PAHs,³ can compromise the ability to use stormwater for recharging aquifers or apply it in grey-water operations. The concentrations of *Escherichia coli* (*E.coli*) in runoff can exceed 104 colony-forming units (CFU) per 100 ml,⁶ making stormwater runoff one of the major contributors of pathogens into surface and coastal waters^{5,7}. The sources of pathogens in stormwater runoff are attributed to wildlife or pets⁸ and, to some degree to human fecal contamination.⁷ Exposure to pathogens can lead to serious illness, such as gastroenteritis or cholera.^{5, 9} Ideally, structural BMPs should simultaneously attenuate organic, inorganic, and microbiological contaminants. However, most stormwater BMPs are only effective in treating heavy metals and petroleum hydrocarbons^{10,11,12} through filtration and sorption^{13,11,12}. They are largely ineffective in treating pathogens^{14, 15, 16, 17}. Previous studies showed that materials such as organoclays amended with quaternary ammonium compounds exhibit higher sorption for PAHs and metals.¹⁸⁻²¹ The quaternary ammonium polymer 3-(trihydroxysilyl) propyldimethyloctadecyl ammonium chloride (TPA) is used as a disinfectant material in environmental and medical applications such as ceramic filters²² and prosthetic devices²³. Silver nanoparticles (AgNPs) are another well-known antimicrobial agent. Impregnating filters media with AgNPs effectively removes pathogens from aqueous solutions.^{24, 25} To our knowledge these nanoparticles and the TPA polymer have never been used for stormwater runoff treatment.

One commonly used BMP is a tree filter, which consists of a subsurface biofiltration system that combines filtration, sorption, and phytoremediation processes for contaminant removal. However,

previous studies have shown that contaminant removal is limited.¹³ Hence, there is a need to find filter materials that can treat a variety of pollutants and can enhance the stormwater treatment performance of BMPs, such as tree filters. Hence, the objective of this study was to develop and test filter materials amended with nanoparticles or polymers that are capable of simultaneously removing PAHs, metals and pathogens from stormwater runoff. For this study, red cedar (RC) wood chips and expanded shale (ES) were selected as the filter matrices. Expanded shale is a commonly used filter material in commercial tree filters, while the rot-resistance of red cedar, even under saturated conditions,²⁶ makes it a promising filter material. Here, we investigated the efficacy of TPA and AgNPs as amendments to RC and compared the contaminant removal performance to the unmodified expanded shale. The ultimate goal of this study is to offer new, multifunctional filter materials for stormwater treatment.

2. Methods

2.1 Materials

Untreated red cedar wood was obtained locally (Liberty Cedar, West Kingston, RI). The wood was chipped, and the fraction of RC chips retained between 10 and 3.3 mm sieves was used for the experiments. This sieve size was chosen to avoid fines and larger wood chips as the former can reduce hydraulic conductivity and the latter could induce preferential flow paths. Expanded shale (ES; trade name Norlite), sorted between 13 and 19 mm (the size of ES used in tree filters), was obtained from Read Custom Soils (Hanover, MA). Both materials were washed and soaked in deionized water for a minimum of 2 weeks to leach out soluble matter. A 5% solution of 3-(trihydroxysilyl)propyldimethyloctadecyl ammonium chloride solution (TPA) (EPA product Reg. No. 83019-2) was obtained from Biosafe (Pittsburgh, PA). AgNPs were synthesized via Tollens method as described elsewhere,²⁷ using polyvinylpyrrolidone (PVP, average molecular weight 29,000 g/mol, Sigma-Aldrich) as a stabilizer.

Two common stormwater PAH compounds, acenaphthene and fluorene (purity grade of 98% or higher) were obtained from Sigma-Aldrich. The PAH solutions were prepared as described elsewhere.²¹ PAH standards and deuterated PAH standards were obtained from Ultra Scientific, U.S.A. Metal reference standards containing 1000 mg/L \pm 1% certified cadmium, copper, lead, nickel, and zinc were obtained from Fisher Chemical. Sodium sulfate (Na₂SO₄), disodium phosphate (Na₂HPO₄), and sodium nitrate (NaNO₃) were obtained from Sigma-Aldrich. A nonpathogenic wild strain of *Escherichia coli* (*E. coli*) was obtained from IDEXX laboratories.

2.2 Material Characterization

The hydrodynamic sizes of the AgNPs were measured with dynamic light scattering (DLS) using a Zetasizer (Nano ZS, ZEN 3600, Malvern) at 25 °C in 1.3 mmol/L ionic strength medium. The surface area of the sorbents was measured using a multipoint BET method (Quantachrome NOWA 2200) with N₂ as the sorbate. The hydrophobicity of the materials was determined by measuring the contact angle of water to modified red cedar using a contact angle goniometer (Rame-Hart)

2.3 Laboratory Analysis

TPA concentrations were analyzed using Hach Method 8337 on a Hach DR 2800 spectrophotometer. Metals, along with AgNPs (measured as total silver), were analyzed using a PerkinElmer inductively coupled plasma optical emission spectrometer (ICP-OES) 3100 XL. The fractions of silver nanoparticles and Ag ions were measured by filtering the samples through Amicon ultra-14 centrifugal filters (Millipore) at 3500 rpm for 30 min. All PAH samples were prepared according to EPA method 610 and analyzed using a gas chromatograph coupled with a mass spectrometer (Shimadzu GC-MS QP2010). PAH samples were spiked with acenaphthene-d10 to quantify the extraction efficiency. E. coli concentrations were determined using membrane filtration, applying m-FC broth with Rosolic acid (Millipore) and incubating the samples at 44.5 °C for 24 h. To enumerate E. coli sorbed onto the solid phase, samples were sonicated (QSonica, Q125) twice for 10 min at 20% amplitude in a phosphate buffer solution. The liquid phase was then analyzed by the aforementioned method.

2.4 Experimental Methodology

The laboratory experiments were divided into two phases. During the first phase, the loading capacity and stability of TPA and AgNP amendments on RC and ES were tested. This was achieved through batch sorption isotherms (loading capacity) followed by sequential desorption for a week (stability). In the second phase, building on the isotherm results obtained during the first phase, RC was modified with different TPA and AgNP loadings and evaluated in batch experiments for sorption capacity of PAHs and heavy metals and also *E. coli* disinfection performance.

2.4.1 Phase I: Nanoparticle and Polymer Loading Capacity of Sorbents

Batch isotherms were carried out in triplicates to determine the loading capacity of TPA and AgNPs onto the sorbent materials. For all experiments, a 1.3 mmol/L ionic strength medium using sodium chloride (NaCl) was used as a background solution in order to mimic surface water conditions in Rhode Island.²⁷ Detailed experimental procedures are in Text S1 of the Supporting Information. After conducting the sorption experiment, the samples were decanted and dried at 60 °C. Desorption of TPA and AgNPs from modified sorbent materials was determined through sequential desorption in DI water for a minimum of 24 h and up to 168 h, i.e., until aqueous concentrations were below the method detection limit of 0.2 mg/L for TPA and 0.01 mg/L for Ag. The method detection limit for Ag is below EPA MCL of 0.1 mg/L, while for TPA, no EPA MCL limit is defined. TPA is categorized as slightly toxic with oral LD₅₀ above 5000 mg/L. The results from the desorption experiment were reported as total silver and TPA, respectively. The fractions of desorbed AgNPs and Ag ions are also measured and reported in Table S2 of the Supporting Information.

2.4.2 Phase II: Organic and Inorganic Contaminant Removal Efficiency of Modified Sorbents

Using the results obtained in phase I, RC was modified at different loadings of TPA and AgNPs (Table 1) to assess the ability to remove organic, inorganic, and microbiological contaminants as a function of loading. This process was required to adapt the lab-scale amending procedure to a large scale due to the large amount of the material required to perform all tests; details of this procedure are presented in Text S2 of the Supporting Information. Due to disintegration of ES when agitated for modification, this material was no longer tested. However, unmodified ES was used as baseline comparison for modified RC.

Batch tests were carried out to determine the sorption capacity of the modified and unmodified sorbent materials for PAHs and heavy metals. A synthetic stormwater runoff stock solution, containing PAHs, metals, and inorganic salts, was prepared (Table S3, Supporting Information). All solutions were adjusted to a pH of 5.5. Details of the batch tests are described in Text S3 of the Supporting Information. Visual MINTEQ Ver.3.0, an equilibrium speciation software, was used to determine the speciation of metals in the synthetic runoff.

Microbiological Contaminant Removal Efficiency by Modified Sorbents

Two of the modified RC sorbents (6 mg/g TPA-RC and 0.6 mg/g AgNP-RC) along with unmodified RC and ES were selected to test bacteria deactivation efficiency. Five different initial *E. coli* concentrations relevant to stormwater runoff, ranging from 10^2 – 10^6 CFU/100 mL, were used in the experiments.^{6, 7} Detailed experimental procedures are provided in Text S4 of the Supporting.

2.5 Cost Analysis and Limitations

The cost for the preparation of modified red cedar was calculated based on material costs incurred from lab-scale modifications. The total initial cost calculation for incorporating modified red cedar in a full-scale tree filter BMP system was based on a 5 cm thick layer of modified RC for a tree box filter with dimensions of 1.22 m × 1.83 m and a drainage area of 0.5 acre.

3. Results and Discussion

3.1 Material Characterization

The average hydrodynamic size of the AgNPs was 38.5 ± 3.5 nm. The surface area of the modified RC increased with increased loading of AgNPs and TPA, for example, the surface area increased from 4.89 ± 0.092 m²/g for UM-RC to 7.98 ± 0.42 m²/g and 6.01 ± 0.23 m²/g for 9TPA-RC and 0.6AgNP-RC. The contact angle of water for modified RC increased with loading of TPA and AgNPs (Table S4, Supporting Information). The contact angle was greater than 90° for 9TPA-RC and was greater than 70° for 6TPA-RC and 0.6AgNP-RC, indicating that modification with TPA and AgNPs made the material more hydrophobic.

3.2 Phase I: Nanoparticle and Polymer Loading Capacity of Sorbents

The TPA batch sorption on RC showed that between 37% and 98% of the initial mass of TPA in the aqueous phase was sorbed to the RC, with a maximum loading of 0.93 ± 0.03 mg/g. For expanded shale (ES), the total mass of TPA sorbed was in the range of 30% to 75%, with a maximum loading of 0.30 ± 0.03 mg/g. During the sequential desorption study, only $0.54 \pm 0.30\%$ of the TPA initial mass sorbed was released from RC, while for ES, it was $1.13 \pm 0.60\%$.

The higher sorption of TPA to RC is likely due to stronger interaction with the wood's molecules, such as lignin and cellulose.²⁸ The nonlinear shape of the sorption isotherm model (Figure 3-S1a, Supporting Information) supports that TPA predominantly sorbs onto RC rather than diffusing into it, which would have been by linear sorption isotherm, indicative of Fickian transport processes. In comparison, ES contains little or no organic matter due to the extreme heating during expansion process.²⁹ This likely resulted in fewer sorption sites for TPA. The linearity of the ES isotherm (Figure 3-S1a, Supporting Information) indicates that TPA may be partitioning into porous spaces in the shale.

The amount of AgNPs sorption to RC depended on the initial concentration of the AgNP solution. That is, RC sorbed up to 97% when the initial concentrations of AgNPs were below 21 mg/L.

However, the AgNPs sorption to RC decreased to 75% and 10% when initial concentrations were at 52 and 104 mg/L, respectively. Maximum loading of AgNPs to RC was 0.63 ± 0.10 mg/g.

Independent of the initial solution concentration, ES sorbed 96% to 99% of the initial mass of AgNPs with a maximum loading of 0.40 ± 0.02 mg/g. In the case of AgNPs, desorption was variable for RC and depended on the AgNP mass sorbed to the sorbent. That is, $2.50 \pm 2.94\%$ were desorbed if the AgNP loading was low (0.33 mg/g) and $14.4 \pm 9.28\%$ if the loading was high (0.63 mg/g) (Figure 3-1b). Depending on the initial aqueous phase concentration of AgNPs, between 88% and 98% of the mass desorbed is in the form AgNPs, while the remainder is in form of Ag ions (Table 3-S2, Supporting Information). For ES, desorption of AgNP was $<0.01\%$ relative to the initial mass of AgNPs sorbed, regardless of the initial aqueous phase AgNP concentration or mass sorbed (Figure 1b). The fraction of AgNPs and Ag ions desorbed from ES were below method detection limit. The uptake of AgNPs can be due to trapping of AgNPs in the pores of the sorbent material and sorption due to van der Waal forces of attraction between AgNPs and the sorbents.

At concentrations below 52 mg/L, the hydrodynamic size of AgNPs is ≤ 40 nm, whereas at higher concentrations (104 mg/L), the average hydrodynamic size of the AgNPs increased to >80 nm due to aggregation. This phenomenon was confirmed by TEM imaging (Figure 3-S2, Supporting Information). The larger size could have hindered the sorption of AgNPs to the micropores in wood chips, whereas it did not reduce the uptake by ES due to the large pores present in expanded shale.²⁹

3.3 Phase II: Organic and Inorganic Contaminant Removal Efficiency of Modified Sorbents

The results of the batch isotherm experiments for PAHs and heavy metals onto unmodified ES as well as unmodified and modified RC are nonlinear (Figure 3-2). Assuming that the number of sorption sites is limited, the results were fitted to the Langmuir model

$$q = \frac{Qb c_e}{(1+bc_e)} \quad \text{Equation 1}$$

where q is the amount of solute sorbed ($\mu\text{g/g}$), Q is the Langmuir maximum amount of solute that can be absorbed by the sorbent ($\mu\text{g/g}$), b is the Langmuir adsorption coefficient, and C_e is the equilibrium aqueous solute concentration ($\mu\text{g/L}$). The results from batch experiments show that during the experimental conditions RC and ES had reached saturation indicating a limited number of sorption sites (Figure 3-S3, Supporting Information), thus confirming the appropriateness of the Langmuir type isotherm model. In order to compare the performance of all the materials, the Langmuir type model was applied to all data sets. The isotherm parameters for PAHs and metals for all sorbents were obtained using SigmaPlot 11 (Systat Software, Inc.) (Table 3-2). Except for ES, the goodness-of-fit using the Langmuir model was high ($R^2 > 0.90$) for all isotherms.

Polycyclic Aromatic Hydrocarbons

The Langmuir maximum sorption capacity of PAH for ES is much lower compared to both unmodified and modified RC (Table 3-2), which may be a result of the vitrification process the expanded shale has undergone during thermal expansion, making it more inert by removing potential organic sorption sites.²⁹ In the case of RC, the value of Q for acenaphthene and fluorene increased with increased loadings of TPA and AgNPs (Figure 3-2). For example, for acenaphthene, Q increased from $48.6 \mu\text{g/g}$ for UM-RC to $1703.5 \mu\text{g/g}$ for 9TPA-RC and to $1429.2 \mu\text{g/g}$ for 0.6AgNP-RC (Table 3-2).

Finally, the modification with TPA and AgNPs increased the hydrophobicity of the RC as confirmed by contact angle measurements (Table 3-S4, Supporting Information). While the

C18chain of the TPA molecule is enhancing the hydrophobicity of RC, in the case of AgNP-RC, it is the PVP coating on AgNPs. The increase in surface hydrophobicity of RC resulted in an increase in PAH sorption after the amendment of RC with both AgNPs and TPA. This is due to the hydrophobic interactions between PAH and modified RC. In addition, PAHs can also partition onto the organic phase created by TPA and PVP on modified RC.

Heavy Metals

The results obtained from the Visual MINTEQ model show that at pH 5.5 the metal speciation in the synthetic stormwater is dominated (73.5% to 87.6%) by the divalent cations (Pb^{2+} , Cd^{2+} , Zn^{2+} , Ni^{2+} , and Cu^{2+}) and otherwise consists of predominantly sulfate salts of, e.g., $PbSO_4$ (Table 3-S6, Supporting Information). The percentage of metals available for sorption was taken into account for batch isotherm calculations, and the Langmuir isotherm model was used for quantitative comparison of the sorption capacity between the unmodified and modified materials. Of all sorbents tested, the unmodified ES exhibited the lowest Q for all metals (Table 3-2). In the case of RC, Q for Pb increased from 85.14 $\mu g/g$ for unmodified RC to 625 $\mu g/g$ for 9TPA-RC and 153.8 $\mu g/g$ for 0.6AgNP-RC (Table 3-2). For Cu, the TPA and AgNP amendments enhanced the sorption of Cu compared to unmodified RC. However, no correlation could be identified between amendment loading and Cu sorption (Table 3-2). The modification of RC with TPA and AgNPs did not have an impact on Q for Cd and slightly decreased in the case of Zn and Ni (Table 3-2).

The enhanced maximum sorption capacity Q of modified RC for Pb and Cu, as well as the unchanged Q for Cd, indicates that modification of RC is not limiting the retention of these metals and in fact increases it. The hydroxyl groups present in the TPA molecule provides attractive sorption sites for metals, whereas the oxygen and nitrogen present in PVP can form metal complexes.³⁰ The increase in Pb and Cu sorption could be due to bonding with hydroxyl groups on TPA and formation of complexes with PVP present on AgNPs. In addition, the

increase in surface area of modified RC (Table 3-S4, Supporting Information) likely provided more sorption sites for these metals. However, the reasons for the slight decrease in Q for Zn and Ni (Table 3-2) is unclear. No correlations with physiochemical properties or interactions with the amendments were found to explain the different sorption behavior of these metals to modified RC. Therefore, further studies are required to gain insight on the sorption behavior of these metals onto modified RC.

Microbiological Contaminant Removal Efficiency of Modified Sorbents

Two modified sorbents (6TPA-RC and 0.6AgNP-RC) were tested for bacteria deactivation efficiency and were compared to unmodified RC and ES. The disinfection performance of the materials was calculated as log removal value (LRV)

$$\text{LRV} = \log (\text{initial } E. \text{ coli concentration}) - \log (\text{final } E. \text{ coli concentration}) \quad \text{Equation 2}$$

Final *E. coli* concentration is the total *E. coli* in aqueous phase and sorbed to the sorbents. The average LRV for the unmodified RC and ES was always below 1 (Figure 3-3). For the modified materials, the average LRV values ranged from 1.74 ± 1.04 log to 2.90 ± 0.50 log for 6TPA-RC. In the case of 0.6AgNP-RC, the average LRV value ranged from 2.03 ± 0.60 log to 2.10 ± 0.90 log. Overall, the deactivation performance shows that the modified materials are significantly more effective at deactivating bacteria compared to unmodified ES and RC ($p < 0.001$) (Figure 3-3). Previous studies showed that the impregnation of TPA and AgNPs onto surfaces enhanced the deactivation of *E. coli*.²² Several mechanisms have been suggested for disinfection using AgNPs. These include damage to bacteria by pitting the cell membrane, lysis of cells caused by silver ion release, or damage of the cell by the reactive oxygen species formed on the surface of the AgNPs. The biotoxicity of TPA has been explained mainly by the positively charged quaternary amine groups attracting *E. coli* and C18 groups the piercing membrane and causing cell disruption³¹

3.4 Cost Analysis and Limitations

The contaminant removal performance and bacterial deactivation of both TPA- and AgNP-modified RC compare well and significantly enhanced water quality compared to unmodified RC. However, the selection of which antimicrobial agent to use for modification will be driven by the costs of amending the materials. The initial modification cost for RC using AgNPs is higher compared to TPA (Table 3-S7, Supporting Information). For instance, to modify 1 kg of RC at loading of 6 mg/g of TPA and 0.6 mg/g of AgNP, as both of these materials have similar treatment capability regarding PAHs, heavy metals, and *E. coli* modification costs \$57.90/kg versus \$10.30/kg for TPA (Table 3-S7, Supporting Information). When installing these amendments in a field-scale BMP, such as a tree filter, less than 8% of the total initial cost incurred was for the TPA amendment compared to a 35% increase for AgNP. The toxicological data as determined by previous studies also suggests that TPA is less toxic compared to AgNPs (Table 3-S8, Supporting Information). Further, the antimicrobial performance of AgNPs primarily depends on silver ion release. Over time, the silver ion release from AgNPs may decrease and thus could result in the reduction of antimicrobial efficiency. Overall, TPA has a cost advantage over AgNPs in addition to lower toxicity and better contaminant removal performance. The long-term performance of TPA is currently unknown and requires further studies. These need to include investigations of TPA behavior at different water chemistry conditions.

In summary, this study reveals that conventional materials such as unmodified expanded shale and red cedar have very limited pathogen treatment capabilities. However, RC amended with TPA and AgNPs both increased antimicrobial properties by orders of magnitude. The amendments also enhanced PAH sorption while not hindering the sorption of most metals. These findings show that modified sorbent materials can enhance the stormwater treatment efficiency of BMP filters. The high cost involved in amending the sorbent with AgNPs and the higher toxicity

may prevent the use of AgNP-modified materials in BMPs. Conversely, TPA-modified RC has the advantage of lower cost, lower toxicity, and higher contaminant and pathogen removal performance, making it the overall better choice as a filter medium for use in BMPs, such as tree filters. However, the long-term performance and effectiveness of TPA-modified RC under natural environmental conditions has yet to be studied.

Table 3-1: Amendment loadings achieved by exposing red cedar to aqueous solutions of either TPA or AgNPs.

Bioactive agent	Concentrations (mg/l)	Amendments (Abbreviation)
TPA	26	3.6 mg/g TPA Red Cedar (3TPA-RC)
	72	6.7 mg/g TPA Red Cedar (6TPA-RC)
	150	*9.3 mg/g TPA Red Cedar (9TPA-RC)
AgNP	20.8	0.33 mg/g AgNP Red Cedar (0.3AgNP-RC)
	52	*0.68 mg/g AgNP Red Cedar (0.6AgNP-RC)

*Maximum possible loading.

Table 3-2: Langmuir maximum sorption capacity (Q) for PAHs and metals for all sorbents. Both, Langmuir adsorption coefficients (b) and goodness-of-fit values (R²) are provided in the supplementary information.

		ES	Unmodified-RC	3TPA-RC	6TPA-RC	9TPA-RC	0.3AgNP-RC	0.6AgNP-RC
Acenaphthene	Q (µg/g)	20.3	48.6	114.6	133.7	1703.5	282.7	1429.2
Fluorene	Q (µg/g)	10.2	26.1	43.9	83.8	391.1	87.7	380.0
Lead	Q (µg/g)	33	85.14	193.3	352.6	625.1	148.4	153.8
Cadmium	Q (µg/g)	60.3	13.0	13.7	11.8	14.2	13.8	15.1
Copper	Q (µg/g)	18.7	62.3	173.4	81.8	93.2	127.1	97.06
Zinc	Q (µg/g)	31.7	124.9	95.6	84.1	95.7	106.7	45.8
Nickel	Q (µg/g)	11.6	35.3	13.25	15.8	20.36	14.23	9.2

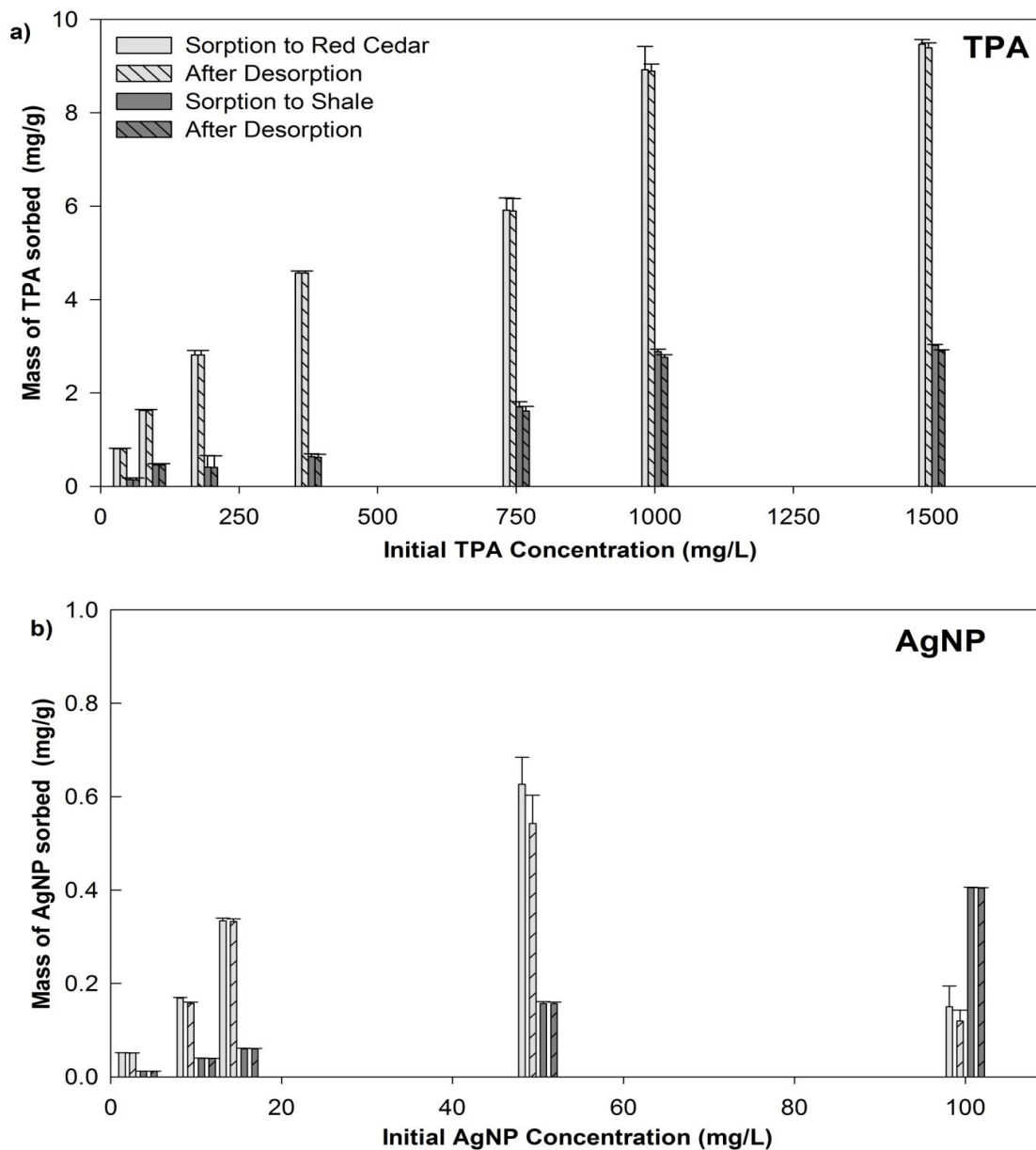


Figure 3-1: Polymer and nanoparticle loading capacity of sorbents. Mass sorbed during sorption experiments and mass retained after desorption for (a) TPA and (b) AgNPs on red cedar (RC) and expanded shale (ES). The data suggests that once amended, the active compounds remain largely fixed on the substrate.

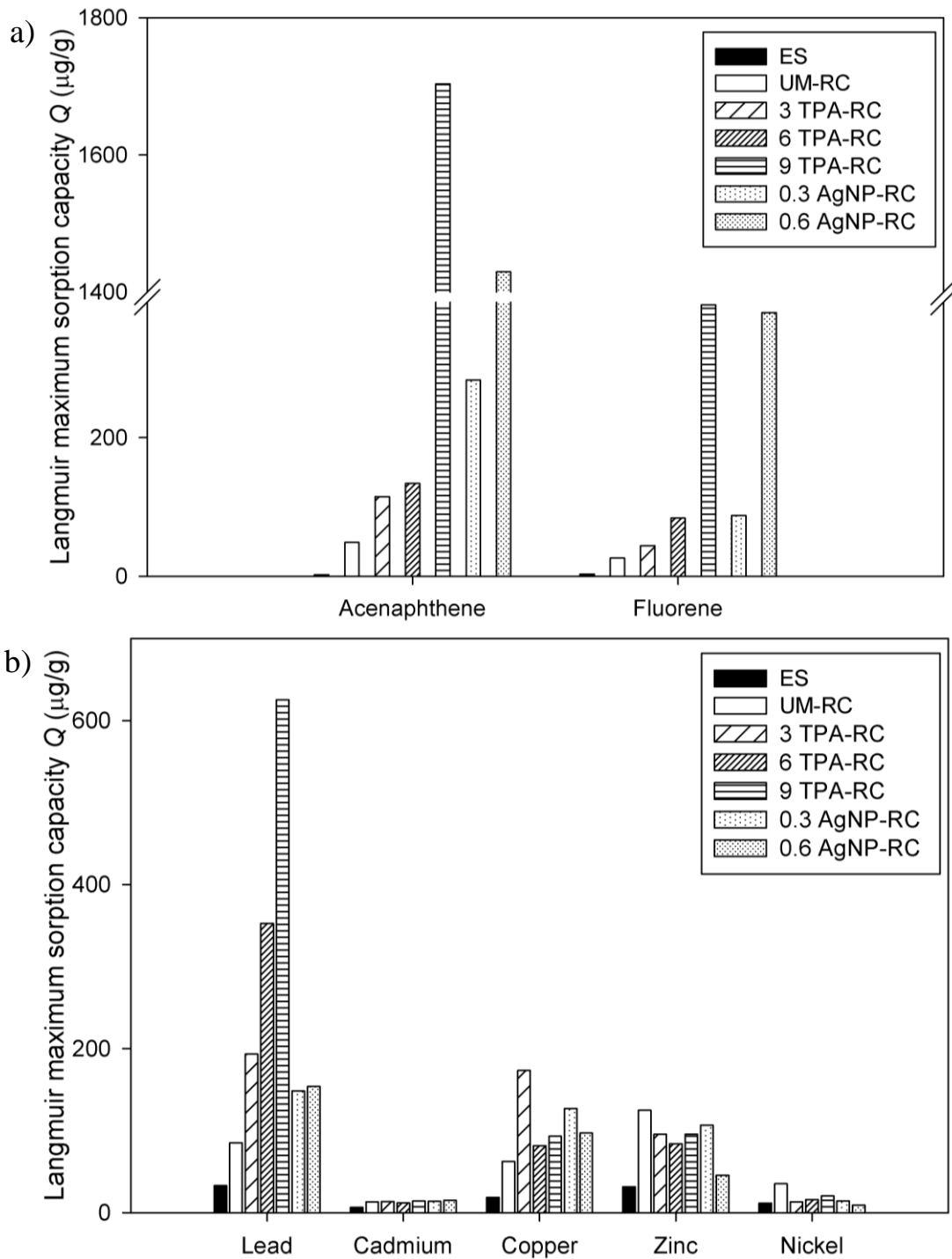


Figure 3-2: Langmuir maximum sorption coefficient Q of a) PAHs and b) heavy metals for expanded shale (ES), unmodified red cedar (UM-RC) and RC modified with TPA and AgNPs.

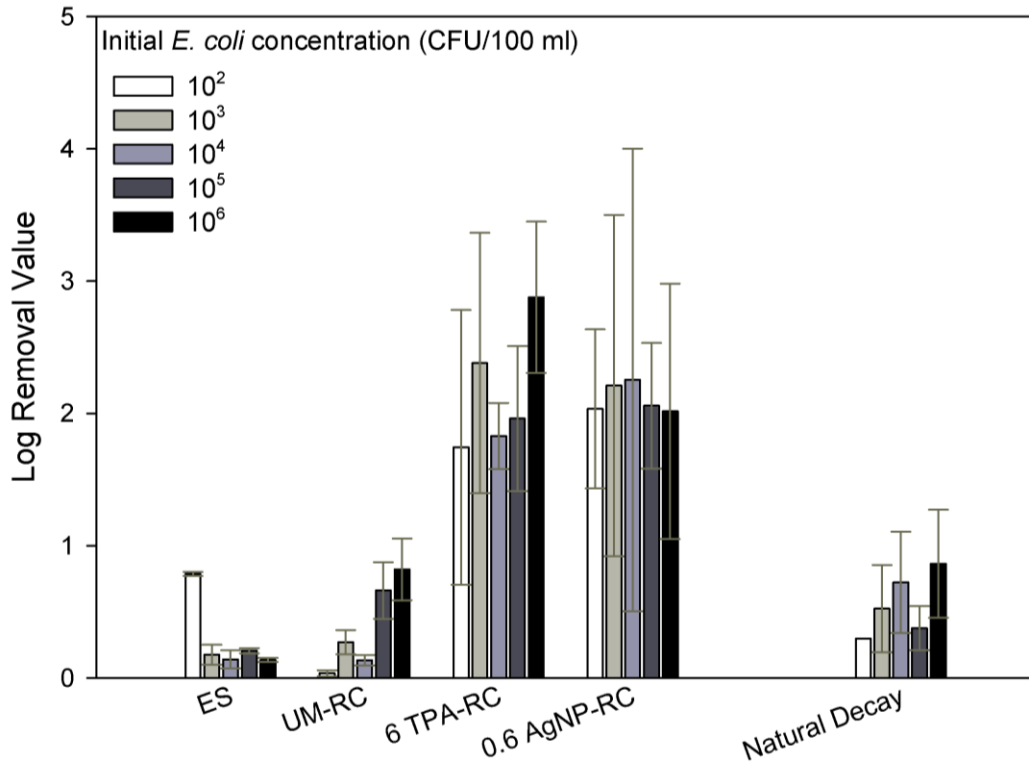


Figure 3-3: Deactivation of *E. coli* at increasing concentrations using unmodified and modified materials (6 TPA-RC, and 0.6Ag-RC). Both the 6 TPA-RC and 0.6Ag-RC were significantly more effective at deactivating *E. coli* compared to the unmodified materials ($p < 0.001$). The data presented is an average of nine samples. Individual significant differences between the materials are indicated by the letters a and b in the figure.

References

- 1) Ahn, J. H.; Grant, S. B.; Surbeck, C. Q.; DiGiacomo, P. M.; Nezlin, N. P.; Jiang, S. Coastal water quality impact of stormwater runoff from an urban watershed in southern California. *Environ. Sci. Technol.* 2005, 39, 5940-5953.
- 2) Brown, J. N.; Peake, B. M. Sources of heavy metals and polycyclic aromatic hydrocarbons in urban stormwater runoff. *Sci. Total Environ.* 2006, 359, 145-155.
- 3) Göbel, P.; Dierkes, C.; Coldewey, W. G. Storm water runoff concentration matrix for urban areas. *J. Contam. Hydrol.* 2007, 91, 26-42.
- 4) McLellan, S.; Salmore, A. Evidence for localized bacterial loading as the cause of chronic beach closings in a freshwater marina. *Water Res.* 2003, 37, 2700-2708.
- 5) Dorfman, M.; Rosselot, K. *Testing the Water: A Guide to Water Quality at Vacation Beaches.* Natural Resources Defense Council 2012, 22.
- 6) Schueler, T. R.; Holland, H. Microbes and urban watersheds: concentrations, sources, and pathways. *The Practice of Watershed Protection* 2000, 74-84.
- 7) Parker, J.; McIntyre, D.; Noble, R. Characterizing fecal contamination in stormwater runoff in coastal North Carolina, USA. *Water Res.* 2010, 44, 4186-4194.
- 8) Mallin, M. A.; Williams, K. E.; Esham, E. C.; Lowe, R. P. Effect of human development on bacteriological water quality in coastal watersheds. *Ecol. Appl.* 2000, 10, 1047-1056.
- 9) Stewart, J. R.; Gast, R. J.; Fujioka, R. S.; Solo-Gabriele, H. M.; Meschke, J. S.; Amaral-Zettler, L. A.; del Castillo, E.; Polz, M. F.; Collier, T. K.; Strom, M. S. The coastal environment and human health: microbial indicators, pathogens, sentinels and reservoirs. *Environ. Health* 2008, 7, S3.
- 10) Boving, T. B.; Zhang, W. Removal of aqueous-phase polynuclear aromatic hydrocarbons using aspen wood fibers. *Chemosphere* 2004, 54, 831-839.
- 11) Boving, T. B.; Neary, K. Attenuation of polycyclic aromatic hydrocarbons from urban stormwater runoff by wood filters. *J. Contam. Hydrol.* 2007, 91, 43-57.
- 12) Genç-Fuhrman, H.; Mikkelsen, P. S.; Ledin, A. Simultaneous removal of As, Cd, Cr, Cu, Ni and Zn from stormwater: Experimental comparison of 11 different sorbents. *Water Res.* 2007, 41, 591-602.
- 13) UNHSC; Roseen, R.; Ballestero, T.; Houle, J. UNH Stormwater Center 2007 Annual Report. 2007.
- 14) Zhang, X.; Lulla, M. Evaluation of pathogenic indicator bacteria in structural best management practices. *Journal of Environmental Science and Health Part A* 2006, 41, 2483-2493.

- 15) Scholes, L.; Revitt, D. M.; Ellis, J. B. A systematic approach for the comparative assessment of stormwater pollutant removal potentials. *J. Environ. Manage.* 2008, 88, 467-478.
- 16) Davis, A. P.; Hunt, W. F.; Traver, R. G.; Clar, M. Bioretention technology: Overview of current practice and future needs. *J. Environ. Eng.* 2009, 135, 109-117.
- 17) Li, H.; Davis, A. P. Water quality improvement through reductions of pollutant loads using bioretention. *J. Environ. Eng.* 2009, 135, 567-576.
- 18) Celis, R.; Hermosin, M. C.; Cornejo, J. Heavy metal adsorption by functionalized clays. *Environ. Sci. Technol.* 2000, 34, 4593-4599.
- 19) Oyanedel-Craver, V. A.; Smith, J. A. Effect of quaternary ammonium cation loading and pH on heavy metal sorption to Ca bentonite and two organobentonites. *J. Hazard. Mater.* 2006, 137, 1102-1114.
- 20) Lee, S. M.; Tiwari, D. Organo and inorgano-organo-modified clays in the remediation of aqueous solutions: An overview. *Appl. Clay. Sci.* 2012, 59, 84-102.
- 21) Kasaraneni, V.; Kohm, S. E.; Eberle, D.; Boving, T.; Oyanedel-Craver, V. Enhanced containment of polycyclic aromatic hydrocarbons through organic modification of soils. *Environmental Progress & Sustainable Energy* 2013.
- 22) Zhang, H.; Oyanedel-Craver, V. Comparison of the bacterial removal performance of silver nanoparticles and a polymer based quaternary amine functionalized silsesquioxane coated point-of-use ceramic water filters. *J. Hazard. Mater.* 2013.
- 23) Oosterhof, J. J.; Buijssen, K. J.; Busscher, H. J.; van der Laan, Bernard FAM; van der Mei, Henny C Effects of quaternary ammonium silane coatings on mixed fungal and bacterial biofilms on tracheoesophageal shunt prostheses. *Appl. Environ. Microbiol.* 2006, 72, 3673-3677.
- 24) Dankovich, T. A.; Gray, D. G. Bactericidal paper impregnated with silver nanoparticles for point-of-use water treatment. *Environ. Sci. Technol.* 2011, 45, 1992-1998.
- 25) Rayner, J.; Zhang, H.; Lantagne, D.; Schubert, J.; Lennon, P.; Craver, V. O. Laboratory investigation into the effect of silver application on the bacterial removal efficacy of filter material for use on locally-produced ceramic water filters for household drinking water treatment. *ACS Sustainable Chemistry & Engineering* 2013.
- 26) Bilby, R. E.; Heffner, J. T.; Fransen, B. R.; Ward, J. W.; Bisson, P. A. Effects of immersion in water on deterioration of wood from five species of trees used for habitat enhancement projects. *N. Am. J. Fish. Manage.* 1999, 19, 687-695.

- 27) Zhang, H.; Smith, J. A.; Oyanedel-Craver, V. The effect of natural water conditions on the anti-bacterial performance and stability of silver nanoparticles capped with different polymers. *Water Res.* 2012, 46, 691-699.
- 28) Boving, T. B.; Rowell, R. In *Environmental Applications of Lignocellulosic Filter Materials*; Rowell, R., Ed.; Sustainable Development in the Forest Products Industry; UFP Editions: Lisbon, Portugal, 2010.
- 29) Forbes, M. G.; Dickson, K. R.; Golden, T. D.; Hudak, P.; Doyle, R. D. Dissolved phosphorus retention of light-weight expanded shale and masonry sand used in subsurface flow treatment wetlands. *Environ. Sci. Technol.* 2004, 38, 892-898.
- 30) Tokman, N.; Akman, S.; Ozeroglu, C. Determination of lead, copper and manganese by graphite furnace atomic absorption spectrometry after separation/concentration using a water-soluble polymer *Talanta* 2004, 63, 699-703.
- 31) Kim, H. W.; Kim, B. R.; Rhee, Y. H. Imparting durable antimicrobial properties to cotton fabrics using alginate–quaternary ammonium complex nanoparticles. *Carbohydr. Polym.* 2010, 79, 1057-1062.

Supporting Information

Enhancement of Surface Runoff Quality Using Modified Sorbents

¹Kasaraneni, Varun K; ²Schifman, Laura A.; ^{1,2}Boving, Thomas B; ¹Oyanedel-Craver, Vinka

Is published in ACS Sustainable Chemistry & Engineering

¹Department of Civil and Environmental Engineering, University of Rhode Island, 1 Lippitt Rd,
Kingston, RI USA 02881

²Department of Geosciences, University of Rhode Island, 9 E. Alumni Ave, Kingston, RI USA
02881.

Text 3-S1: Nanomaterials loading capacity on sorbents

The loading capacity of nanomaterials and polymers on sorbent materials was determined using batch tests. A 1.3 mmol/L ionic strength solution was used to mimic surface water conditions in Rhode Island¹. Water saturated sorbent materials were weighed out in triplicates (1.89 ± 0.43 g for RC, 6.92 ± 0.72 g for ES) in 50 ml polyethylene tubes and combined with TPA or AgNP solutions with concentrations ranging from 93 to 1500 mg/L for TPA and 1.6 mg/L to 105 mg/L for AgNPs. In addition, tubes containing only TPA and AgNP solutions were prepared for quality control and quality assurance. All samples were placed in a rotisserie incubator at 5 rpm and 25 °C until equilibrium was reached. Kinetic studies were performed to determine equilibrium times (Table 3-S1) between sorbent and sorbate for all compounds of interest.

Text 3-S2: Nanoparticle and polymer loading capacity of sorbents

RC was amended by exposing them to TPA or AgNP solutions at previously determined concentrations established through the above mentioned isotherm studies. The concentrations used, and loadings achieved are listed in Table 3-1. Based on previously carried out isotherm studies (described in “Batch Scale for Modification” in the main text), the materials were allowed to equilibrate for 6 days on a shaker table set at 100 rpm at 25 °C. After each material amendment, the dried material was submerged in frequently exchanged deionized water and the aqueous concentration of the TPA or AgNP was measured until desorption ceased or the concentrations were below the detection limit of the instruments (0.2 mg/L for TPA and 0.1 µg/L for Ag). The difference between initial mass sorbed and mass desorbed was taken into consideration for the final loading of antimicrobial onto RC. Attempts were made to amend ES with TPA and AgNPs; however, due to disintegration of ES when agitated on a shaker table or roller mill, it was concluded that this material cannot feasibly be modified on a larger scale. Instead, unmodified ES was used a baseline for comparison with modified RC.

Text 3-S3: Organic and inorganic contaminant removal efficiency of the modified sorbents

The sorption capacity of modified and unmodified sorbent materials for PAHs and heavy metals were determined through batch tests. A synthetic stormwater runoff stock solution, containing PAHs, metals, and inorganic salts was prepared (Table 3-S2). Acenaphthene and Fluorene were chosen as representative PAHs due to their high solubility and consistent presence in stormwater runoff 4, while cadmium, copper, lead, nickel, and zinc were chosen as representative heavy metals due to the high concentrations found in runoff ^{5,6}. To prevent heavy metal precipitation the pH of the solution was adjusted to 5.5 using sodium hydroxide. The study was conducted by combining water saturated sorbent material (1.52 ± 0.052 g for RC and 3.50 ± 0.076 g for ES) with the synthetic runoff solution into 40 ml amber glass tubes with Teflon (PTFE) lined caps. Dilutions over three orders of magnitude were prepared. Triplicates and appropriate controls were set for QC/QA. All samples were placed in a rotisserie incubator at five rpm and 25 °C for six days, as determined by kinetic study to determine equilibrium time (data not shown). Visual MINTEQ Ver.3.0 an equilibrium speciation model was used to determine the speciation of metals in the synthetic runoff.

Text 3-S4: Microbiological contaminant removal efficiency of the modified sorbents

The water saturated sorbent materials were weighed (1.59 ± 0.181 g for RC and 3.48 ± 0.059 g for unmodified ES) and exposed to E. coli prepared in 1.3 mmol/l ionic strength solution 1 for three hours at 25 °C and five rpm in a rotisserie incubator. The three hour exposure time was based on a kinetic study where a ~50% reduction of E. coli was observed within that time when exposed to RC and ES at 25 °C (data not shown). Five different initial E. coli concentrations relevant to stormwater runoff, ranging from 10^2 - 10^6 CFU/100ml were used in the experiments^{7,8}. In addition, controls containing only sorbent material with background sodium chloride solution and bacteria solutions without any sorbent were prepared to establish natural decay of bacteria

over the three hour time period. These experiments were performed in triplicates and repeated three times.

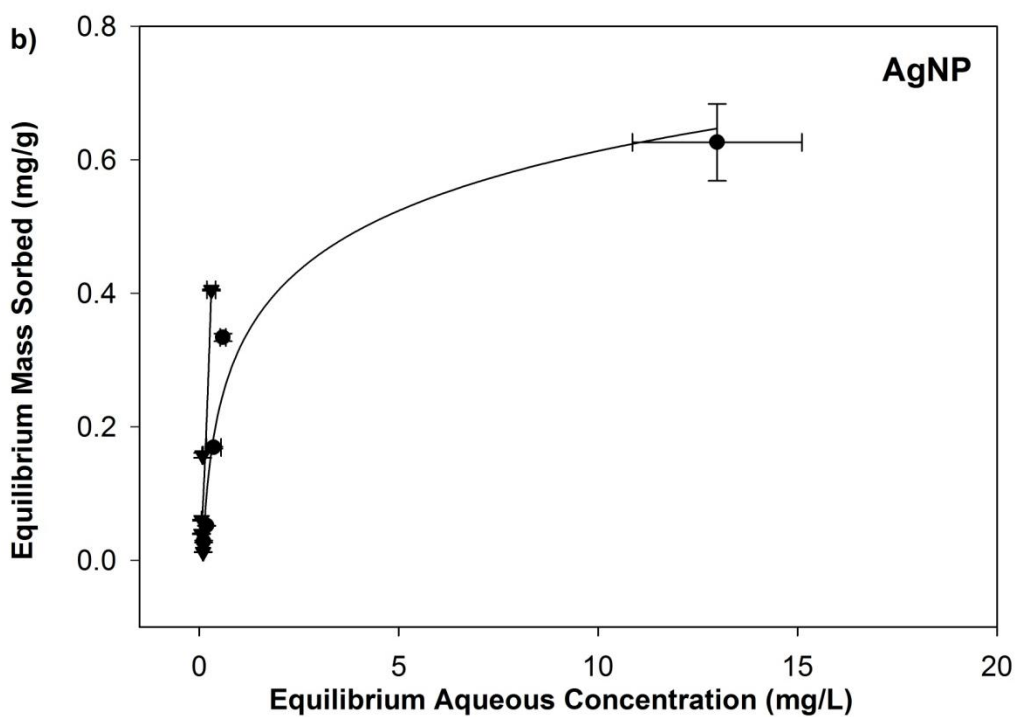
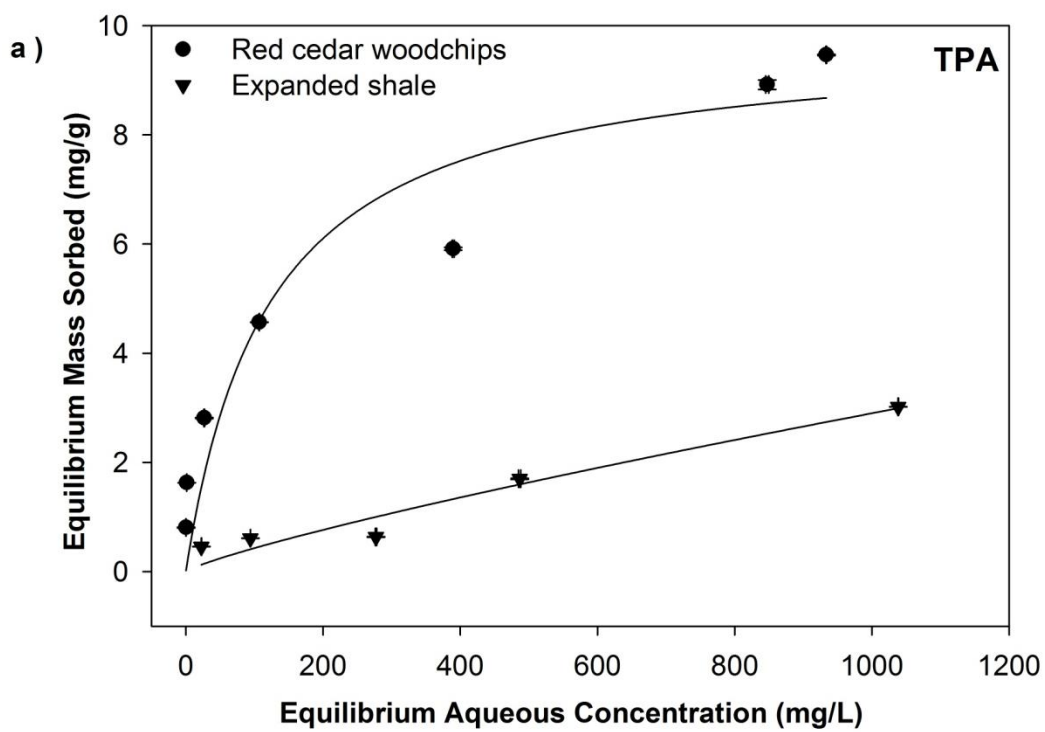


Figure 3-S1: Sorption isotherm for red cedar and expanded shale for a) TPA and b) AgNP

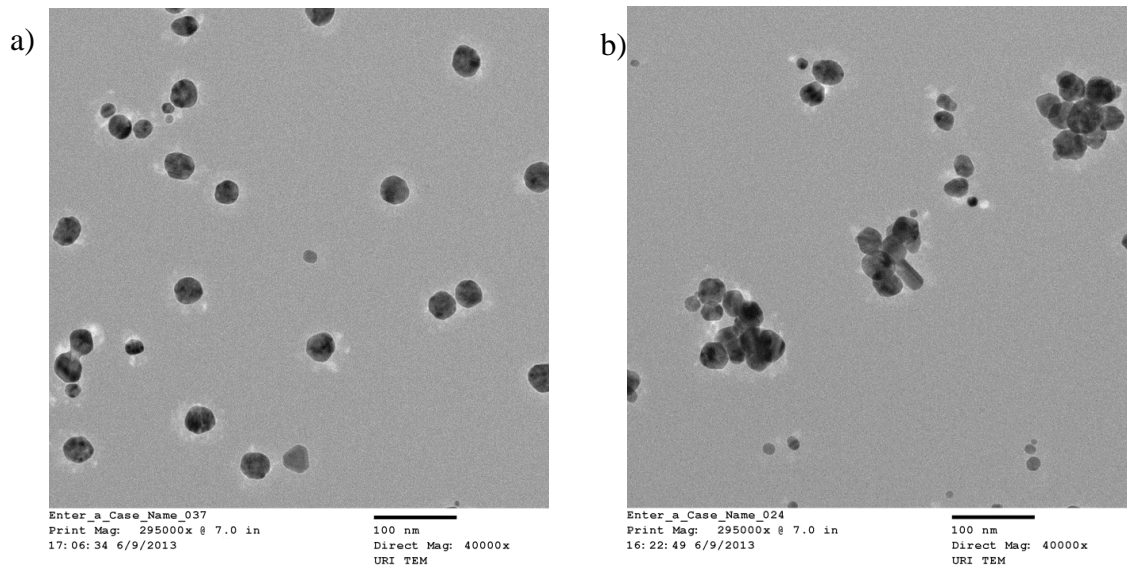


Figure 3-S2: TEM image of AgNPs at a) 10mg/l and b) 104 mg/l concentration. The images show that AgNPs increase in size at higher concentrations due to aggregation.

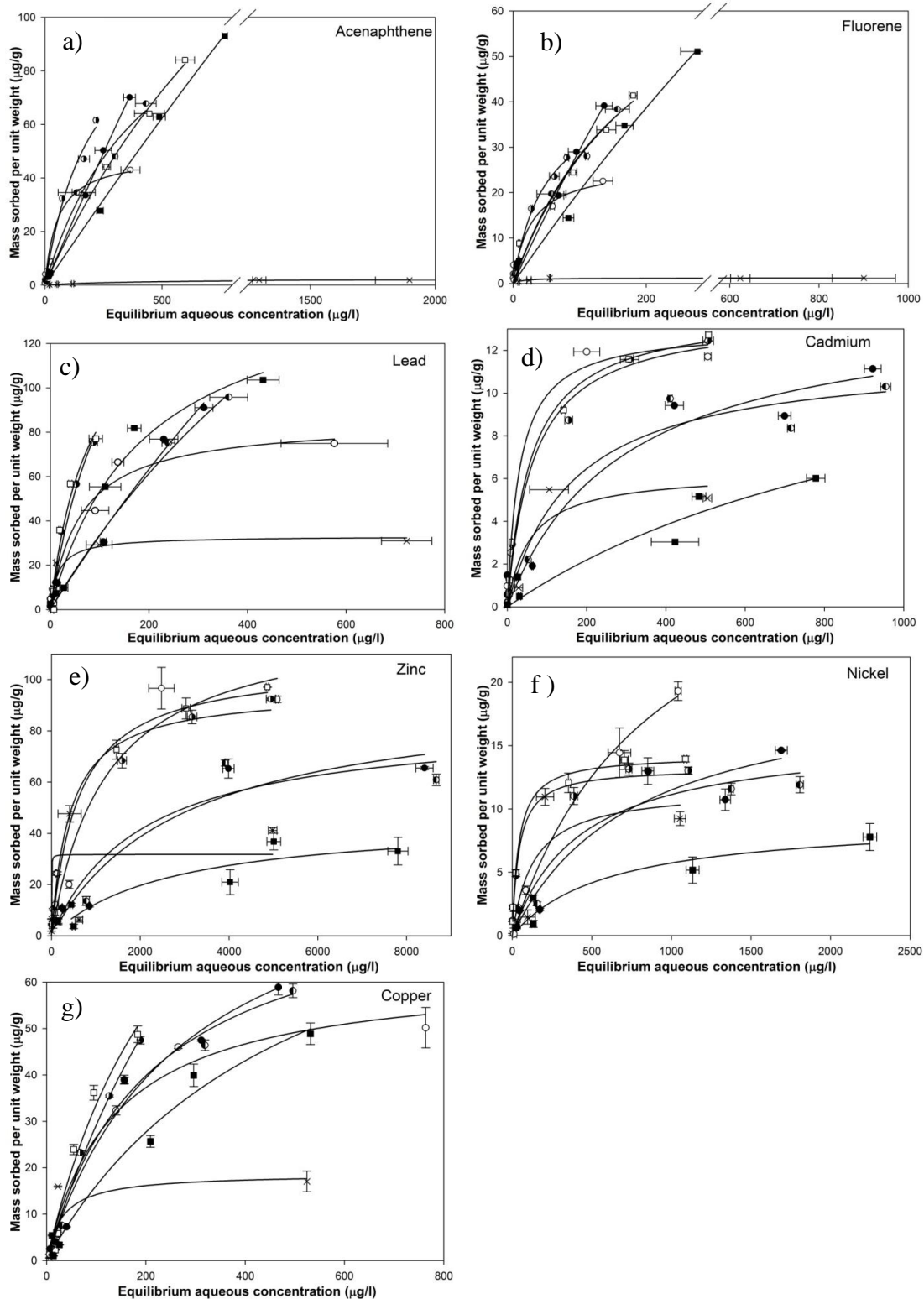


Figure 3-S3: Batch Isotherm results of a) Acenaphthene, b) Fluorene, c) Lead, d) Cadmium, e) Zinc, f) Nickel, and g) Copper for \times Expanded Shale, \circ UM-RC, \bullet 3 TPA-RC \blacklozenge 6 TPA-RC, \star 9 TPA-RC, \square 0.3 AgNP-RC, \blacksquare 0.6 AgNP-RC fitted using the Langmuir model.

Table 3-S1: Equilibrium times of batch isotherms for TPA and AgNPs modifications of red cedar and shale.

Material	Equilibrium Time (Days)	
	TPA	AgNPs
Red cedar	4	5
Expanded shale	4	6

Table 3-S2: Fraction of AgNPs and Ag ions desorbed during desorption study.

Initial AgNP concentration (mg/l)	Mass desorbed (mg/g)	Percentage of AgNP (%)	Percentage of Ag ion (%)
3.2	-NA-	-NA-	-NA-
10.4	0.02	-NA-	-NA-
20.8	0.03	88.4	11.6
52	0.132	98.2	1.8
104	0.06	98.4	1.6

-NA- : The concentrations of Ag were below detection limits.

Table 3-S3: Composition of the synthetic runoff stock solution. Five dilutions were prepared from this solution to cover 3 orders of magnitude for each compound of interest.

Contaminant	Concentration (mg/l)
Acenaphthene	3.2
Fluorene	1.8
Lead	5.0
Cadmium	1.2
Nickel	2.5
Zinc	10.0
Copper	2.5
Nitrate	50
Sulfate	100
Phosphate	10

Table 3-S4: N₂ BET specific surface areas and contact angle measurements for all sorbent materials.

Sorbent material	Specific surface area	Contact angle
	m ² /g	°
ES	1.31±0.23	NA
UM-RC	4.89±0.092	30.45 ± 6.68
3 TPA-RC	5.64 ±0.30	52.67 ± 4.74
6 TPA-RC	5.78 ±0.26	70.30 ± 3.05
9 TPA-RC	7.98 ±0.42	106.27 ± 12.68
0.3 AgNP-RC	5.23±0.47	59.60 ± 4.44
0.6 AgNP-RC	6.01±0.23	75.28 ± 2.32

Table 3-S5: Isotherm parameters for PAHs and metals for all sorbents, b is the Langmuir adsorption coefficient (l/μg), and R2 represents the goodness of fit for the model.

		ES	UM-RC	3TPA-RC	6TPA-RC	9TPA-RC	0.3Ag-RC	0.6Ag-RC
Acenaphthene	b	0.0024	0.0180	0.0048	0.0022	0.0001	0.0007	0.0001
	R2	0.99	0.99	0.98	0.98	0.99	0.99	0.99
Fluorene	b	0.0717	0.0370	0.0200	0.0050	0.0008	0.0046	0.0006
	R2	0.88	0.95	0.99	0.99	0.99	0.97	0.98
Lead	b	0.0061	0.0160	0.0075	0.0011	0.0006	0.0126	0.0053
	R2	0.88	0.97	0.96	0.98	0.98	0.94	0.97
Cadmium	b	0.0175	0.0320	0.0152	0.0060	0.0034	0.0166	0.0009
	R2	0.86	0.98	0.99	0.94	0.95	0.99	0.91
Copper	b	0.0032	0.0074	0.0020	0.0047	0.0036	0.0036	0.0019
	R2	0.75	0.97	0.98	0.98	0.98	0.96	0.98
Zinc	b	0.0530	0.0008	0.0023	0.0005	0.0003	0.0016	0.0003
	R2	0.50	0.95	0.98	0.92	0.93	0.99	0.90
Nickel	b	0.0075	0.0011	0.024	0.00235	0.0013	0.0247	0.00166
	R2	0.72	0.99	0.99	0.93	0.93	0.99	0.90

Table 3-S6: Speciation data for metals at pH 5.5. This data was obtained using Visual MINTEQ Version 3.0.

Metal	Species	Percentage (%)
Pb	Pb+2	73.518
	PbOH+	0.352
	PbSO4 (aq)	24.474
	Pb(SO4)2-2	0.399
	PbNO3+	0.694
	PbH2PO4+	0.337
	PbHPO4 (aq)	0.225
Cd	Cd+2	84.783
	CdSO4 (aq)	13.509
	Cd(SO4)2-2	0.493
	CdNO3+	0.171
	CdHPO4 (aq)	1.044
Ni	Ni+2	87.668
	NiSO4 (aq)	11.889
	NiNO3+	0.14
	NiH2PO4+	0.107
	NiHPO4 (aq)	0.192
Zn	Zn+2	86.281
	ZnOH+	0.016
	ZnSO4 (aq)	12.83
	Zn(SO4)2-2	0.302
	ZnNO3+	0.138
	ZnHPO4 (aq)	0.433
	Cu	Cu+2
CuOH+		0.505

Metal	Species	Percentage (%)
	CuSO ₄ (aq)	13.017
	CuNO ₃ ⁺	0.169
	CuHPO ₄ (aq)	2.706

Table 3-S7: Cost of modification of red cedar wood chips using TPA and AgNPs at various loadings.

Modification	Cost per kg of red cedar (\$)
0.3 TPA-RC	2.8
0.6 TPA-RC	10.3
0.9 TPA-RC	19.8
0.3 AgNP-RC	24.4
0.6 AgNP-RC	57.9

Table 3-S8: Toxicity data of AgNPs and TPA [9-10]

	Acute oral toxicity (LD50)
AgNPs	100 mg/kg 9
TPA	> 5000 mg/kg 10

References

- 1) Zhang, H.; Smith, J. A.; Oyanedel-Craver, V. The effect of natural water conditions on the anti-bacterial performance and stability of silver nanoparticles capped with different polymers. *Water Res.* 2012, 46, 691-699.
- 2) Scholes, L.; Revitt, D. M.; Ellis, J. B. A systematic approach for the comparative assessment of stormwater pollutant removal potentials. *J. Environ. Manage.* 2008, 88, 467-478.
- 3) Kasaraneni, V.; Kohm, S. E.; Eberle, D.; Boving, T.; Oyanedel-Craver, V. Enhanced containment of polycyclic aromatic hydrocarbons through organic modification of soils. *Environmental Progress & Sustainable Energy* 2013.
- 4) Boving, T. B.; Neary, K. Attenuation of polycyclic aromatic hydrocarbons from urban stormwater runoff by wood filters. *J. Contam. Hydrol.* 2007, 91, 43-57.
- 5) Göbel, P.; Dierkes, C.; Coldewey, W. G. Storm water runoff concentration matrix for urban areas. *J. Contam. Hydrol.* 2007, 91, 26-42.
- 6) Metcalf, L.; Eddy, H.; Tchobanoglous, G. *Wastewater engineering: treatment, disposal, and reuse*; McGraw-Hill: 2010; .
- 7) Schueler, T. R.; Holland, H. Microbes and urban watersheds: concentrations, sources, and pathways. *The Practice of Watershed Protection* 2000, 74-84.
- 8) Parker, J.; McIntyre, D.; Noble, R. Characterizing fecal contamination in stormwater runoff in coastal North Carolina, USA. *Water Res.* 2010, 44, 4186-4194.
- 9) Drake, P. L.; Hazelwood, K. J. Exposure-Related Health Effects of Silver and Silver Compounds: A Review. *Ann. Occup. Hyg.* 2005, 49, 575–585.
- 10) Getman, G.D. An advanced non-toxic polymeric antimicrobial for consumer products. *rubber world* 2011, 22-

Chapter 4

Levels, sources and risk assessment of polycyclic aromatic hydrocarbons (PAH) in San Mateo Ixtatán, Guatemala.

By

¹Kasaraneni, Varun K; ^{1,2}Boving, Thomas B; ¹Oyanedel-Craver, Vinka

¹Department of Civil and Environmental Engineering, University of Rhode Island, 1 Lippitt Rd, Kingston, RI USA 02881

²Department of Geosciences, University of Rhode Island, 9 E. Alumni Ave, Kingston, RI USA 02881.

Is prepared for submission to Journal of Hazardous Materials

Abstract

Twenty four surface soil (0 - 5 cm) samples from a urban, peri-urban and agricultural land and six sediment samples from the river were collected in San Mateo Ixtatán, Guatemala were analyzed for 17 polycyclic aromatic hydrocarbons ($\Sigma 17\text{PAH}$). The $\Sigma 17\text{PAH}$ concentrations at town sites ranged between 460.62 $\mu\text{g}/\text{kg}$ to 3251.83 $\mu\text{g}/\text{kg}$ (mean 1401.75 $\mu\text{g}/\text{kg}$), representing mean contribution of 55.2% from lower molecular weight (LMW: 2 and 3-ring) PAHs. The agricultural soil samples have $\Sigma 17\text{PAH}$ concentrations ranging from 350.93 $\mu\text{g}/\text{kg}$ to 2086.94 $\mu\text{g}/\text{kg}$ (mean 1037.81 $\mu\text{g}/\text{kg}$) with LMW PAH contribution greater than 60%. The PAH profiles, isomer pair ratios, principal component analysis/multiple linear regression (PCA/MLR) suggest that combustion of wood, diesel vehicular emissions, and biomass combustion as main PAH sources. Wood combustion contributes more than 70.6% and 75.5% in town samples and agricultural soils, respectively. The estimated accumulation of $\Sigma 16\text{PAH}$ in corn grains cultivated in contaminated agricultural soils ranged between 0.73 $\mu\text{g}/\text{kg}$ and 11.82 $\mu\text{g}/\text{kg}$ of corn. The cancer risk assessment showed that incremental life time cancer risks (ILTCR) were greater than the acceptable level of 10^{-6} . Main routes of exposure are through soil ingestion and dermal contact. The dietary uptake of PAH through ingestion of corn resulted in a significantly higher cancer risk (ILTCR_{corn}) of 1.95×10^{-3} and 4.54×10^{-3} for adults and children, respectively. Analysis of sediment samples revealed that the $\Sigma 17\text{PAH}$ concentrations in the river sediments were three times higher for samples taken in the town compared to the upstream sediment samples. The study concludes that the contamination of surface soils and the high cancer health risk to local residents is due to the usage of wood as domestic fuel source. Alternative fuels sources and improvements to existing stoves should be considered to reduce the exposure.

1. Introduction

Polycyclic aromatic hydrocarbons (PAHs) are a class of persistent organic pollutants in the environment that possess carcinogenic and mutagenic properties. The US Environmental Protection Agency (US EPA) has listed 16 PAHs as priority pollutants of which seven, i.e., benzo[a] anthracene, chrysene, benzo[a] pyrene, benzo[b]fluoranthene, benzo[k]fluoranthene, dibenz[a,h] anthracene and indeno [1,2,3-cd] pyrene, are listed as probable human carcinogens. Although PAHs can have natural sources, they can also be released into environment through anthropogenic sources such as: oil spills, vehicle exhaust, industrial smoke stack emissions, combustion of fossil fuels and biomass. Fossil fuel and biomass combustion are the major sources of PAH contamination in urban and rural environments [1–3]. PAHs emitted into the atmosphere can be deposited on soils and water systems.

Atmospheric deposition of PAHs on soils occurred via solid, gaseous, and gaseous processes. Soil ecosystems are therefore considered major reservoirs and sinks for these hydrophobic organic contaminants [4]. PAHs accumulated in surface soils bond strongly to the soil's organic matter. PAHs with three or more rings (i.e. higher molecular weight, HMW) have low water solubility, very low vapor pressures and high octanol/water partition coefficients, therefore they can strongly sorb to soil. Because of that, most PAH are persistent in the environment. High concentrations of PAH in soils and sediments have been reported around the world in a number of studies [5,6][1,7,8][9] [10][11]. Soil PAH concentrations correlate well with the corresponding levels in air and atmospheric concentrations are considered a good indicator of environmental pollution [4]. Non-point sources, such as atmospheric deposition or stormwater runoff from urban communities, can contaminate sediments and surface waters ([5], [6]).

Occurrence of PAHs in agricultural soils is a public health concern, because they can be introduced into fruits and vegetables [10] and humans can get exposed through direct contact and ingestion. Assessment of PAH contamination and source apportionment are important for

pollution control, remediation to minimize risk of exposure and can help plan intervention studies.

In developing countries nearly 90% of rural households rely on biomass for their energy needs [11]. Combustion of wood and other biomass fuels can release many pollutants including particulate matter, carbon monoxide and PAHs [12,13]. In developing countries, the pollution generated combustion of wood and biomass for domestic purposes has been linked to respiratory diseases [14,15]. In several developing countries traditional wood stoves have been modified to reduce in door emissions through the venting of the smoke outside the buildings [15-18]. This can result in increasing PAH atmospheric deposition on soils posing a health risk to humans.

The objectives of this study were to 1) to investigate PAH contamination in surface soils and sediments in the town of San Mateo Ixtatán, Guatemala, 2) determine the sources of PAH contamination, 3) estimate life time health risk for adults and children due to soil contamination.

2. Materials and methods

PAH standards and deuterated PAH standards were obtained from Ultra Scientific, USA. All solvents (Dichloromethane, n-Hexane, Acetone) were of HPLC grade and were obtained from Fisher Scientific.

2.1 Description of study area and sampling sites

The town of San Mateo Ixtatán (SMI) is located in Huehuetenango department, Guatemala (elevation 2540m) with a population of approximately 10,000. About 98% of the households use wood as a primary source of fuel for cooking and heating purposes [19]. In August 2012, surface soil samples (0-5cm) were collected at 24 sampling sites (18 town sites and 6 agricultural soils). The 18 town sampling sites (T1 to T18) include residential areas with high and low housing density and commercial areas (Figure 4-1). Six agricultural soil samples (A1 to A6) three samples (A2 to A4) were taken in rural areas while the rest were collected in urban agricultural settings. In addition, six sediment samples (SD1 to SD6) were collected along the river passing through the town in order to determine the contamination caused by PAHs from the town. The sediment samples SD1 and SD2 were taken at the beginning of the river and 0.5 km from SD1 to establish a baseline. Sample SD3, SD4, and SD5 were taken in the town. Locations SD4 and SD5 are where tributaries running through the town carrying household waste water and rainwater runoff merge into the river (Figure 4-1). The sampling of surface soil and sediments were done following EPA standard operating procedures[20][21].

2.2 Sample preparation, extraction, cleanup and analysis

All samples were air dried for one week at room temperature and sieved through a 2 mm mesh to remove stones and residual roots. The extraction of PAHs from soil and sediment samples was done using a Dionex ASE 350 (Dionex Corporation, CA, USA) accelerated solvent extraction device using hexane and acetone (1:1,v/v). Between 3g to 5g of sample was used for extractions. Air dried samples were spiked with deuterated standards (Acenaphthene-D10, Phenanthrene-D10,

Benz[a]anthracene-D12, Benzo[a]pyrene-D12) prior to extraction. Extractions were performed with a 1:1 mixture of hexane and acetone at 140 °C and 1500 psi. The concentrated extracts were cleaned using solid phase extraction cartridges Strata SI-1 (Phenomenex). Extracts were concentrated to a final volume of 0.5 ml using N-EVAP nitrogen evaporator (Organomation Associates, Inc). The determination of 17 PAHs (Table 4-1) was performed using gas chromatography coupled with mass spectrometry (Shimadzu QP2010S GC-MS).

2.3 Quality assurance/quality control (QA/QC) and statistical analysis

A five point calibration was used for the GC-MS with a detection limit of 10 ng/μl for PAH and D-PAH. Procedural blanks were run periodically to detect false positives. The average recoveries for deuterated standards ranged from 44.5% to 94% for acenaphthene-D10, and phenanthrene-D10 while it was between 51% to 132% for benz[a]anthracene-D12 and benzo[a]pyrene-D12. All statistical analyses were carried out using R version 3.0.3 or SigmaPlot 11 (Systat Software Inc.).

2.4 Estimation of carcinogenic potency

Benzo[a]pyrene (BaP) is the only PAH which has enough toxicological data to estimate carcinogenic potency. The carcinogenic potency due to contamination of soil samples with PAHs can be estimated using the BaP equivalent concentrations of all PAHs using toxicity equivalency factors (TEFs) (Table 4-1) [22,23]. The BaP toxic equivalent concentration (TBaP_{eq}) for each site was calculated using equation 1.

$$TBaP_{eq} = \sum_i C_i * TEF_i \quad (1)$$

Where, C_i is the concentration of the individual PAH and TEF_i is the corresponding toxicity equivalency factor. As a TEF value for Retene was unavailable, it was not considered for toxicity and cancer risk calculations.

2.5 Estimation of PAH accumulation in corn grains and dietary intake

Corn is a widely used staple of the local cuisine and was therefore selected to evaluate the potential risk associated with the intake of the food staple. The accumulation of PAH in corn grains were estimated based on the model developed by Paraíba et al 2010[24]. The assumptions for developing the model are 1) in the soil-plant system PAH are degraded, dissipated, and transformed according to first order kinetics and 2) the uptake, transport, and accumulation of PAH in corn plants is via transpiration stream from contaminated soil solution. Equations 2 to 5 were used to estimate the concentration of PAH in corn and the definitions and the values of parameters used are listed in Table 4-2

$$C_g = \frac{\rho_w A Q_f C_w(0)}{\rho_g(B-k_s)} [e^{(-k_s t)} - e^{(-Bt)}] \quad (2)$$

Where the constants A and B represents the PAH total uptake rate by corn plants and the PAH total dissipation rate, both in the soil-plant system and are given by

$$A = \frac{Q_x TSCF}{M_p} \quad (3)$$

$$B = k_e + k_g + \frac{Q_x}{M_p(f_l k_{lw} + f_c k_{cw})} \quad (4)$$

C_w is the concentration of PAH in soil solution and is calculated using equation 5

$$C_w(t) = \frac{\rho_w t C_s(0) e^{-k_s t}}{(\rho_s k_d + f_\theta + f_\delta k_{aw})} \quad (5)$$

2.6 Cancer health risk assessment

The lifetime average daily exposure (LADD) due to exposure to 16 PAHs through dietary uptake of corn, soil ingestion, and dermal contact was calculated for each exposure pathway according to the USEPA framework [44] using the equations 6 through 8

$$LADD_{\text{corn}} = \frac{(C_c * EF * ED * IR)}{(BW * AT)} \quad (6)$$

$$LADD_{\text{ing}} = \frac{(C_s * ET * EF * ED * IR * C_f)}{(BW * AT)} \quad (7)$$

$$LADD_{\text{der}} = \frac{(C_s * ET * EF * ABS * SA * ED * AF_d * C_f)}{(BW * AT)} \quad (8)$$

$LADD_{\text{corn}}$, $LADD_{\text{ing}}$ and $LADD_{\text{der}}$ are lifetime average daily doses associated with uptake of PAH by corn, ingestion of soil, and dermal exposure (mg/kg/d), C_c and C_s are concentrations of TBaP_{eq} PAH in corn and soil (mg/kg), ET is exposure time (hrs/day), EF is exposure frequency (days/year), IR is ingestion rate (mg/kd/day), BW is body weight (kg), AT is average time (days), C_f is conversion factor, ABS is dermal adsorption fraction (-), SA is surface area (cm²) and AF_d is soil to skin adherence factor (mg/cm²/event)

$$ILTCR_i = LADD_i * SF_i \quad (9)$$

The average incremental lifetime cancer risks (ILTCR_i) is cancer risk for an exposure route (i) and SF_i = cancer slope factor for an exposure route (i).

The exposure parameters used in the risk assessment were obtained from USEPA and listed in Table 4-3. The cancer slope factors (SF_i) for BaP used in this study were 30.5, 12 and 7.3 mg kg⁻¹ d⁻¹ for dermal contact, ingestion and oral uptake routes, respectively [22]. The lower end of the

range for acceptable risk is defined by a single constraint on the 95th percentile of risk distribution that must be equal or lower than $1E^{-6}$ for carcinogens [25].

3. Results and Discussion

3.1 Concentrations and composition profiles of PAHs in surface soil samples

The concentrations of 17 individual PAHs, sum of 16 PAHs ($\Sigma 16\text{PAH}$), sum of 17 PAHs ($\Sigma 17\text{PAH}$) and seven carcinogenic PAHs ($\Sigma 7\text{CarPAH}$) in surface soil samples are shown in Table 4-4. A wide range of PAH concentrations were observed in soil samples (Figure 4-2) with $\Sigma 16\text{PAH}$ concentrations in range of 434.54 $\mu\text{g}/\text{kg}$ to 2560.47 $\mu\text{g}/\text{kg}$ (mean 1226.63 $\mu\text{g}/\text{kg}$) for town samples and 328.40 $\mu\text{g}/\text{kg}$ to 1642.49 $\mu\text{g}/\text{kg}$ (mean 921.23 $\mu\text{g}/\text{kg}$) for agricultural soil samples. The $\Sigma 16\text{PAH}$ concentrations found in SMI are higher than the $\Sigma 16\text{PAH}$ concentrations previously reported in urban soils, such as Tokushima, Japan (mean of 611 $\mu\text{g}/\text{kg}$) [26] or Hong Kong, China (21–554 $\mu\text{g}/\text{kg}$) [27]. The concentrations were also higher than in soils from a natural reserve close to industrial plants in Italy (range 35 to 545 $\mu\text{g}/\text{kg}$) [28], industrial soils samples from Tarragona, Spain (range 112 to 1002 $\mu\text{g}/\text{kg}$) [29], Norwegian soils (range 8.6 to 1050 $\mu\text{g}/\text{kg}$) [30]. However, the concentrations are in range with those reported from industrial areas in Linz, Austria (mean 1450 $\mu\text{g}/\text{kg}$) [31], agricultural soils in Delhi, India (mean 1910 $\mu\text{g}/\text{kg}$) [1], and soils from vegetable fields in the Pearl River delta, China (range 16 to 3700 $\mu\text{g}/\text{kg}$) [32]. The concentrations are lower compared to soil samples from New Orleans, United States (mean 3730 $\mu\text{g}/\text{kg}$) [7] and in Beijing, China range (366–27,800 $\mu\text{g}/\text{kg}$) [33]. The concentrations of seven carcinogenic PAHs ($\Sigma 7\text{CarPAH}$) accounted for 5.54 % to 72.09% (mean 29.96%) of $\Sigma 16\text{PAH}$ in town samples and 12.78% to 51.22 % (mean 26.82%) for agricultural sites.

The $\Sigma 17\text{PAHs}$ were divided in to two groups, representing LMW PAHs (2,3 ring) and HMW PAHs (3,4,5 ring). The composition profiles of soil PAHs have higher proportions of LMW PHA 55.2% \pm 20.1 % (mean \pm standard deviation) in town samples and 60.2% \pm 12.7% in agricultural

soil samples (Figure 4-3). In general, $\Sigma 16\text{PAH}$ concentrations were dominated by acenaphthene ($13.6\% \pm 15.8\%$) (mean \pm standard deviation), phenanthrene ($9.3\% \pm 6.0\%$), fluoranthene ($10.9\% \pm 6.6\%$), and pyrene ($12.3\% \pm 9.7\%$) in town samples. In agricultural soils, acenaphthene ($19.4\% \pm 12.5\%$), phenanthrene ($8.6\% \pm 5.5$), fluoranthene ($7.0 - 19.3\%$, 11.9%), and pyrene ($10.6\% \pm 5.8\%$) were dominant. Retene, a molecular marker for wood combustion [34] was dominant in both, town samples and agricultural soils (Table 4-4). The dominant occurrence of LMW PAH (2, 3-ring) at all the sampling sites reflects the presence of low temperature combustion related sources.

3.2 Correlation among individual PAH and with soil organic carbon (TOC)

The relationship between individual PAHs and soil organic carbon (TOC) was examined using Pearson correlation analysis. Only correlation coefficients (r) greater than 0.5 with $p < 0.05$ were considered for interpretation of the results. Overall, no correlation was found between soil TOC and PAH concentrations for town samples and agricultural soils. (Tables 4-4 a & b). The lack of correlation might be related to PAH concentration in the atmosphere not having reached equilibrium with the TOC in the soil. This would mean that other factors such as land use, wind direction, rainfall etc. might have a stronger influence on deposition of PAHs [35,36].

The $\Sigma 17\text{PAH}$ concentrations at town sites are strongly correlated ($r > 0.75$, $p < 0.05$) with Phn, Ant, Fln, Pyr, and Ret while for agricultural samples a stronger correlation was observed with Phn, Ant, Fln, Pyr, Ret, and BaA, suggesting a common source for the majority of the contamination at each type of site. Among individual PAHs, a significant correlation was observed between two groups of PAHs in town samples, the first group comprised of Phn, Ant, Fln, Pyr, and Ret while the second group is the HMW PAHs BbF, BkF, BgP and IP. This distribution is indicative of multiple sources. In agricultural samples significantly higher correlations ($r > 0.8$, $p < 0.05$) were observed among Fln, Pyr, Ret, BaA, Chr, and BaP.

3.3 PAH Source identification and estimation

3.3.1 Isomer ratios of PAHs

The PAH isomer pair ratios for Ant/(Ant+Phn), Fln/(Fln+Pyr), BaA/(BaA+Chr), and IP/(IP+BgP) can be used as tracers to identify sources of PAH contamination [1,37,38]. In the present study, the ratio of Ant/(Ant+Phn) was higher than 0.1 for all the sampling sites (Figure 4-4a). This indicates a dominance of combustion source rather than petroleum source[38]. The ratio of BaA/(BaA+Chr) was greater than 0.35 for both, town and agricultural soils, which implies combustion of coal and biomass, such as grass and wood, as primary source. For the town soil samples, the ratios of Fln/(Fln+Pyr) and IP/ (IP+BgP) varied from 0.21 to 0.63 and 0.33 to 0.86, respectively, while these ratios for agricultural soils varied from 0.48 to 0.71 and 0.47 to 0.81, respectively. These data sets imply that multiple sources (petroleum, petroleum combustion and biomass and coal combustion) as the source of PAH contamination in surface soils. The cross plot (figure 4-4) shows that at town and agricultural sampling sites most of the soils had Fln/(Fln+Pyr) and IP/ (IP+BgP) ratios greater than 0.5 which is indicative for biomass and/or coal combustion. [38,39]. In SMI, coal is not commonly used, but wood and other biomass are the predominant domestic fuels. Thus, combustion of wood and biomass likely is the primary sources of surface soil contamination.

3.3.2 Principal component analysis/Multiple linear regression

Principal component analysis (PCA) as a multivariate analytical tool has been widely used in environmental studies for source identification [1,2]. PCA reduces the total variability in the original data to a minimum number of factors. The factor loadings indicate the correlations of among the contaminants and related source emission composition [40]. The PCA was performed using R software R version 3.0.3. The principal components were identified by varimax rotation and Eigen values greater than one. The percentage mean contribution of each source was

determined using multiple linear regression as described by [41]. PCA was performed separately on the data sets of town samples and agricultural soil samples. Four components were extracted from the PCA (PC1, PC2, PC3, and PC4) for town samples accounting for 90.7% of the variability and two components (PC1 and PC2) for agricultural soils accounting for 89.0% of variance (Table 4-4). As the loadings were low in most cases, a factor loading of 0.15 was selected as the lowest level of significance within a component.

For town samples the first component, PC1, was responsible for 68.0 % of the variance in the data. PC1 had high loadings of LMW PAH: Phn , Ant, Fln, Pyr, and Ret . The occurrence of 3, 4-ring compounds, Phn, Ant, Flu and Pyr are indicative of a combustion source. The use of Retene has been suggested as a marker for wood combustion [34] and its presence along with Phn, Fln and Pyr suggests that wood burning is the main contributing source. The second component, PC2, accounts for 10.4% of variance and is dominated by Ret, BbF, BaP, BgP , and IP. The HMW PAHs BaP, DAnt, BgP and IP are associated with traffic emissions [42,43,44], while BbF and BgP are indicators of diesel combustion [45]. The third component, PC3, was responsible for 6.8% with higher loadings of LMW PAHs Ace , Flu, Phn, Ant, Fln , BaA , and Chr and indicative of biomass combustion [46][44]. PC4 with predominance of Ace, Flu, Pyr, Ret , BbF, BaP , BgP, and IP is indicative of diesel combustion as source[42,45].

At agricultural sites, the two components PC1 and PC2 accounted for 68.6% and 20.4% of the variance in the data. PC1 is predominantly weighted with Phn, Ant , Fln, Pyr , Ret , and BaA and represents combustion of wood as source of PAH [45][44]. The second component, PC2, is dominated by Ace, Ant, Fln and Pyr and suggests combustion of biomass as a source.

The percent mean contribution of sources determined by PCA is obtained by performing principal component analysis/ multiple linear regression (PCA/MLR). The PCA/MLR indicates that wood combustion contributes 70.6% of $\Sigma 17$ PAH to in town samples, while emissions from diesel

powered vehicles contribute 24.1% and combustion of biomass account for 5.3% of $\sum 17\text{PAH}$. For agricultural soil samples, 75.5% of the $\sum 17\text{PAH}$ originated from wood combustion with 24.5% from combustion of biomass such as agricultural residue. Inferences drawn from PCA/MLR are similar to those of isomer pair ratios which pointed to wood, biomass combustion, and emissions from diesel powered vehicles as the main sources of PAH contamination in surface soils of San Mateo Ixtatán.

3.4 Estimation of carcinogenic potency

The calculated TBaP_{eq} for 18 town sample sites ranged from 9.0 $\mu\text{g}/\text{kg}$ to 257.7 $\mu\text{g}/\text{kg}$ with a mean value of 109.0 $\mu\text{g}/\text{kg}$. The TBaP_{eq} of the agricultural samples ranged from 17.1 $\mu\text{g}/\text{kg}$ to 214.0 $\mu\text{g}/\text{kg}$ with a mean of 104.1 $\mu\text{g}/\text{kg}$ (figure 4-5). The HMW PAHs BaP (32.9%), DAnt (32.6%), BaA (9.5%), BbF (6.7%), Chr (5.7%), IP (3.9%) contributed more than 90% to TBaP_{eq} . The TBaP_{eq} concentrations in this study are higher compared to previous reported mean concentrations around the world. For example, TBaP_{eq} in natural reserve soil samples in Italy were (18 $\mu\text{g}/\text{kg}$) [28], rural soils in Norway (14.3 $\mu\text{g}/\text{kg}$ [30]), and soils of Tarragona, Spain (64 $\mu\text{g}/\text{kg}$) [29]. Our data are in range with agricultural soils in Delhi, India (45.6 $\mu\text{g}/\text{kg}$ to 387.13 $\mu\text{g}/\text{kg}$, [1]. This suggests that concentrations of PAH in the surface soils of San Mateo Ixtatán are high and carcinogenic potency of PAH needs to be considered.

3.5 Estimation of PAH accumulation in corn grains and dietary intake

In SMI corn or maize is the primary crop cultivated at the sites where agricultural soil samples were collected. The accumulation of individual PAHs in corn grains at all six agricultural soil sites were estimated and are shown in table 4-7. The $\sum 16\text{PAH}$ concentrations estimated in corn ranged from 0.73 $\mu\text{g}/\text{kg}$ to 11.82 $\mu\text{g}/\text{kg}$ with a mean of 4.99 $\mu\text{g}/\text{kg}$. With the exception of f Pyr, the 2, 3-ring PAHs were dominant and the mean contribution to $\sum 16\text{PAH}$ were in the order of Ace > Phn > Ant > Pyr > Nap > Acy > Flu > Fln. The total BaP equivalent TBaP_{eq} concentrations are between 0.01 $\mu\text{g}/\text{kg}$ and 0.08 $\mu\text{g}/\text{kg}$ with a mean 0.03 $\mu\text{g}/\text{kg}$. The average

$\Sigma 16$ PAH uptake based on daily corn intake was set at 454 g for adults and 227g for children [47]. This is equivalent to an estimated PAH uptake of 2.26 $\mu\text{g}/\text{day}$ for adults and 1.13 $\mu\text{g}/\text{day}$ for children (below 6 years) (Table 4-8).

3.6 Risk assessment

The aim of the risk assessment was to investigate the possibility of cancer development in adults and children (below 6 years) in San Mateo Ixtatán as a result of dietary uptake of PAH through corn consumption and exposure to PAHs in soil via ingestion and dermal exposure routes. The average incremental lifetime cancer risks (ILTCR) due to soil ingestion ($\text{ILTCR}_{\text{ing}}$) and dermal contact ($\text{ILTCR}_{\text{der}}$) are higher (figure 4-6) than US EPA acceptable cancer risk level of 1×10^{-6} [25]. Children are at higher risk than adults with average $\text{ILTCR}_{\text{ing}}$ and $\text{ILTCR}_{\text{der}}$ at 1.61×10^{-5} and 1.49×10^{-5} respectively. The average incremental lifetime cancer risks due to dietary uptake ($\text{ILTCR}_{\text{corn}}$) of PAHs are 1.93×10^{-3} for adults and 4.54×10^{-3} for children. All the calculated ILTCRs exceed the US EPA acceptable cancer risk level of 1×10^{-6} indicating high potential carcinogenic health risk [48]. Dietary uptake of PAH through corn consumption was the major contributor for total incremental lifetime cancer risk ($\text{ILTCR}_{\text{total}}$) accounting for >99% of $\text{ILTCR}_{\text{total}}$. The individual PAH contributions to $\text{ILTCR}_{\text{corn}}$ are dominated by 2 and 3- ring PAHs (Table 4-7), which are associated with low temperature combustion sources, such as wood burning. From source apportionment it was established that more than 75 % of the PAH in agricultural soils have wood combustion as a source. Therefore it can be concluded that use of wood as domestic fuel is primary contributor to higher cancer risk for the people of SMI and should be taken into account for health protection.

3.7 Contamination of river sediments

The $\Sigma 17$ PAH concentrations at the starting of the river (SD1) and upstream of the town (SD2) were 311.57 $\mu\text{g}/\text{kg}$ and 529.70 $\mu\text{g}/\text{kg}$, respectively. For the sediment samples taken in town SD4 and SD5, the $\Sigma 17$ PAH concentrations were 1005.36 $\mu\text{g}/\text{kg}$ and 1198.46 $\mu\text{g}/\text{kg}$, respectively

(Table 4-9). The deposition of atmospheric PAH, erosion of surface soils contaminated with PAHs in to the river, and household waste water discharged into the river are likely sources for higher sediment PAH concentrations at SD4 and SD5. However, it has not been studied which of these contamination sources might be more dominant. In comparison, the concentrations of PAH found in these sediments are higher than in sediments from Galveston Bay and the Mississippi River Delta [49]. They are in comparable range with sediment concentrations in Tonghui River of Beijing, China [50]. Finally, the ratios of Ant/ (Ant+Phn), Fln/(Fln+Pyr), BaA/(BaA+Chr), IP/(IP+BgP) suggest that most of the PAH contamination in river sediments is due to the combustion of wood and biomass (Table 4-9).

4 Conclusions

The data from this study suggest that in the rural town of San Mateo Ixtatán in the northwestern highlands of Guatemala the PAH contamination in surface soils is higher or are in range with urban and industrial regions around the world. The source apportionment concludes that the use of wood as domestic fuel is the primary source of this contamination in surface soils. The results of a cancer risk assessment indicate that both, children and adults face a high potential risk of cancer development as a result of the exposure to PAH via soil ingestion, dermal contact, and dietary uptake through corn cultivated in the contaminated soils. Alternative domestic fuel sources or improving existing stove models should be considered to reduce the health risk resulting from high PAH exposure.

Table 4-1: List of PAHs analyzed, molecular weight, number of rings and BaP toxicity equivalent factors.

No.	Compound	Abbreviation	Molecular Wt	Number of Rings	TEF	
1	Naphthalene	Nap	128.1	2	0.001	LMW
2	Acenaphthylene	Acy	152.1	2	0.001	
3	Acenaphthene	Ace	154.2	2	0.001	
4	Fluorene	Flu	166	2	0.001	
5	Phenanthrene	Phn	178	3	0.001	
6	Anthracene	Ant	178	3	0.001	
7	Fluoranthene	Fln	202.2	3	0.001	
8	Retene	Ret	234.3	3	-NA-	
9	Pyrene	Pyr	202.2	4	0.001	HMW
10	Benz[a]anthracene	BaA	228	4	0.1	
11	Chrysene	Chr	228.2	4	0.01	
12	Benz[b]Fluoranthene	BbF	252.3	4	0.1	
13	Benz[k]Fluoranthene	BkF	252.3	4	0.1	
14	Benzo[a]pyrene	BaP	252.3	5	1	
15	Dibenz[a,h]anthracene	DAnt	278.3	5	1	
16	Benzo[ghi]perylene	BgP	276.3	6	0.01	
17	Indeno [1,2,3]pyrene	IP	276	5	0.1	

LMW is low molecular weight and HMW is high molecular weight

Table 4-2: Soil, corn plant and grain physical–chemical parameters applied to the model to estimate the polycyclic aromatic hydrocarbons (PAH) accumulation in corn grains. The references for values of individual parameters can be found in Paraiba et al 2010.

Parameter	Unit	Symbol	Value
Total daily volume of water lost by plant transpiration	L day ⁻¹ ha ⁻¹	Q _x	5.0E+04
Plant fresh biomass	kg ha ⁻¹	M _p	2.0E+04
Plant growth rate	day ⁻¹	k _e	0.71
Corn grain cellulose volumetric fraction	g g ⁻¹	f _c	0.25
Corn grain lignin volumetric fraction	g g ⁻¹	f _l	0.06
Phloem sap flow rate necessary to produce 1.0 kg fresh corn grains	L kg ⁻¹	Q _f	3
Corn grain density	kg L ⁻¹	ρ _g	1.2
Soil solution density	kg L ⁻¹	ρ _w	0.98
Soil water volumetric fraction	g g ⁻¹	f _θ	0.25
Soil air volumetric fraction	g g ⁻¹	f _δ	0.16
Soil organic matter volumetric fraction*	g g ⁻¹	f _{om}	0.09 – 0.53
Dry soil density*	kg L ⁻¹	ρ _s	0.79 – 0.85
Humid soil density*	kg L ⁻¹	ρ _{wt}	1.02 – 1.1
Plant age at grain harvest (days after sowing)	day	t _h	120

*values used were obtained from soil samples in this study

Table 4-3: Exposure parameter values

Variable	Children	Adult
EF (d/y)^	350	
ED (y)^	6	30
BW (kg)^	15	70
AT (d)^	70 x 365	
IngR (mg/d)^	100	50
ABS^	0.13	
SA (cm2)^	2800	5700
Corn consumption * (kg/day)	0.484	0.242

^ Values obtained from EPA risk assessment guide [48] * Value based on [41]

Table 4-4: Concentrations of PAHs ($\mu\text{g}/\text{kg}$ dry weight) in soils from different functional areas in San Mateo Ixtatán, Guatemala.

	Town sites			Agricultural sites		
	Minimum	Maximum	Average	Minimum	Maximum	Average
Nap	0.50	82.93	38.33	0.50	40.96	24.82
Acyl	4.66	110.05	33.07	18.90	57.87	33.48
Ace	15.43	329.22	110.65	25.40	408.16	152.97
Flu	10.58	203.50	64.46	9.92	104.46	39.13
Phn	11.25	469.14	140.57	15.68	301.59	97.70
Ant	8.33	370.37	98.17	12.49	141.20	72.52
Fln	13.84	493.83	168.26	29.39	317.46	124.59
Py	11.53	675.15	187.90	18.86	269.84	112.46
BaA	6.36	477.78	92.68	3.26	116.07	42.31
Chr	6.13	277.43	62.99	1.63	68.45	17.95
BbF	6.61	288.21	73.28	2.35	116.28	50.53
BkF	1.95	63.61	20.80	2.81	44.80	22.39
BaP	1.29	123.24	39.53	8.28	71.98	31.41
DAnt	1.36	133.55	39.40	5.52	179.21	55.36
BgP	0.97	163.98	25.12	6.61	54.08	18.93
IP	5.27	151.06	31.42	10.12	47.43	24.69
Ret	23.12	691.36	175.12	22.54	444.44	116.57
$\Sigma 17\text{PAH}$	460.62	3251.83	1401.75	350.93	2086.94	1037.81
$\Sigma 16\text{PAH}$	434.54	2560.47	1226.63	328.40	1642.49	921.23
$\Sigma 7\text{CarPAH}$	34.60	795.43	360.10	41.98	485.19	244.63

Table 4-5b: Pearson correlation coefficients for TOC and 17 individual PAHs at agricultural sites

	Nap	Acy	Ace	Flu	Phn	Ant	Fln	Pyr	Ret	BaA	Chr	BbF	BkF	BaP	DAnt	BgP	IP	Σ16PAH	
TOC (%)	0.17	-0.46	0.01	0.48	-0.53	-0.68	-0.55	-0.64	-0.41	-0.51	-0.19	0.25	0.36	-0.04	0.39	0.61	0.66	-0.39	
Nap	1.00	0.15	0.31	0.11	0.41	0.50	0.47	0.51	0.35	0.47	0.38	0.59	0.16	0.50	-0.26	0.46	0.63	0.61	
Acy		1.00	-0.69	-0.38	0.60	0.51	0.61	0.64	0.55	0.83*	0.46	0.03	-0.40	0.67	-0.15	-0.45	0.18	0.45	
Ace			1.00	0.09	-0.26	0.19	-0.18	-0.09	-0.38	-0.41	-0.45	-0.11	0.27	-0.58	-0.15	0.12	-0.29	-0.05	
Flu				1.00	-0.52	-0.65	-0.55	-0.55	-0.37	-0.45	-0.09	0.06	-0.47	-0.20	-0.57	0.71	0.48	-0.46	
Phn					1.00	0.77	0.99*	0.95*	0.97*	0.93*	0.85*	0.62	0.18	0.81	-0.06	-0.28	0.08	0.96*	
Ant						1.00	0.84*	0.92*	0.58	0.77	0.34	0.17	0.10	0.39	-0.14	-0.52	-0.21	0.80*	
Fln							1.00	0.98*	0.93*	0.94*	0.79	0.57	0.17	0.77	-0.08	-0.31	0.06	0.97*	
Pyr								1.00	0.84*	0.94*	0.68	0.44	0.07	0.68	-0.19	-0.39	0.00	0.94*	
Ret									1.00	0.87*	0.95*	0.73	0.17	0.86*	-0.06	-0.13	0.19	0.91*	
BaA										1.00	0.77	0.47	-0.07	0.85*	-0.17	-0.30	0.22	0.87*	
Chr											1.00	0.84*	0.10	0.90*	-0.15	0.13	0.41	0.81	
BbF												1.00	0.45	0.76	0.05	0.54	0.60	0.72	
BkF													1.00	0.11	0.79	0.21	0.01	0.31	
BaP														1.00	0.01	0.15	0.60	0.77	
DAnt															1.00	-0.03	-0.07	-0.06	
BgP																1.00	0.80	-0.11	
IP																	1.00	0.18	
Σ16PAH																			1.00

Table 4-6: Factor loadings and source contribution obtained from PCA/MLR

	Town sites				Agricultural sites	
	PC1	PC2	PC3	PC4	PC1	PC2
Nap	0.03	-0.02	0.02	0.00	0.02	0.05
Acy	0.03	0.06	0.13	0.04	0.04	-0.05
Ace	-0.14	-0.35	0.42	0.64	-0.20	0.91
Flu	-0.09	-0.15	0.16	0.39	-0.07	-0.04
Phn	0.41	0.02	0.31	-0.06	0.42	0.08
Ant	0.28	-0.20	0.18	-0.26	0.18	0.25
Fln	0.47	-0.06	0.35	0.01	0.41	0.15
Pyr	0.52	-0.53	-0.57	0.20	0.36	0.22
Ret	0.49	0.44	0.04	0.21	0.62	-0.06
BaA	0.14	0.14	0.16	-0.11	0.16	-0.01
Chr	0.09	0.11	0.17	-0.06	0.09	-0.04
BbF	0.07	0.40	-0.14	0.40	0.10	0.01
BkF	0.03	0.07	-0.03	0.07	0.01	0.03
BaP	0.05	0.17	-0.13	0.20	0.08	-0.05
DAnt	0.05	0.09	-0.29	0.07	-0.02	-0.10
BgP	-0.01	0.15	-0.07	0.19	-0.02	-0.01
IP	0.00	0.16	-0.14	0.17	0.01	-0.03
% variance	68.0	10.4	6.8	5.5	68.6	20.4
Eigen value	6.64	3.86	1.99	1.41	8.29	3.52
Estimated source % mean contribution	Wood combustion	Diesel combustion	Biomass combustion	Diesel combustion	Wood combustion	Biomass Combustion
	70.6	6.3	5.3	17.8	75.5	24.5

Table 4-7: Estimated concentrations of individual PAHs ($\mu\text{g}/\text{kg}$ of corn) and BaP equivalent concentrations estimated in corn grain cultivated at agricultural sites

Site	Nap	Acy	Ace	Flu	Phn	Ant	Fln	Pyr	BaA	Chr	BbF	BkF	BaP	DAnt	BgP	IP	$\Sigma 16\text{PAH}$	TBaP _{eq}
A1	0.005	0.289	1.953	0.404	0.173	0.188	0.029	0.200	0.008	0.006	0.002	0.002	0.004	0.001	0.001	0.001	3.27	0.01
A2	0.336	0.312	0.744	0.079	0.591	0.915	0.076	0.609	0.043	0.003	0.005	0.002	0.010	0.003	0.001	0.002	3.73	0.02
A3	0.585	0.160	6.886	0.110	1.034	1.799	0.132	1.021	0.030	0.002	0.034	0.015	0.004	0.004	0.001	0.001	11.82	0.03
A4	0.048	0.041	0.459	0.015	0.060	0.053	0.009	0.026	0.001	0.001	0.009	0.005	0.002	0.005	0.001	0.001	0.73	0.01
A5	0.137	0.035	0.622	0.107	0.061	0.030	0.009	0.053	0.004	0.004	0.015	0.002	0.003	0.001	0.001	0.001	1.09	0.01
A6	0.614	0.486	0.476	0.059	3.183	1.931	0.300	1.889	0.119	0.066	0.113	0.015	0.032	0.007	0.002	0.003	9.30	0.08
Mean	0.287	0.220	1.857	0.129	0.850	0.820	0.093	0.633	0.034	0.014	0.030	0.007	0.009	0.004	0.001	0.001	4.99	0.03

Table 4-8: Dietary uptake of $\Sigma 16\text{PAH}$ ($\mu\text{g}/\text{day}$)

	Adult	Child
A1	1.48	0.74
A2	1.69	0.85
A3	5.37	2.68
A4	0.33	0.17
A5	0.49	0.25
A6	4.22	2.11
Mean	2.26	1.13

Table 4-9: Concentrations of $\Sigma 17\text{PAH}$ and $\Sigma 7\text{CarPAH}$ in sediments and the isomer pair ratios.

	$\Sigma 17\text{PAH}$	$\Sigma 7\text{CarPAH}$	Fln / (Fln+Py)	Ant / (Ant+Phn)	IP/ (IP+BgP)	BaA / (BaA+Chr)
SD1	311.57	104.11	0.53	0.80	0.50	0.84
SD2	529.70	120.24	0.50	0.47	0.61	0.79
SD3	734.32	145.79	0.52	0.45	0.48	0.60
SD4	1005.36	159.72	0.49	0.48	0.64	0.78
SD5	1198.46	112.30	0.50	0.47	0.98	0.68
SD6	608.23	120.80	0.49	0.41	0.20	0.69

FIGURES

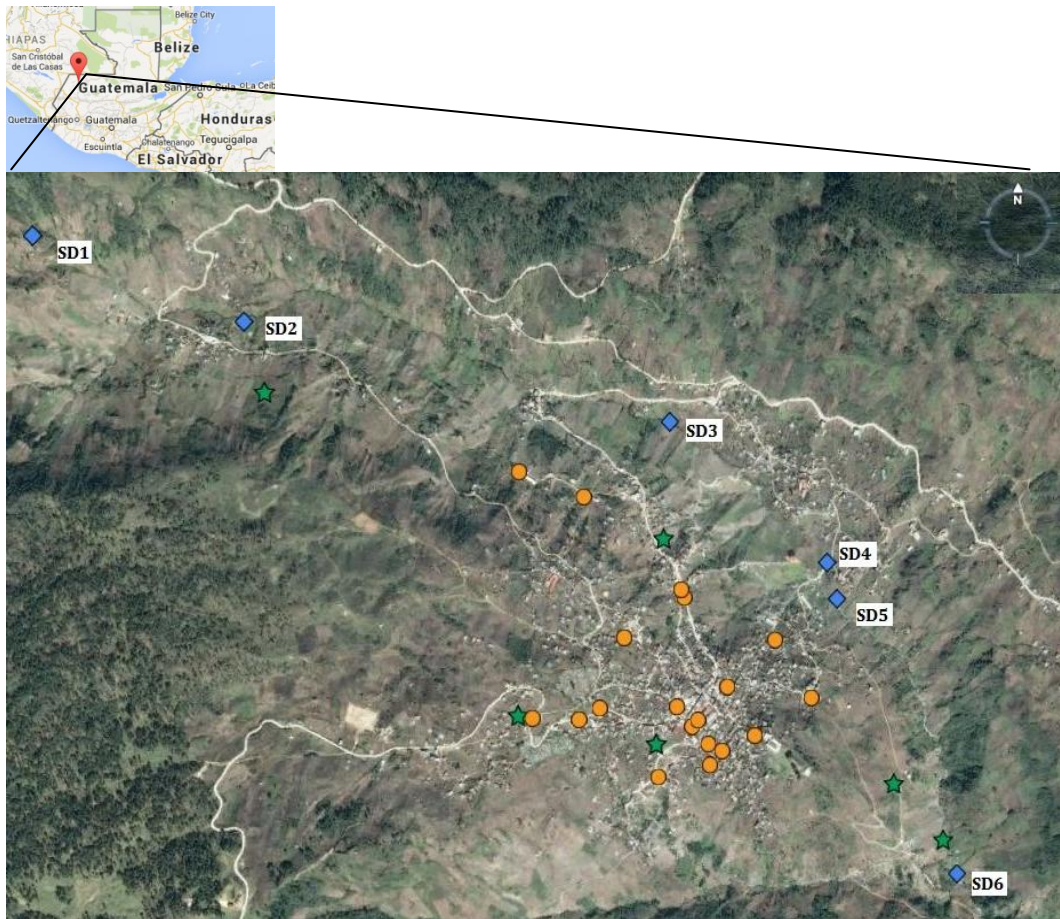





Figure 4-1: Location of San Mateo Ixtatán and the sampling sites.  Represents sediment sampling location,  represents agricultural soil samples and  represents samples taken in town.

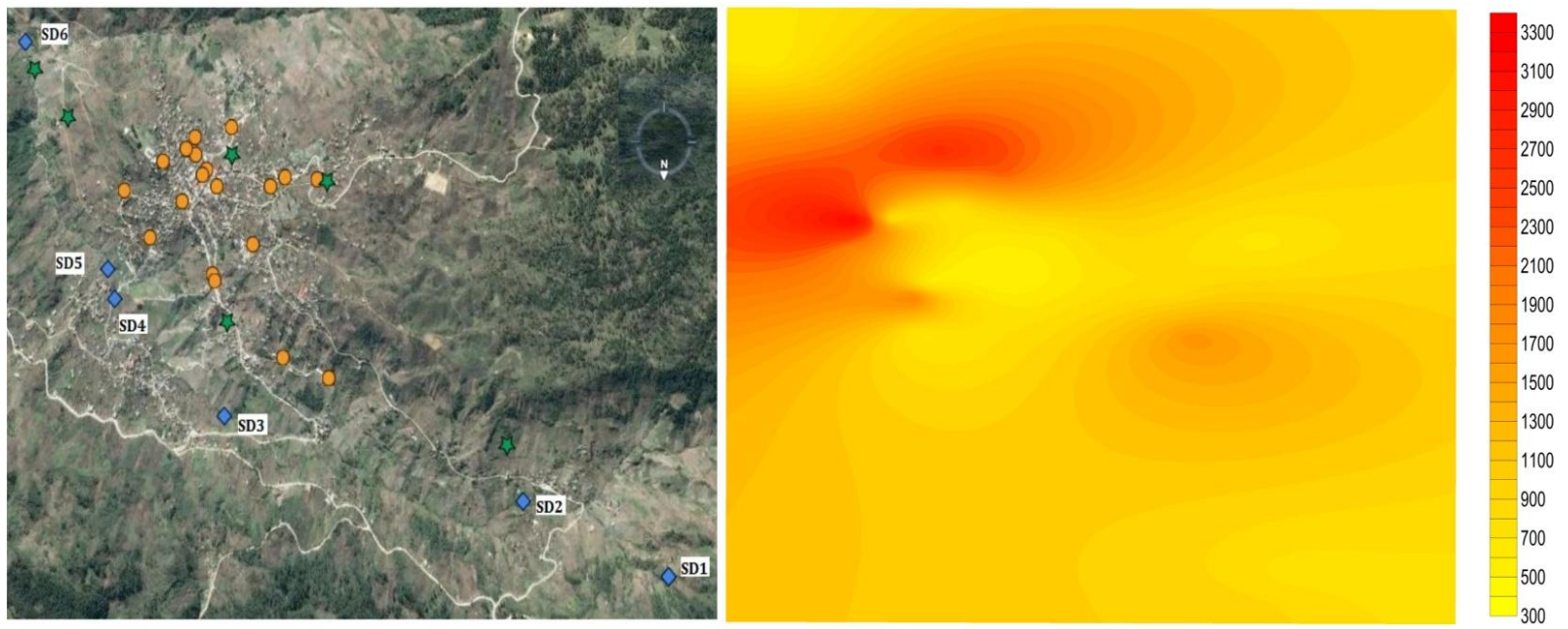


Figure 4-2: Spatial distribution of PAH in surface soils of San Mateo Ixtatán, Guatemala. Concentrations in µg/kg of dry weight.

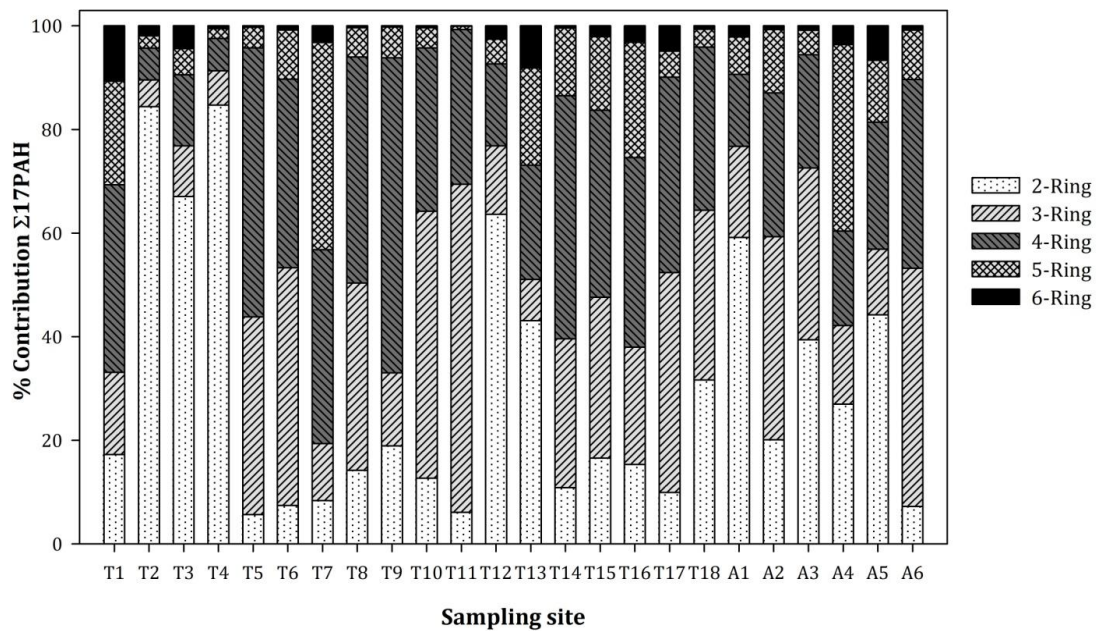


Figure 4-3: Percent contribution of 2, 3, 4, 5, 6-ring PAHs in surface soils of San Mateo Ixtatán.

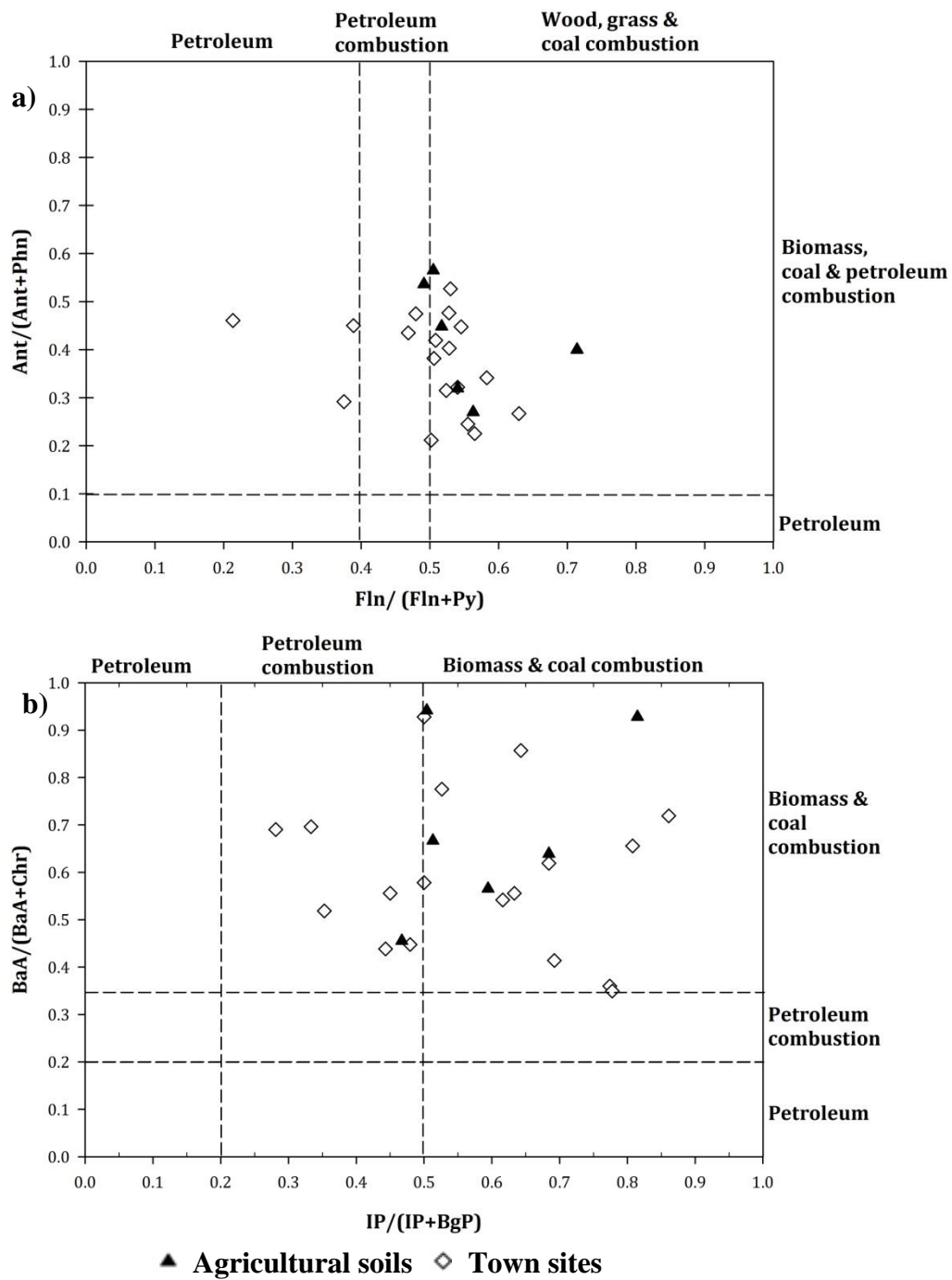


Figure 4-4: Cross plot of the Isometric ratios of (a) Ant/(Ant+Phn) vs Fln/(Fln+Pyr), and (b) BaA/(BaA+Chr) vs IP/(IP+BgP) in surface soil samples of San Mateo Ixtatán.

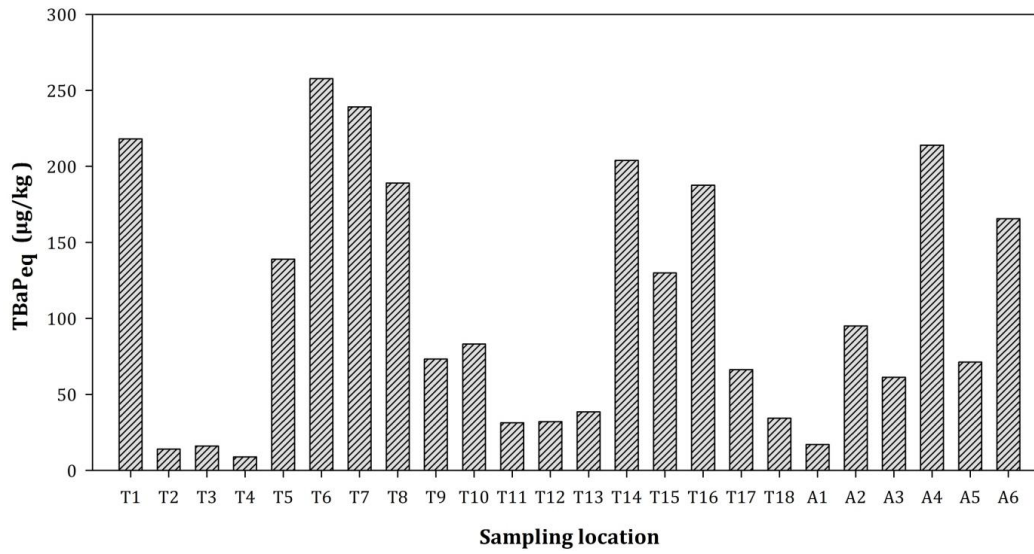


Figure 4-5: Graph showing the soil toxicity at various sampling sites expressed in terms of Benzo[a]pyrene equivalent concentrations.

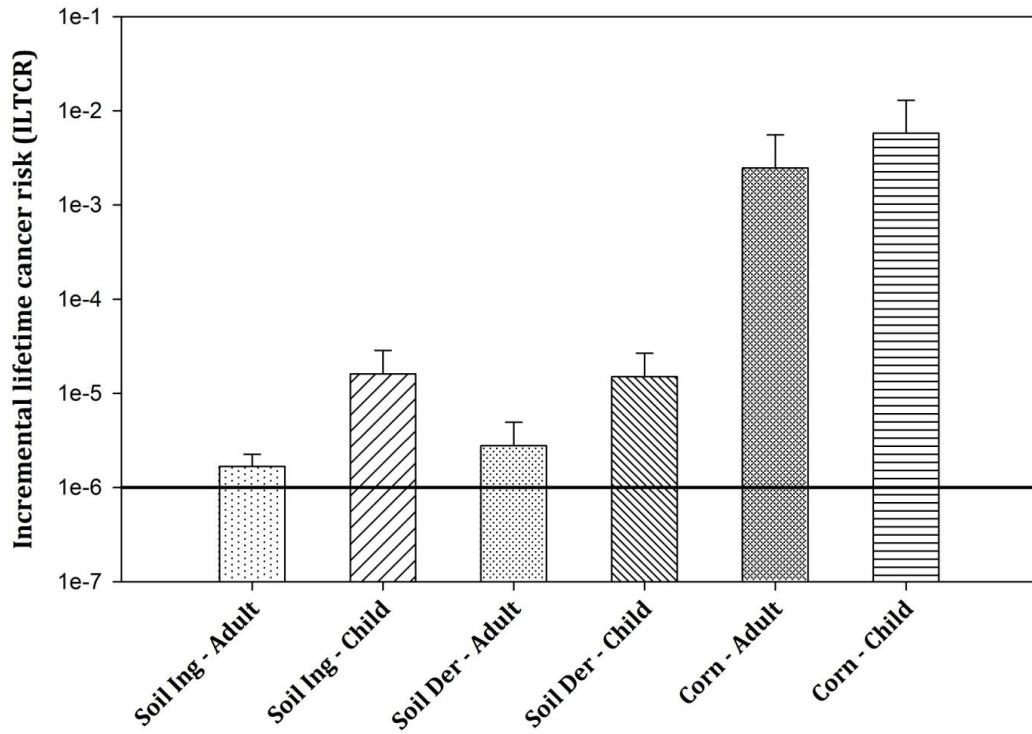


Figure 4-6: The estimated Incremental lifetime cancer risk due to ingestion of soil, through dermal contact and dietary uptake of PAH through corn. The line indicates acceptable risk level of 1×10^{-6}

References

- [1] T. Agarwal, P.S. Khillare, V. Shridhar, S. Ray, Pattern, sources and toxic potential of PAHs in the agricultural soils of Delhi, India, *J. Hazard. Mater.* 163 (2009) 1033–1039. doi:10.1016/j.jhazmat.2008.07.058.
- [2] Y.-F. Jiang, X.-T. Wang, F. Wang, Y. Jia, M.-H. Wu, G.-Y. Sheng, et al., Levels, composition profiles and sources of polycyclic aromatic hydrocarbons in urban soil of Shanghai, China, *Chemosphere*. 75 (2009) 1112–1118. doi:10.1016/j.chemosphere.2009.01.027.
- [3] R. Xiao, J. Bai, J. Wang, Q. Lu, Q. Zhao, B. Cui, et al., Polycyclic aromatic hydrocarbons (PAHs) in wetland soils under different land uses in a coastal estuary: Toxic levels, sources and relationships with soil organic matter and water-stable aggregates, *Chemosphere*. 110 (2014) 8–16. doi:10.1016/j.chemosphere.2014.03.001.
- [4] S.R. Wild, K.C. Jones, Polynuclear aromatic hydrocarbons in the United Kingdom environment: A preliminary source inventory and budget, *Environ. Pollut.* 88 (1995) 91–108. doi:10.1016/0269-7491(95)91052-M.
- [5] M. Trapido, Polycyclic aromatic hydrocarbons in Estonian soil: contamination and profiles, *Environ. Pollut.* 105 (1999) 67–74. doi:10.1016/S0269-7491(98)00207-3.
- [6] Z. Wang, J. Chen, X. Qiao, P. Yang, F. Tian, L. Huang, Distribution and sources of polycyclic aromatic hydrocarbons from urban to rural soils: A case study in Dalian, China, *Chemosphere*. 68 (2007) 965–971. doi:10.1016/j.chemosphere.2007.01.017.
- [7] H.W. Mielke, G. Wang, C.R. Gonzales, B. Le, V.N. Quach, P.W. Mielke, PAH and metal mixtures in New Orleans soils and sediments, *Sci. Total Environ.* 281 (2001) 217–227. doi:10.1016/S0048-9697(01)00848-8.
- [8] S.A. Stout, T.P. Graan, Quantitative Source Apportionment of PAHs in Sediments of Little Menomonee River, Wisconsin: Weathered Creosote versus Urban Background, *Environ. Sci. Technol.* 44 (2010) 2932–2939. doi:10.1021/es903353z.
- [9] H. Budzinski, I. Jones, J. Bellocq, C. Piérard, P. Garrigues, Evaluation of sediment contamination by polycyclic aromatic hydrocarbons in the Gironde estuary, *Mar. Chem.* 58 (1997) 85–97. doi:10.1016/S0304-4203(97)00028-5.
- [10] A.M. Kipopoulou, E. Manoli, C. Samara, Bioconcentration of polycyclic aromatic hydrocarbons in vegetables grown in an industrial area, *Environ. Pollut.* 106 (1999) 369–380. doi:10.1016/S0269-7491(99)00107-4.
- [11] WHO. *Bulletin of the World Health Organization*, (2000).
- [12] C. Boman, E. Pettersson, R. Westerholm, D. Boström, A. Nordin, Stove Performance and Emission Characteristics in Residential Wood Log and Pellet Combustion, Part 1: Pellet Stoves, *Energy Fuels*. 25 (2011) 307–314. doi:10.1021/ef100774x.

- [13] E. Pettersson, C. Boman, R. Westerholm, D. Boström, A. Nordin, Stove Performance and Emission Characteristics in Residential Wood Log and Pellet Combustion, Part 2: Wood Stove, *Energy Fuels*. 25 (2011) 315–323. doi:10.1021/ef1007787.
- [14] WHO. The health effects of indoor air pollution exposure in developing countries, (2002).
- [15] Z. Li, A. Sjödin, L.C. Romanoff, K. Horton, C.L. Fitzgerald, A. Eppler, et al., Evaluation of exposure reduction to indoor air pollution in stove intervention projects in Peru by urinary biomonitoring of polycyclic aromatic hydrocarbon metabolites, *Environ. Int.* 37 (2011) 1157–1163. doi:10.1016/j.envint.2011.03.024.
- [16] I. Romieu, H. Riojas-Rodríguez, A.T. Marrón-Mares, A. Schilmann, R. Perez-Padilla, O. Masera, Improved Biomass Stove Intervention in Rural Mexico, *Am. J. Respir. Crit. Care Med.* 180 (2009) 649–656. doi:10.1164/rccm.200810-1556OC.
- [17] L.P. Naeher, Biomass-fueled Intervention Stoves in the Developing World, *Am. J. Respir. Crit. Care Med.* 180 (2009) 586–587. doi:10.1164/rccm.200907-1115ED.
- [18] T.S.-S. M.fl, Reducing indoor air pollution with a randomised intervention design - a presentation of the Stove Intervention Study in the Guatemalan Highlands, *Nor. Epidemiol.* 14 (2004). <https://www.ntnu.no/ojs/index.php/norepid/article/view/236> (accessed November 1, 2014).
- [19] G. Rosa, L. Miller, T. Clasen, Microbiological Effectiveness of Disinfecting Water by Boiling in Rural Guatemala, *Am. J. Trop. Med. Hyg.* 82 (2010) 473–477. doi:10.4269/ajtmh.2010.09-0320.
- [20] U.S. EPA, Standard operating procedures; SOP 2012. soil sampling, (2000).
- [21] U.S. EPA, standard operating procedures; SOP 2016. sediment sampling, (1994).
- [22] K.-C. Chiang, C.-P. Chio, Y.-H. Chiang, C.-M. Liao, Assessing hazardous risks of human exposure to temple airborne polycyclic aromatic hydrocarbons, *J. Hazard. Mater.* 166 (2009) 676–685. doi:10.1016/j.jhazmat.2008.11.084.
- [23] I.C.T. Nisbet, P.K. LaGoy, Toxic equivalency factors (TEFs) for polycyclic aromatic hydrocarbons (PAHs), *Regul. Toxicol. Pharmacol.* 16 (1992) 290–300. doi:10.1016/0273-2300(92)90009-X.
- [24] L.C. Paraíba, S.C.N. Queiroz, A. de H.N. Maia, V.L. Ferracini, Bioconcentration factor estimates of polycyclic aromatic hydrocarbons in grains of corn plants cultivated in soils treated with sewage sludge, *Sci. Total Environ.* 408 (2010) 3270–3276. doi:10.1016/j.scitotenv.2010.04.026.
- [25] O. of S.W.E.R. US EPA, Risk Assessment Guidance for Superfund (RAGS), Volume I: Human Health Evaluation Manual (Part E, Supplemental Guidance for Dermal Risk Assessment) Interim, (n.d.). <http://epa.gov/oswer/riskassessment/ragse/index.htm> (accessed October 30, 2014).

- [26] Y. Yang, X.-X. Zhang, T. Korenaga, Distribution of Polynuclear Aromatic Hydrocarbons (PAHs) in the Soil of Tokushima, Japan, *Water, Air, Soil Pollut.* 138 (2002) 51–60. doi:10.1023/A:1015517504636.
- [27] M.K. Chung, R. Hu, K.C. Cheung, M.H. Wong, Pollutants in Hong Kong soils: Polycyclic aromatic hydrocarbons, *Chemosphere.* 67 (2007) 464–473. doi:10.1016/j.chemosphere.2006.09.062.
- [28] S. Orecchio, Polycyclic aromatic hydrocarbons (PAHs) in indoor emission from decorative candles, *Atmos. Environ.* 45 (2011) 1888–1895. doi:10.1016/j.atmosenv.2010.12.024.
- [29] M. Nadal, M. Schuhmacher, J.L. Domingo, Levels of PAHs in soil and vegetation samples from Tarragona County, Spain, *Environ. Pollut.* 132 (2004) 1–11. doi:10.1016/j.envpol.2004.04.003.
- [30] J.J. Nam, G.O. Thomas, F.M. Jaward, E. Steinnes, O. Gustafsson, K.C. Jones, PAHs in background soils from Western Europe: Influence of atmospheric deposition and soil organic matter, *Chemosphere.* 70 (2008) 1596–1602. doi:10.1016/j.chemosphere.2007.08.010.
- [31] P. Weiss, A. Riss, E. Gschmeidler, H. Schentz, Investigation of heavy metal, PAH, PCB patterns and PCDD/F profiles of soil samples from an industrialized urban area (Linz, Upper Austria) with multivariate statistical methods, *Chemosphere.* 29 (1994) 2223–2236. doi:10.1016/0045-6535(94)90390-5.
- [32] Q.-Y. Cai, C.-H. Mo, Y.-H. Li, Q.-Y. Zeng, A. Katsoyiannis, Q.-T. Wu, et al., Occurrence and assessment of polycyclic aromatic hydrocarbons in soils from vegetable fields of the Pearl River Delta, South China, *Chemosphere.* 68 (2007) 159–168. doi:10.1016/j.chemosphere.2006.12.015.
- [33] L. Tang, X.-Y. Tang, Y.-G. Zhu, M.-H. Zheng, Q.-L. Miao, Contamination of polycyclic aromatic hydrocarbons (PAHs) in urban soils in Beijing, China, *Environ. Int.* 31 (2005) 822–828. doi:10.1016/j.envint.2005.05.031.
- [34] T. Ramdahl, Retene—a molecular marker of wood combustion in ambient air, *Nature.* 306 (1983) 580–582. doi:10.1038/306580a0.
- [35] R. Lohmann, E. Nelson, S.J. Eisenreich, K.C. Jones, Evidence for Dynamic Air–Water Exchange of PCDD/Fs: A Study in the Raritan Bay/Hudson River Estuary, *Environ. Sci. Technol.* 34 (2000) 3086–3093. doi:10.1021/es990934r.
- [36] R. Lohmann, G.L. Northcott, K.C. Jones, Assessing the Contribution of Diffuse Domestic Burning as a Source of PCDD/Fs, PCBs, and PAHs to the U.K. *Atmosphere, Environ. Sci. Technol.* 34 (2000) 2892–2899. doi:10.1021/es991183w.
- [37] S. Tao, Y.H. Cui, F.L. Xu, B.G. Li, J. Cao, W.X. Liu, et al., Polycyclic aromatic hydrocarbons (PAHs) in agricultural soil and vegetables from Tianjin, *Sci. Total Environ.* 320 (2004) 11–24. doi:10.1016/S0048-9697(03)00453-4.

- [38] M.B. Yunker, R.W. Macdonald, R. Vingarzan, R.H. Mitchell, D. Goyette, S. Sylvestre, PAHs in the Fraser River basin: a critical appraisal of PAH ratios as indicators of PAH source and composition, *Org. Geochem.* 33 (2002) 489–515. doi:10.1016/S0146-6380(02)00002-5.
- [39] Ravindra, A.K. Mittal, R. Van Grieken, Health risk assessment of urban suspended particulate matter with special reference to polycyclic aromatic hydrocarbons: a review, *Rev. Environ. Health.* 16 (2001) 169–189.
- [40] R.C. Henry, C.W. Lewis, P.K. Hopke, H.J. Williamson, Review of receptor model fundamentals, *Atmospheric Environ.* 1967. 18 (1984) 1507–1515. doi:10.1016/0004-6981(84)90375-5.
- [41] R.K. Larsen, J.E. Baker, Source Apportionment of Polycyclic Aromatic Hydrocarbons in the Urban Atmosphere: A Comparison of Three Methods, *Environ. Sci. Technol.* 37 (2003) 1873–1881. doi:10.1021/es0206184.
- [42] Duval, M. M., and S. K. Friedlander. "Source resolution of polycyclic aromatic hydrocarbons in the Los Angeles atmosphere application of a CMB with first-order decay." *United States Environmental Protection Agency, Washington, DC*(1981).
- [43] R.M. Harrison, D.J.T. Smith, L. Luhana, Source Apportionment of Atmospheric Polycyclic Aromatic Hydrocarbons Collected from an Urban Location in Birmingham, U.K., *Environ. Sci. Technol.* 30 (1996) 825–832. doi:10.1021/es950252d.
- [44] K. Ravindra, R. Sokhi, R. Van Grieken, Atmospheric polycyclic aromatic hydrocarbons: Source attribution, emission factors and regulation, *Atmos. Environ.* 42 (2008) 2895–2921. doi:10.1016/j.atmosenv.2007.12.010.
- [45] N.R. Khalili, P.A. Scheff, T.M. Holsen, PAH source fingerprints for coke ovens, diesel and, gasoline engines, highway tunnels, and wood combustion emissions, *Atmos. Environ.* 29 (1995) 533–542. doi:10.1016/1352-2310(94)00275-P.
- [46] B.M. Jenkins, A.D. Jones, S.Q. Turn, R.B. Williams, Emission Factors for Polycyclic Aromatic Hydrocarbons from Biomass Burning, *Environ. Sci. Technol.* 30 (1996) 2462–2469. doi:10.1021/es950699m.
- [47] O.A. Torres, E. Palencia, L.L. de Pratdesaba, R. Grajeda, M. Fuentes, M.C. Speer, et al., Estimated Fumonisin Exposure in Guatemala Is Greatest in Consumers of Lowland Maize, *J. Nutr.* 137 (2007) 2723–2729.
- [48] O. of S.W.E.R. US EPA, Risk Assessment Guidance for Superfund (RAGS) Part A, (n.d.). <http://www.epa.gov/oswer/riskassessment/ragsa/index.htm> (accessed October 30, 2014).
- [49] P.H. Santschi, B.J. Presley, T.L. Wade, B. Garcia-Romero, M. Baskaran, Historical contamination of PAHs, PCBs, DDTs, and heavy metals in Mississippi River Delta, Galveston Bay and Tampa Bay sediment cores, *Mar. Environ. Res.* 52 (2001) 51–79. doi:10.1016/S0141-1136(00)00260-9.

- [50] Z. Zhang, J. Huang, G. Yu, H. Hong, Occurrence of PAHs, PCBs and organochlorine pesticides in the Tonghui River of Beijing, China, *Environ. Pollut.* 130 (2004) 249–261. doi:10.1016/j.envpol.2003.12.002.

Appendices

Selecting an antimicrobial filter media for improved stormwater best management practices

By

Laura A. Schifman^{1*}, Varun K. Kasaraneni², Ryan K. Sullivan¹, Vinka Oyanedel-Craver², Thomas B. Boving^{1,2}

Submitted to water research

¹ Department of Geosciences, University of Rhode Island, Kingston RI 02881, USA

² Department of Civil and Environmental Engineering, University of Rhode Island, Kingston RI 02881, USA

ABSTRACT

Stormwater runoff can contain high concentrations pathogens that can impair water bodies used for drinking or recreational purposes. Currently, stormwater best management practices (BMP) are not designed to treat bacteria. In this study, we amended red cedar wood chips with different loadings of two antimicrobial compounds: 3-(trihydroxysilyl)propyldimethyloctadecyl ammonium chloride (TPA) and silver nanoparticles (AgNP) for use in BMPs. After exposing *Escherichia coli* suspensions to the modified wood for three hours, the culturable bacteria in the aqueous and attached phase were determined. Results showed that *E. coli* inactivation, at 25°C, can be achieved with log₁₀ removal values (LRV) up to 3.71 ± 0.38 (mean ± standard error) for TPA-red cedar and 2.25 ± 1.00 for AgNP-red cedar, while unmodified red cedar only achieved 0.45 log₁₀. Similar trends were obtained when a temperature of 17.5°C was used. At even lower temperature (10°C) there was no difference in the level of bacteria inactivation between modified and unmodified cedar wood. The stability of the amended materials, in terms of efficiency, was also tested through storage under saturated conditions for 120 days, (equivalent to ~4.25 years of projected field use). It was observed that the level of bacteria inactivation for concentrations of 10⁶ CFU/100ml using 6 mg/g TPA modified red cedar was reduced from 2.20 log₁₀ to 1.62 log₁₀ over the storage period, which was still elevated compared to unmodified red cedar at 0.42 log₁₀. This study demonstrated that cedar wood chips amended to have antimicrobial properties could be applied as a filter media in structural BMP systems, such as tree filters.

1. INTRODUCTION

Stormwater runoff mobilizes microorganisms into surface and ground water bodies, potentially impairing their quality (Schueler and Holland 2000; Ahn et al. 2005; Göbel, Dierkes and Coldewey 2007; Parker, McIntyre and Noble 2010). Research links microbial inputs from stormwater runoff and other nonpoint sources with elevated prevalence of waterborne diseases (Rose et al. 2000; Curriero et al. 2001). *Escherichia coli* (*E. coli*) and fecal coliforms are typically monitored in watersheds, as their presence is used as indicator of pathogenic microbial contamination (U.S. Environmental Protection Agency. 2001; U.S. Environmental Protection Agency 2012). In runoff, *E. coli* concentrations often exceed 10^4 colony-forming units (CFU) per 100 ml (Schueler and Holland 2000; U.S. Environmental Protection Agency 2001; Ahn et al. 2005). These levels are considered a public health hazard in recreational waters according to the current environmental regulations (U.S. Environmental Protection Agency. 2001; U.S. Environmental Protection Agency 2012). Coastal areas are vulnerable to microbiological contamination, as high bacteria loads are introduced through untreated surface water runoff during storm events, resulting in beach closures and impacting the economic activities of coastal communities (Mallin et al. 2000; McLellan and Salmore 2003; Ahn et al. 2005; Lee et al. 2006; Parker, McIntyre and Noble 2010; Dorfman and Rosselot 2012). Despite the risks to human health, there are very few regulations pertaining to the removal of pathogens from stormwater runoff. Currently, Rhode Island is the only state in the United States that requires bacteria removal of 60% from stormwater runoff through the use of structural best management practices (BMPs) (Rhode Island Department of Environmental Management 2010; EPA 2011). However, 60% removal of bacteria at concentrations of 10^4 CFU/100 ml in runoff may not result in acceptable water quality, depending on the level of mixing in the receiving water body. There are currently very few BMP technologies that advertise bacterial removal capacities, e.g. *BactoLoxx* (Filtrexx, Goffstown, NH) or *Bacterra* (Filtterra Bioretention Designs, Ashland, VA). The *BactoLoxx* technology relies on proprietary flocculation agents that result in the settling of

bacteria (Faucette et al. 2009), and *Bacterra* relies on physical filtration and predation from biomat formation (Coffman, Ruby and Beach 2008). Their stated bacteria removal efficiency reaches up to 99%, however field studies indicated that bacteria removal is variable and can range from 0-80%, which is not considered sufficient from a public health perspective when taking into consideration bacteria concentrations in runoff (U.S. Environmental Protection Agency 2012; Schueler and Holland 2000; U.S. Environmental Protection Agency. 2001; Ahn et al. 2005.) Additionally, recent studies on a wide range of structural BMPs concluded that their removal was less effective, as the removal of pathogens primarily relied on attachment/collection and not inactivation (Stevik et al. 2004; Zhang and Lulla 2006). This is because sorbed pathogens can remain viable during attachment (Davies and Bavor 2000; Mohanty et al. 2013) and therefore can be remobilized/detached during intermittent flow conditions (Mohanty et al. 2013). This is especially relevant in areas with high water tables, because not enough soil depth is present to filter out pathogens effectively, therefore increasing the risk of bacterial contamination (Morales et al. 2014). New approaches are therefore needed to enhance the inactivation of pathogenic organisms in stormwater and possibly implement these technologies in the next generation BMPs. Materials with antimicrobial properties, such as nanoparticles and polymeric compounds, are widely and successfully used in many applications, ranging from treated fabrics in the medical industry (Li et al. 2006; Song, Kong and Jang 2011) to point of use water filtration (Oyanedel-Craver and Smith 2007; Zhang and Oyanedel-Craver 2013). Other, chemically less complex compounds suggested for removing bacteria include iron oxide or copper (Mohanty et al. 2013; Ren et al. 2009). Prior studies investigated various media, including wood chips and shale to enhance stormwater treatment of BMPs (Kasaraneni et al. 2014; Li, Deletic and McCarthy 2014). However, these studies focused primarily on the amendment procedures and did not evaluate these modified materials for their antimicrobial properties. Particularly, the use of 3-trihydroxy silylpropyldimethyloctadecyl ammonium chloride solution (TPA) and silver nanoparticles (AgNP) antimicrobials in stormwater treatment applications has not been documented. Here, we

hypothesize that antimicrobial properties of TPA and AgNP can be transferred to cedar wood and that the resulting material can significantly enhance the microbial treatment of stormwater runoff under a range of environmental conditions.

Recent studies compared bacteria transport, removal, and mobilization through natural and amended porous media (Mohanty et al. 2013; Li, Deletic and McCarthy 2014). It was found that the performance of antimicrobial materials in the aqueous phase or materials containing an antimicrobial coating is primarily a function of dose, contact time, and temperature (Gayán et al. 2011; Raffellini et al. 2011; Zhang and Oyanedel-Craver 2013). For instance, it was shown that bacteria survival rates were higher while inactivation rates were lower at lower temperatures (15°C) relative to temperatures ranging from 20 to 25°C (Stevik et al. 2004; Chandrasena, Deletic and McCarthy 2013).

The scope of this research was to develop materials with antimicrobial properties than can effectively treat stormwater runoff contaminants with emphasis on inactivation of pathogens. Red cedar wood was chosen as the base material and silver nanoparticles (AgNPs) and 3-(trihydroxysilyl) propyldimethyloctadecyl ammonium chloride (TPA) were the antimicrobial agents. Red cedar was chosen due to its high affinity for organic contaminants and heavy metals (Kasaraneni et al. 2014) and its resistance to degradation (Grohs, Wegen and Kunz 1999). Silver nanoparticles (AgNPs) and TPA are antimicrobials with proven environmental applications such as drinking water treatment (Zhang and Oyanedel-Craver 2013). Based on our prior research, both amendments have enhanced removal of organic and inorganic contaminants and are expected to provide antimicrobial properties (Kasaraneni et al. 2014).

The aim of this current study is to select a material based on the inactivation performance for use in a structural BMP. The antimicrobial performance of a material in a complex environment such as a stormwater BMP depends on factors such as amount of antimicrobial in the filtration matrix, microbial loading, temperature, hydraulic loading (contact time), water chemistry etc. Testing several variables in such a complex environment under dynamic real-time conditions is

challenging. Through the use of batch isotherm experiments the abovementioned variables can be individually tested. Therefore the importance of individual variables can be identified. Here we used a batch experiment approach and tested the effect of 1) antimicrobial (AgNP and TPA) loading, 2) exposure time, 3) concentration of microbes, and 4) effects of exposure temperature. The specific objectives of this study were to 1) perform kinetic studies and model the disinfection performance to achieve a desired bacteria inactivation given a specific disinfectant concentration and exposure time; 2) determine the microbial inactivation efficiency of red cedar modified with varying loadings of AgNPs and TPA, 3) evaluate the bacteria removal efficiency of the three most effective materials at lower temperatures, and 4) evaluate the long term saturated storage impacts on the inactivation efficiency of the three most effective materials.

2. METHODS

2.1 Materials

Untreated red cedar (RC) wood, obtained from Liberty Cedar and New England Wood Products (both West Kingston, RI), was chipped, thoroughly mixed, and sieved. Wood chips passing through a 10 mm sieve, but retained on a 3.3 mm sieve were collected and used for the experiments. Wood chips were soaked in deionized water for a minimum of two weeks to leach out soluble matter and remove fines. Biosafe (Pittsburgh, PA) provided a 5% solution of TPA (EPA product Reg.No. 83019-2). The TPA molecule differs from other organosilane quaternary ammonium compounds previously studied (e.g. Torkelson et al. 2012 (Torkelson et al. 2012)) as the structure is a polymer consisting of a mixture of condensed 3-(trihydroxysilyl) propyldimethyloctadecyl ammonium chloride molecules (Figure 3-S1). AgNPs were synthesized in the laboratory via the Tollens method as described by Zhang et al. 2012 (Zhang, Smith and Oyanedel-Craver 2012), using polyvinylpyrrolidone (PVP, average molecular weight: 29,000 g/mol, Sigma Aldrich) as a stabilizer. To achieve various loadings of TPA and AgNPs, red cedar wood chips were amended following procedures described in Kasaraneni et al. (2014) (Table 1).

Briefly, wood chips were submerged in TPA or AgNP solutions of 1.3 mmol/L ionic strength (NaCl) and were allowed to equilibrate for four to six days on a shaker to achieve a range of loadings that include the maximum possible loading of each antimicrobial (Table 1) (more details on modification and desorption in Kasaraneni et al. (2014)). A nonpathogenic wild strain of *E. coli* (IDEXX, Westbrook, ME, USA) was used to test the antimicrobial performance. *E. coli* was chosen as it is commonly used as indicator bacteria for fecal contamination in drinking water and surface waters and is commonly monitored under stormwater regulations (Edberg et al. 2000; Wheeler Alm, Burke and Spain 2003; Ashbolt 2004; Dorfman and Rosselot 2012). In addition it is widely used in testing filter media for drinking water treatment (Zhang, Smith and Oyanedel-Craver 2012; Zhang and Oyanedel-Craver 2013).

2.2 Experimental Methodology

The first part of the study involved batch experiments to test the inactivation kinetics of TPA and AgNP modified RC at 25°C and establishing whether exposure time or disinfectant loading had the main contribution on bacteria inactivation. This was followed by testing the disinfection performance of each material at 25°C and establishing bacteria inactivation efficiency at three different temperatures (25°C, 17.5 °C and 10°C) for the most effective materials. In the last part of the study, the amended materials were submerged in water to test for possible changes in bacteria inactivation efficiency over 120 day period.

During all experiments the solution ratio was 1 g of sorbent to 25 ml of solution containing the desired *E. coli* concentration. This ratio was based on a previous study that tested the performance of contaminant removal from an aqueous solution using the wood chips. All experiments were carried out in triplicates. Controls, buffer blanks, and NaCl blanks were analyzed for quality control purposes and to establish natural decay of bacteria over the experimental period. All solutions, glassware and other materials used for the experiments were sterilized through autoclaving.

2.2.1 Bacteria Culturing and Enumeration

Bacteria were cultured in LB broth (10 g/L Sodium Chloride, 10 g/L Tryptone, and 5 g/L Yeast Extract, Sigma Aldrich) at 37.5 °C for 13 hrs. After culturing, the bacteria were removed from the LB broth, washed and stored in phosphate buffer solution (11.2 g/L K₂HPO₄, 4.8 g/L KH₂PO₄, and 20 mg/L ethylenediaminetetraacetic acid, all Sigma Aldrich; pH: 7.3). *E. coli* concentration was determined using the membrane filtration technique, applying m-FC with Rosalic Acid Broth (Millipore) with subsequent incubation at 44.5 °C for 24-48 hrs. To enumerate bacteria attached onto the solid phase, samples were carefully sonicated (QSonica, Q125) twice at 20% amplitude in 25 ml phosphate buffer solution for 10 minutes each and filtered following the above procedure. The sonication procedure was previously established by Rayner et al. (2013) (Rayner et al. 2013), further tests were performed to determine the number of cycles required and the effect of sonication on *E.coli* (data not shown). The test results indicated that two cycles for 10 min is sufficient to remove *E.coli* that can detach from the wood chips and the sonication did not inactivate *E.coli*.

2.2.2 Inactivation Kinetics

The experiments were conducted with solutions containing *E. coli* at 10⁶ CFU/100 ml and 10⁵ CFU/100 ml in 1.3 mM NaCl solution at 25°C in a rotisserie incubator set to 5 rpm (Major Science, Saratoga, CA, USA). Contact times were 30 min, 90 min, to 180 min. The resulting data was fitted to the Chick-Watson model (Equation 1)(Haas and Karra 1984)

$$\ln\left(\frac{N_t}{N_0}\right) = -k'C^n t \quad \text{Equation 1}$$

where N_t/N_0 [-] is the ratio of *E. coli* concentration at time t [min] relative to the initial *E. coli* concentration, k' [mg/g t] is the die-off constant, C [mg/g] is the disinfectant concentration, and n [-] is the coefficient of dilution, which determines the importance of disinfectant concentration. In

the Chick-Watson model, if $n=1$ both time and disinfectant concentration are equally important. If $n>1$, the disinfectant concentration is more important than time and vice-versa if $n<1$ (Tchobanoglous, Burton and Stensel).

The parameterized model (details in SI) was tested against the experimental data and a percentage difference was calculated to determine whether the model over or underestimated inactivation kinetics.

2.2.3 Inactivation Efficiency of Amended Red Cedar

To test the bacteria inactivation efficiency as a function of antimicrobial amendment loading, batch experiments with *E. coli* solutions at five different concentrations ranging from 10^2 to 10^6 CFU/100ml were prepared in 1.3 mM NaCl solution. These solutions were exposed to unmodified, TPA modified (loading range: 3.6 mg/g to a maximum loading of 9.3 mg/g TPA) and AgNP modified (0.33 mg/g to a maximum loading of 0.68 mg/g AgNP) red cedar (from now on test materials are abbreviated as shown in Table 1) at 25 °C in a rotisserie incubator set to 5 rpm (Major Science, Saratoga, CA, USA). The exposure time was 180 minutes. This time was based on a preliminary kinetic study in which a ~50% reduction of *E. coli* was measured when exposed to unmodified red cedar (UM) at 25 °C (data not shown). The inactivation efficiency of the materials was calculated as \log_{10} removal value (LRV):

$$\text{LRV} = \log_{10} (C_0) - \log_{10} (C_t) \quad \text{Equation 3}$$

Where C_0 is the initial *E. coli* concentration and C_t is the final *E. coli* concentration, which is the sum of the *E. coli* that survived in both the aqueous phase and the *E. coli* attached to the unmodified or modified RC material.

To observe the differences in active *E. coli* present on the surface of unmodified and 6mg/g TPA modified red cedar, scanning electron microscope (SEM) images were taken. Each of the wood chips were put in contact with 10^6 CFU/100 ml for three hours in a rotary incubator at 25°C set to 5 rpm (Major Science, Saratoga, CA, USA) and prepared for SEM analysis (details in SI and

Pathan et al. (2013)). Although all the materials were test in the same set of experiments, the inactivation efficiency data for unmodified red cedar, 6TPA and 0.6 Ag were published as part of a proof of concept paper (Kasaraneni et al. 2014) and the data for these three materials was supplemented with four additional amended materials to compare the whole spectrum of materials (Table 1)

2.2.4 Temperature Effect on Inactivation Performance

From the seven materials tested, the three best performing amended materials (6TPA, 9TPA, and 0.6AgNP; abbreviations explained in Table 1) along with UM were selected for testing possible effects of temperature on bacteria inactivation. The materials were exposed to an *E. coli* solution containing 10^6 CFU/100 ml in 1.3 mmol/L NaCl, at temperatures of 25°C, 17.5°C, or 10°C for 180 minutes in a temperature controlled rotisserie incubator set to 5 rpm (Major Science, Saratoga, CA, USA). Bacteria that survived the antimicrobial treatment were counted in the aqueous phase and the solid phase (*E. coli* culturable after attachment to the solid phase are measured as mentioned in Section 2.2.1) to determine removal through attachment and inactivation.

2.2.5 Long-term storage of modified materials and its impact on inactivation efficiency

Tests were conducted to determine how long term storage impacts the inactivation performance of the TPA and AgNP modified materials. Three amended RC sorbents (0.6AgNP, 6TPA, and 9TPA) were stored in the dark at room temperature without mixing under saturated conditions in sterile, deionized water for 120 days at the same ratio as the batch experiments (1:25). The reason deionized water was chosen as the medium for storage was that it provides the greatest concentration gradient from the modified red cedar wood chip into the aqueous phase. Therefore, if any desorption should take place, the gradient is favorable. The 120 day length of storage is equivalent to 4.25 years of an installed tree filter (TF) BMP assuming that the filter matrix in such

a BMP would be saturated for a maximum of 48 hours after a rain storm of ≥ 25 mm, which on average occurs 14 times per year in the Northeast United States, based on a 10-year data set obtained from a NOAA operated meteorological station in Providence, RI (NOAA, National Oceanic and Atmospheric Administration 2014). Antimicrobials have been observed to degrade over time when stored under saturated conditions (No et al. 2006). In comparison, it is assumed that unsaturated or dry storage will have lesser impact on inactivation efficiency over time as degradation occurs more slowly, however this has not been validated.

The inactivation efficiency was quantified immediately after modification (0 days), 60 days (equivalent to ~ 2.1 years), 94 days (equivalent to ~ 3.3 years), and 120 days (equivalent to ~ 4.25 years) after modification. At those times, subsamples of the stored material were exposed to 10^6 CFU/100 ml *E. coli* solutions (worst case scenario for stormwater loading (Schueler and Holland 2000)) in 1.3 mM NaCl. Exposure time was, once again, 180 minutes. The exposure temperature was set to 25°C in a temperature controlled rotary incubator that rotated at 5 rpm (Major Science, Saratoga, CA, USA). All modified materials were compared to unmodified red cedar. After 120 days, the storage solutions were tested for desorbed AgNPs or TPA. The storage solution containing AgNP modified red cedar was subsampled and digested using 2% nitric acid and filtered through a 0.45µm filter before analysis in a Perkin Elmer 3100 XL ICP-OES with a method detection limit of 0.01 mg/l for Ag. To test the TPA storage solution, a subsample was prepared following Hach Method 8337 and was analyzed on a Hach DR 2800, which had a method detection limit of 0.2 mg/L for TPA.

The disinfection efficiency at a specific time was modeled using Equation 4:

$$LRV(t) = (LRV_0 - LRV_{Final})e^{(-kt)} + LRV_{Final} \quad \text{Equation 4}$$

where LRV_0 is the initial LRV that was achieved by the freshly amended material, LRV_{Final} is the final LRV achieved after the material has been stored for 120 days, k is the disinfection efficiency rate loss constant, and t is the time of storage.

2.3 Statistical Analysis

To compare the overall inactivation efficiency of the different materials for all bacteria concentrations tested, a one-way ANOVA was performed. Post-hoc comparisons were carried out using Tukey's Honest Significant Difference. Analysis was carried out to analyze the fraction of culturable attached bacteria and the fraction of culturable bacteria in the aqueous phase. The data were compared based on \log_{10} removal at different temperatures using log-normalized data. In this ANCOVA, the culturable attachment *E. coli* concentrations were the response variable and the explanatory variables were the exposure temperature and the type of material. The model was simplified using a stepwise model simplification and AIC (Akaike's Information Criterion (Akaike 1998)) was used as a criterion for the minimal adequate model. The difference in disinfection performance using total *E. coli* survival as the reference at the three different temperatures (10°C, 17.5°C, and 25°C) were compared with a two-way ANOVA, where \log_{10} removal values (LRV) was the response variable and exposure temperature and material type were the factors.

To compare the inactivation kinetics of the different materials, an ANCOVA was carried out where LRV was the response variable and exposure time was the explanatory variable for each different type of red cedar treatment. The comparison between the LRV of the amended materials before and after long term storage was tested using a two-tailed t-test for each material. All statistical analyses had the alpha value set to 0.05 and were carried out using R version 3.0.3.

3. RESULTS AND DISCUSSION

3.1 Inactivation Kinetics

The kinetic studies data were evaluated with the Chick-Watson model (Haas and Karra 1984) (Equation 1) to determine the concentration-time dependency necessary to achieve a 2 \log_{10} (99%) reduction of total culturable *E. coli*. In addition, the Chick-Watson model parameters

differentiate whether the exposure time or antimicrobial loading had a greater impact on the reduction of the number of total culturable *E. coli*.

Over the 180 minute sampling period, the *E. coli* LRV increased with increased exposure time, following a generally log-linear trend for all materials (Figure 1). The order of calculated inactivation rates was as follows: 9TPA > 6TPA > 0.6AgNP > 0.3AgNP > 4TPA ~ 3TPA > UM. Except for 4TPA and 3TPA, the inactivation rates of 9TPA, 6TPA, 0.3AgNP, and 0.6AgNP are statistically different from the unmodified red cedar inactivation kinetics, while 3TPA and 4TPA are similar to unmodified red cedar (Table 2).

For both, TPA and AgNP amended red cedar, the coefficient of determination (r^2) for all regression equations created to parameterize the Chick-Watson model was 0.99, indicating that modeling the data using the Chick-Watson model is a valid approach even though the model was developed for aqueous phase inactivation kinetics (Tchobanoglous, Burton and Stensel). The model can be used to describe the inactivation kinetics of the amended materials using first order reaction kinetics.

Verifying the predictions of the model with the experimental data shows that there is good agreement between the modeled and observed data, as the predicted LRVs for both TPA and AgNP modified RC were within 25% of the observed LRV (Table 2).

In the parameterized model, the coefficient of dilution, n , indicates that the loading of TPA is more important than exposure time ($n = 1.99$ and $k' = -0.03$); whereas for AgNP modified red cedar exposure time is key for its disinfection performance ($n = 0.58$ and $k' = -1.18$). The model predicts that with 6TPA a 99% reduction of total number of culturable organisms of *E. coli* can be achieved within 3.7 hrs, while it is 5.9 hrs with 0.6AgNP (Table 2, Figure 1). The different bacteria inactivation mechanisms of TPA and AgNP support these findings. AgNPs slowly release Ag^+ ions and it therefore takes time to reach the ion concentration required for reduction of culturable organisms. (Sondi and Salopek-Sondi 2004; Kim et al. 2007) On the other hand,

while the positive charge of TPA attracts bacteria, it is the long carbon chains on the TPA molecule (SI Figure S1) that pierces the bacteria cell membrane. Therefore, reduction of total number of culturable organisms by TPA relies heavily on the TPA loading, i.e. the more TPA molecules, the better the chance of contact (Kim, Kim and Rhee 2010).

3.2 Inactivation Efficiency of Amended Red Cedar

Comparing all seven amended materials demonstrates that highly modified materials (0.6AgNP, 6TPA, 9TPA) are overall significantly more effective at deactivating *E. coli* over a three hour time period compared to unmodified and low modified materials (0.3AgNP, 3TPA, 4TPA; Figure 1).

The LRV of unmodified RC was less than 1 and similar results were obtained using low loading on RC (3TPA, 4TPA and 0.3 AgNP; Table 1, Figure 2). At high loadings (6TPA, 9TPA and 0.6AgNP), *E. coli* reduction increased significantly ($p < 0.001$, $DF=6$, $F=32.8$, ANOVA table in SI Table S1a&b) and the LRV was measured to be up to 3.71 ± 0.38 (>99.9%; Figure 2). The LRV for TPA or AgNP modified RC was independent of the initial *E. coli* concentration, which ranged from 10^2 CFU/100 ml to 10^6 CFU/100 ml. Instead the LRV was influenced by the antimicrobial amendment loading on the material. The natural decay in Figure 2 depicts the natural die-off of bacteria in the control solution containing only NaCl and cannot be attributed to the antimicrobial.

The SEM images support these findings, as the unmodified red cedar shows much higher numbers of *E. coli* and denser clusters of live bacteria present (Figure 3 a&b) on the surface of the wood compared to 6TPA red cedar, which shows fewer bacteria (Figure 3 c&d). At higher magnification, the bacteria cells that are present on the 6TPA material are damaged and/or ruptured (Figure 3d), compared to those on the unmodified red cedar (Figure 3b). The structure of the bacteria cells in the SEM images from Figure 3 can be compared to those in Figure S2 in the

supplemental information where active and TPA treated (inactive) bacteria were analyzed on the SEM. This visual observation suggests that TPA lowers the number of active *E.coli* on the surface of the wood and prohibits growth of cells on the wood surface.

Both, TPA and AgNP modified RC were successful at deactivating *E. coli* but in order to archive significantly higher LRV, a minimum loading of ~6 mg/g is required for TPA and 0.6 mg/g for AgNP. Based on these results, the materials with higher antimicrobial agent loading (6TPA, 9TPA, and 0.6AgNP) were chosen for testing the effect of lower exposure temperatures and storage time on inactivation efficiency.

3.3 Temperature Effect on Performance of Amended Red Cedar

The performance of the highly amended materials (6TPA, 9TPA, and 0.6AgNP) was tested at three temperatures (10°C, 17.5°C, and 25 °C). Unmodified RC was used as a baseline comparison.

Over the 180 minutes exposure period and at all temperatures (10°C, 17.5°C, and 25 °C), *E. coli* remained culturable in both the aqueous solution and after attachment for all treatments (Figure 4). Fewer *E. coli* survived in total when in contact with amended materials at 25 °C and 17.5 °C compared to 10°C ($p < 0.001$, $DF=2$, $F\text{-value}= 14.78$, ANOVA Table in SI Table S2a). At 25°C, the type of material impacted the number of total culturable *E. coli* in this order: 9TPA < 6TPA ~ 0.6AgNP < UM, indicating that 9TPA has the highest inactivation value.

Bacteria can be permanently removed through inactivation, but can also be temporarily retained through attachment to surfaces (Mohanty et al. 2013). Generally, bacteria attachment is lower at elevated temperatures, compared to lower temperatures (McCaulou, Bales and Arnold 1995; 2010; Stevik et al. 2004). The higher modified materials (6TPA, 0.6 AgNP, and 9 TPA) showed that the survival of bacteria attached onto these surfaces is significantly lower at all temperatures compared to unmodified red cedar ($p < 0.001$, $DF=3$, $F\text{-value}=12.317$; ANOVA table in SI Table S2b; Figure 4b).

As the more highly modified materials have a greater concentration of antimicrobial agent on the surface of the red cedar, the likelihood of the bacteria coming in contact with an antimicrobial agent during attachment were greater than for unmodified and low modified materials. As the temperature increased, there are significantly fewer bacteria that survive once they attach to the modified red cedar surface ($p < 0.001$, $DF=2$, $F\text{-value}=49.92$, ANOVA table in Table S2b). This trend was clearly detected when comparing results at 17.5°C and 25°C (Figure 4b), whereas no difference in bacteria survival after attachment to the three amended materials was detected at 10°C. However, at 10°C survival after attachment for unmodified red cedar was two orders of magnitude higher compared to modified materials (Figure 4b). These results are consistent with previously reported studies, where lower temperatures, such as those used in this study, allowed for higher bacteria survival (Gayán et al. 2011; Raffellini et al. 2011). It is proposed that at lower temperatures the movement of the bacteria in solution is reduced and bacteria generally attach to surfaces in fewer numbers (Bales et al. 1991; McCaulou, Bales and Arnold 1995; 2010), resulting in fewer *E. coli* interacting with the antimicrobial agent. The reduced bacteria motility and attachment, along with a change in their cell membrane structure, making them more rigid at low temperature, (Shivaji and Prakash 2010) contribute to an overall reduced *E. coli* inactivation performance at low temperatures.

3.4 Long-term reduction of the disinfection efficiency of modified materials

The three most effective sorbent materials (0.6AgNP, 6TPA, and 9TPA) were tested to quantify if and how saturated bench storage impacts the inactivation performance of the materials. These materials showed changes in efficiency over time that resulted in a 26% to 38% decrease in LRV (Table 3, Figure 5) compared to freshly prepared material. The decay in removal efficiency of these materials fell into the following order: 9TPA > 0.6AgNP > 6TPA, where there decrease in inactivation efficiency was significantly different from the original, freshly prepared inactivation efficiency (Figure 5, Table S4). All models were fitted with $r^2 > 97\%$.

Possible explanations for reduction in performance are: 1) leaching /desorption of TPA and AgNP during storage time, 2) fines clogging the pores of the RC making the antimicrobial inaccessible, 3) degradation of antimicrobial agent, 4) diffusion of TPA and AgNP in to RC thereby becoming inaccessible, and 5) surface aggregation and bridging among TPA polymer molecules or AgNP, depending on the material, making the antimicrobial less accessible. Even though all materials exhibit a decrease in inactivation performance over time (Table 3 and Figure 5), there was non-significant leaching of either TPA (<0.02%) or AgNP (0%) and Ag⁺ ions (0%) from the RC sorbent, even after the full 120 days of storage. These findings are in agreement with Kasaraneni et al. (2014) and further suggest that desorption of antimicrobial agents cannot explain the observed lower inactivation performance. However, even though no total silver or silver ions were present in the storage solution when analyzed on the ICP-OES (detection limit 10ppb), the concentration of total silver or silver ions may be elevated at the wood chip-water interface, but may not be detected in the bulk sample (Unwin and Bard 1992; Barker et al. 1999; Pfeiffer et al. 2014). This phenomenon may not limit the antimicrobial effectiveness of AgNPs, as the concentration of Ag⁺ ions can still be elevated at the interface of the nanoparticle (Pfeiffer et al. 2014).

To test whether eroded red cedar fines might have settled on the wood surface after storage and thus limited access to the antimicrobial coating, all materials were agitated by ultrasound for 10 minutes. Subsequently, the inactivation efficiency of all material was tested again and compared to the non-sonicated materials' performances. Because the LRV for the sonicated and non-sonicated materials was the same, covering the actives sites by wood-derived fines could be ruled out as a reason for decreased inactivation efficiency after storage.

The measured decrease in inactivation performance over time could potentially be due to chemical degradation of the antimicrobial material. However, storing aqueous TPA solutions under the same conditions as the amended wood did not decrease the agent's concentration or its inactivation performance. Thus, degradation of the TPA antimicrobial is also not responsible for a

decrease in inactivation performance. Similarly, PVP stabilized AgNPs in aqueous solutions have been shown to be stable as well (Zhang, Smith and Oyanedel-Craver 2012). Rather than degrading, the antimicrobial amendments may diffuse from the wood's surface into its interior over time. This would make it more difficult for the bacteria to come in contact with the antimicrobial agent. Existing analytical models for diffusion into wood cannot be applied to describe the diffusion processes of these compounds (Burr and Stamm 1947; Behr, Briggs and Kaufert 1953) because the TPA and AgNP sorption processes to amend the red cedar do not behave in a linear fashion (Kasaraneni et al. 2014). It would therefore be necessary to develop a complex numerical model as suggested by Rügner, Kleineidam and Grathwohl (1999) to understand the diffusion dynamics of TPA and AgNP into wood. This was outside of the scope of our research and because the diffusion of comparably large molecules, such as TPA (estimated aqueous diffusion coefficient: $4.310^{-10} \text{ m}^2/\text{s}$), is a very slow process, significant diffusive transport into the wood matrix at the time scale investigated (120 days) was not considered a major contributing factor to the observed decrease in inactivation performance over time. Rather, it is hypothesized that the main reason for the decrease in inactivation efficiency over time is aggregation and bridging of the long carbon chain on TPA polymers and the PVP-stabilized AgNP. Through these processes the antimicrobial amendments enter a lower energy state (Rosen 1975; Rosen and Kunjappu 2012) because bridging/aggregating minimizes contact of the TPA polymer and PVP coated AgNPs with the polar water molecules that surround the wood chips.

While aggregated/bridged TPA and AgNP amendments can explain the decrease in antimicrobial effectiveness, the overall antimicrobial effectiveness of the filter material is not entirely compromised as the amended materials still outperforms the UM red cedar by 3.45 times after 120 days of storage. Further, much of the decrease in inactivation performance occurs after 60 days of storage, whereas the inactivation performance remains essentially stable for the remainder of the time (days 60-120) (Figure 5). Therefore, it can be postulated that the bridging/aggregating

occurs within the first 60 days of storage and thereafter the TPA polymer and PVP-stabilized AgNP have reached a stable state of continued inactivation performance.

3.5 Implications and Benefits to Using Antimicrobial Filter Materials

Red cedar wood chips amended with either TPA or AgNP have been shown to increase the removal of bacteria from water. Even though similar results could be achieved with chlorine or UV disinfection, both of which occur within minutes (Gayán et al. 2011; Tchobanoglous, Burton and Stensel), these two approaches have not found application in stormwater treatment because of complexity and cost of such treatment. (Tchobanoglous, Burton and Stensel) Relative to these technologies, the passive wood filtration approach described herein does not produce disinfection byproducts, as often observed when using chlorine. Further, using a passive approach of disinfection requires less energy, in particular compared to UV disinfection, which also involves frequent maintenance to ensure proper disinfection (Gayán et al. 2011; Tchobanoglous, Burton and Stensel).

Based on these properties, the red cedar wood chips amended with either TPA or AgNP could find use in stormwater treatment systems. An example is a Tree Filter BMP, which treats conventional stormwater pollutants, such as heavy metals or petroleum hydrocarbons, but could be outfitted with a layer of amended wood chips to provide additional antimicrobial treatment functions. Such a BMP system could potentially remove a much higher percentage of bacteria from stormwater runoff than most currently available treatment systems such as *BactoLoxx* (Filtrexx, Goffstown, NH) or *Bacterra* (Filterra Bioretention Designs, Ashland, VA). These currently available systems rely on sorption processes, pH changes, and natural predation by other organisms to achieve the reported removal of up to two \log_{10} units (99%) in *E. coli*, whereas up to 3- \log_{10} (99.9% removal) of *E. coli* can be achieved using the amended red cedar filter materials investigated herein. This removal far exceeds the 60% reduction in stormwater bacteria

levels required in the more recently formulated stormwater treatment manuals (Rhode Island Department of Environmental Management 2010).

More importantly, our laboratory study showed that once the wood has been amended, neither TPA nor AgNP showed significant desorption from red cedar, i.e. no detectable leachate for 0.6AgNP and 6TPA, and less than 0.02% of the mass loaded onto 9TPA. Therefore, introducing these materials into BMPs should not disturb native microbial communities such as denitrifiers that have ecological benefits. However, if leaching does occur, quaternary ammonium compounds have been shown to sorb to clay and other soil particles (Oyanedel-Craver and Smith 2006; Oyanedel-Craver, Fuller and Smith 2007; Kasaraneni et al. 2013). Also, the filter material maintained its ability to effectively remove bacteria from aqueous solutions. These are important findings because antimicrobials should not be introduced into the environment and any structural BMP should remain effective for years without major maintenance requirements. Even though both antimicrobials are strongly sorbed to the red cedar, there are benefits to using TPA over AgNP. This is because AgNP amended materials rely on the slow, but continuous release of Ag⁺ ions (Kim et al. 2007). Therefore the antimicrobial treatment efficiency of AgNP amended wood is expected to decrease eventually. In comparison to AgNP and other antimicrobials, such as copper (Ren et al. 2009) or other nanoparticles, TPA does not release ions from its matrix into solution. Hence, TPA should retain its antimicrobial efficiency for longer than AgNP (Shi, Neoh and Kang 2007; Saif, Anwar and Munawar 2008; Ferreira and Zumbuehl 2009; Kasaraneni et al. 2014). In addition, a cost benefit analysis of TPA versus AgNP modified materials (Zhang, Smith and Oyanedel-Craver 2012; Kasaraneni et al. 2014) shows that TPA is more cost effective than AgNP.

If the proposed amended red cedar were to be implemented as a filtration matrix in structural best management practices, the 6TPA modified red cedar would be favorable compared to the currently used matrix that consists of a shale-sand mix, or even unmodified red cedar. This is because not only does 1 gram of this material (i.e. 6 mg of TPA) achieve >2 log₁₀ removal after

three hours of exposure at room temperature, but it also is effective at removing bacteria at decreased temperatures (17.5°C). These lower temperatures are closer to a natural BMP operating temperature in most temperate climates. However, introducing any type of bioactive material into the environment will require additional field studies to ensure that no unanticipated consequences result from the well-intended use of antimicrobial wood for stormwater treatment.

Limitations

The results in this study indicate that the inactivation performance of amended materials is significantly higher than unmodified materials. However, further testing of these materials under dynamic flow conditions is required to confirm these results. Stormwater is a complex mixture which can include organic contaminants, heavy metals, inorganic salts, humic substances etc. along with several species of microorganisms. A study determining the impact of the complex stormwater chemistry conditions on the inactivation performance of the amended materials is necessary prior to use of these materials in the field.

ACKNOWLEDGEMENTS

We would like to thank the Rhode Island Department of Transportation and the University of Rhode Island Transportation Center for funding this research; Liberty Cedar and New England Wood Products, both in Kingston, RI for supplying the authors with Western red cedar wood; and Biosafe, Pittsburgh, PA for supplying the TPA solution for testing. The wood was chipped by Scott Ahern and Kevin Broccolo, URI.

REFERENCES

Ahn, J. H., Grant, S. B., Surbeck, C. Q., DiGiacomo, P. M., Nezlin, N. P., Jiang, S. 2005. Coastal water quality impact of stormwater runoff from an urban watershed in southern California. *Environmental science & technology* 39 (16), 5940-5953.

Akaike, H. (1998) Information Theory and an Extension of the Maximum Likelihood Principle. In: Parzen, E., Tanabe, K., Kitagawa, G. (Eds.), Springer New York, 199-213.

Ashbolt, N. J. 2004. Microbial contamination of drinking water and disease outcomes in developing regions. *Toxicology* 198 (1), 229-238.

Bales, R. C., Hinkle, S. R., Kroeger, T. W., Stocking, K., Gerba, C. P. 1991. Bacteriophage adsorption during transport through porous media: chemical perturbations and reversibility *Environmental science & technology* 25 (12), 2088 <last_page> 2095.

Barker, A. L., Gonsalves, M., Macpherson, J. V., Slevin, C. J., Unwin, P. R. 1999. Scanning electrochemical microscopy: beyond the solid/liquid interface. *Analytica Chimica Acta* 385 (1), 223-240.

Behr, E., Briggs, D., Kaufert, F. 1953. Diffusion of dissolved materials through wood. *The Journal of physical chemistry* 57 (4), 476-480.

Burr, H. K. and Stamm, A. J. 1947. Diffusion in wood. *The Journal of physical chemistry* 51 (1), 240-261.

Chandrasena, G. I., Deletic, A., McCarthy, D. T. 2013. Survival of *Escherichia coli* in stormwater biofilters *Environmental Science and Pollution Research*.

Coffman, L. S., Ruby, M., Beach, C. (2008) *Bacteria by Filterra® Advanced Bioretention System: Discussion of the Benefits, Mechanisms and Efficiencies for Bacteria Removal*. In: ASCE Conf. Proc. 333, .

Curriero, F. C., Patz, J. A., Rose, J. B., Lele, S. 2001. The Association Between Extreme Precipitation and Waterborne Disease Outbreaks in the United States, 1948–1994 *American Journal of Public Health* 91 (8), 1194 <last_page> 1199.

- Davies, C. M. and Bavor, H. J. 2000. The fate of stormwater-associated bacteria in constructed wetland and water pollution control pond systems *Journal of applied microbiology* 89 (2), 349-360.
- Dorfman, M. and Rosselot, K. 2012. *Testing the Water: A Guide to Water Quality at Vacation Beaches*. 22.
- Edberg, S., Rice, E., Karlin, R., Allen, M. 2000. *Escherichia coli*: the best biological drinking water indicator for public health protection. *Journal of applied microbiology* 88 (S1), 106S-116S.
- EPA 2011. *Performance Standards for Discharges from Newly Developed and Redeveloped Sites*. (June 30, 2011), 1-144.
- Faucette, L., Cardoso-Gendreau, F., Codling, E., Sadeghi, A., Pachepsky, Y., Shelton, D. 2009. Storm water pollutant removal performance of compost filter socks. *Journal of environmental quality* 38 (3), 1233-1239.
- Ferreira, L. and Zumbuehl, A. 2009. Non-leaching surfaces capable of killing microorganisms on contact. *Journal of Materials Chemistry* 19 (42), 7796-7806.
- Gayán, E., Monfort, S., Álvarez, I., Condón, S. 2011. UV-C inactivation of *Escherichia coli* at different temperatures *Innovative Food Science & Emerging Technologies* 12 (4), 531-541.
- Göbel, P., Dierkes, C., Coldewey, W. G. 2007. Storm water runoff concentration matrix for urban areas. *Journal of contaminant hydrology* 91 (1-2), 26-42.
- Grohs, B. M., Wegen, H. -, Kunz, B. 1999. Antifungal activity of red cedar extract and hiba oil on wood-inhabiting moulds. *Holz als Roh- und Werkstoff* 57 (4), 277-281.
- Haas, C. N. and Karra, S. B. 1984. Kinetics of microbial inactivation by chlorine—I Review of results in demand-free systems. *Water research* 18 (11), 1443-1449.
- Kasaraneni, V., Kohm, S. E., Eberle, D., Boving, T., Oyanedel-Craver, V. 2013. Enhanced containment of polycyclic aromatic hydrocarbons through organic modification of soils. *Environmental Progress & Sustainable Energy*.

- Kasaraneni, V. K., Schifman, L. A., Boving, T. B., Oyanedel-Craver, V. 2014. Enhancement of Surface Runoff Quality Using Modified Sorbents. *ACS Sustainable Chemistry & Engineering* 2 (7), 1609-1615.
- Kim, J. S., Kuk, E., Yu, K. N., Kim, J., Park, S. J., Lee, H. J., Kim, S. H., Park, Y. K., Park, Y. H., Hwang, C. 2007. Antimicrobial effects of silver nanoparticles. *Nanomedicine: Nanotechnology, Biology and Medicine* 3 (1), 95-101.
- Kim, H. W., Kim, B. R., Rhee, Y. H. 2010. Imparting durable antimicrobial properties to cotton fabrics using alginate–quaternary ammonium complex nanoparticles *Carbohydrate Polymers* 79 (4), 1057 <last_page> 1062.
- Lee, C. M., Lin, T. Y., Lin, C. C., Kohbodi, G. A., Bhatt, A., Lee, R., Jay, J. A. 2006. Persistence of fecal indicator bacteria in Santa Monica Bay beach sediments *Water research* 40 (14), 2593-2602.
- Li, Y. L., Deletic, A., McCarthy, D. T. 2014. Removal of *E. coli* from urban stormwater using antimicrobial-modified filter media *Journal of hazardous materials* 271, 73 <last_page> 81.
- Li, Z., Lee, D., Sheng, X., Cohen, R. E., Rubner, M. F. 2006. Two-Level Antibacterial Coating with Both Release-Killing and Contact-Killing Capabilities *Langmuir* 22 (24), 9820 <last_page> 9823.
- Mallin, M. A., Williams, K. E., Esham, E. C., Lowe, R. P. 2000. Effect of human development on bacteriological water quality in coastal watersheds. *Ecological Applications* 10 (4), 1047-1056.
- McCaulou, D. R., Bales, R. C., Arnold, R. G. 1995; 2010. Effect of Temperature-Controlled Motility on Transport of Bacteria and Microspheres Through Saturated Sediment Water *Resources Research* 31 (2), 271 <last_page> 280.
- McLellan, S. and Salmore, A. 2003. Evidence for localized bacterial loading as the cause of chronic beach closings in a freshwater marina. *Water research* 37 (11), 2700-2708.
- Mohanty, S. K., Torkelson, A. A., Dodd, H., Nelson, K. L., Boehm, A. B. 2013. Engineering Solutions to Improve the Removal of Fecal Indicator Bacteria by Bioinfiltration Systems during Intermittent Flow of Stormwater *Environmental science & technology* 47 (19), 10791 <last_page> 10798.

- Morales, I., Atoyan, J. A., Amador, J. A., Boving, T. 2014. Transport of Pathogen Surrogates in Soil Treatment Units: Numerical Modeling. *Water* 6 (4), 818-838.
- No, H. K., Kim, S. H., Lee, S. H., Park, N. Y., Prinyawiwatkul, W. 2006. Stability and antibacterial activity of chitosan solutions affected by storage temperature and time. *Carbohydrate Polymers* 65 (2), 174-178.
- NOAA, National Oceanic and Atmospheric Administration 2014. Annual Climatological Summary for Providence, RI.
- Oyanedel-Craver, V. A., Fuller, M., Smith, J. A. 2007. Simultaneous sorption of benzene and heavy metals onto two organoclays. *Journal of colloid and interface science* 309 (2), 485-492.
- Oyanedel-Craver, V. A. and Smith, J. A. 2006. Effect of quaternary ammonium cation loading and pH on heavy metal sorption to Ca bentonite and two organobentonites. *Journal of hazardous materials* 137 (2), 1102-1114.
- Oyanedel-Craver, V. A. and Smith, J. A. 2007. Sustainable colloidal-silver-impregnated ceramic filter for point-of-use water treatment. *Environmental science & technology* 42 (3), 927-933.
- Parker, J., McIntyre, D., Noble, R. 2010. Characterizing fecal contamination in stormwater runoff in coastal North Carolina, USA. *Water research* 44 (14), 4186-4194.
- Pathan, A., Bond, J., Gaskin, R. 2010. Sample preparation for SEM of plant surfaces. *Materials Today* 12, 32-43.
- Pfeiffer, C., Rehbock, C., Huhn, D., Carrillo-Carrion, C., de Aberasturi, D. J., Merk, V., Barcikowski, S., Parak, W. J. 2014. Interaction of colloidal nanoparticles with their local environment: the (ionic) nanoenvironment around nanoparticles is different from bulk and determines the physico-chemical properties of the nanoparticles. *Journal of the Royal Society, Interface / the Royal Society* 11 (96), 20130931.
- Raffellini, S., Schenk, M., Guerrero, S., Alzamora, S. M. 2011. Kinetics of *Escherichia coli* inactivation employing hydrogen peroxide at varying temperatures, pH and concentrations. *Food Control* 22 (6), 920-932.
- Rayner, J., Zhang, H., Lantagne, D., Schubert, J., Lennon, P., Craver, V. O. 2013. Laboratory investigation into the effect of silver application on the bacterial removal efficacy of filter

material for use on locally-produced ceramic water filters for household drinking water treatment. ACS Sustainable Chemistry & Engineering.

Ren, G., Hu, D., Cheng, E. W., Vargas-Reus, M. A., Reip, P., Allaker, R. P. 2009. Characterisation of copper oxide nanoparticles for antimicrobial applications. International journal of antimicrobial agents 33 (6), 587-590.

Rhode Island Department of Environmental Management 2010. Rhode Island Stormwater Design and Installation Standards Manual. , 487.

Rose, J. B., Daeschner, S., Easterling, D. R., Curriero, F. C., Lele, S., Patz, J. A. 2000. Climate and waterborne disease outbreaks. Journal-American Water Works Association 92 (9), 77-87.

Rosen, M. J. and Kunjappu, J. T. (2012) Surfactants and interfacial phenomena. John Wiley & Sons, .

Rosen, M. 1975. Relationship of structure to properties in surfactants. III. Adsorption at the solid-liquid interface from aqueous solution. Journal of the American Oil Chemists Society 52 (11), 431-435.

Rügner, H., Kleineidam, S., Grathwohl, P. 1999. Long term sorption kinetics of phenanthrene in aquifer materials. Environmental science & technology 33 (10), 1645-1651.

Saif, M. J., Anwar, J., Munawar, M. A. 2008. A novel application of quaternary ammonium compounds as antibacterial hybrid coating on glass surfaces. Langmuir 25 (1), 377-379.

Schueler, T. R. and Holland, H. 2000. Microbes and urban watersheds: concentrations, sources, and pathways. The Practice of Watershed Protection, 74-84.

Shi, Z., Neoh, K., Kang, E. 2007. Antibacterial and adsorption characteristics of activated carbon functionalized with quaternary ammonium moieties. Industrial & Engineering Chemistry Research 46 (2), 439-445.

Shivaji, S. and Prakash, J. S. 2010. How do bacteria sense and respond to low temperature? Archives of Microbiology 192 (2), 85-95.

- Sondi, I. and Salopek-Sondi, B. 2004. Silver nanoparticles as antimicrobial agent: a case study on E. coli as a model for Gram-negative bacteria *Journal of colloid and interface science* 275 (1), 177-182.
- Song, J., Kong, H., Jang, J. 2011. Bacterial adhesion inhibition of the quaternary ammonium functionalized silica nanoparticles. *Colloids and Surfaces B: Biointerfaces* 82 (2), 651-656.
- Stevik, T. K., Aa, K., Ausland, G., Hanssen, J. F. 2004. Retention and removal of pathogenic bacteria in wastewater percolating through porous media: a review *Water research* 38 (6), 1355-1367.
- Tchobanoglous, G., Burton, F. L., Stensel, H. D. *Wastewater engineering: treatment and reuse* Boston ; McGraw-Hill, c2003., 1819.
- Torkelson, A., da Silva, A., Love, D., Kim, J., Alper, J., Coox, B., Dahm, J., Kozodoy, P., Maboudian, R., Nelson, K. 2012. Investigation of quaternary ammonium silane-coated sand filter for the removal of bacteria and viruses from drinking water. *Journal of applied microbiology* 113 (5), 1196-1207.
- U.S. Environmental Protection Agency 2012. *Recreational Water Quality Criteria*. Office of Water 820-F-12-058, 1-58.
- U.S. Environmental Protection Agency. (2001) *Protocol for Developing Pathogen TMDLs*. Office of Water (4503F), United States Environmental Protection Agency, Washington, DC, 132.
- Unwin, P. R. and Bard, A. J. 1992. Scanning electrochemical microscopy. 14. Scanning electrochemical microscope induced desorption: a new technique for the measurement of adsorption/desorption kinetics and surface diffusion rates at the solid/liquid interface. *The Journal of physical chemistry* 96 (12), 5035-5045.
- Wheeler Alm, E., Burke, J., Spain, A. 2003. Fecal indicator bacteria are abundant in wet sand at freshwater beaches. *Water research* 37 (16), 3978-3982.
- Zhang, H. and Oyanedel-Craver, V. 2013. Comparison of the bacterial removal performance of silver nanoparticles and a polymer based quaternary amine functionalized silsesquioxane coated point-of-use ceramic water filters. *Journal of hazardous materials*.

Zhang, X. and Lulla, M. 2006. Evaluation of pathogenic indicator bacteria in structural best management practices. *Journal of Environmental Science and Health Part A* 41 (11), 2483-2493.

Zhang, H., Smith, J. A., Oyanedel-Craver, V. 2012. The effect of natural water conditions on the anti-bacterial performance and stability of silver nanoparticles capped with different polymers. *Water research* 46 (3), 691-699.

TABLES

Table 1. Description of the seven test materials used in the study along with their abbreviations. The matrix for all test materials was Red Cedar. Antimicrobial agent loadings are categorized as low for 0.3AgNP, 3TPA, and 4TPA, and as high for 0.6AgNP, 6TPA, and 9TPA.

Antimicrobial Agent	Antimicrobial Loading	Abbreviation	Initial aqueous concentrations (mg/l)
None	Unmodified	UM	-
TPA	3.6 mg/g	3TPA	260
	4.5 mg/g	4TPA	450
	6.7 mg/g	6TPA	720
	9.3 mg/g	9TPA	1500
AgNP	0.33 mg/g	0.3Ag	20.8
	0.68 mg/g	0.6Ag	52

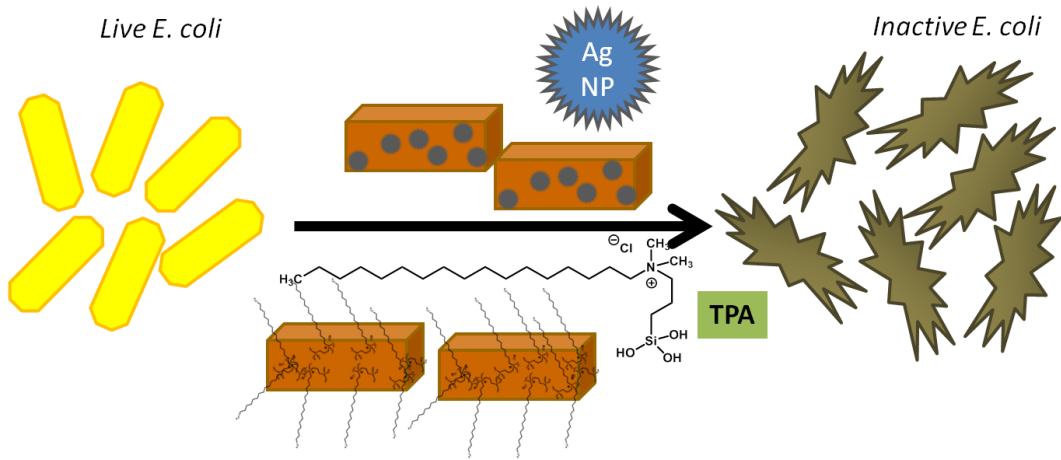
Table 2. Bacteria inactivation kinetics determined by the Chick-Watson Model (Equation 1) for TPA and AgNP modified red cedar. The parameterized model predicts that it takes 1.33 times longer to achieve 3- log₁₀ (99.9%) compared to 2- log₁₀ (99.0%) reduction. Experimental data and the Chick-Watson model predictions are presented in log₁₀ removal values (LRV) with percent differences in parentheses.

Antimicrobial Agent / Model	Antimicrobial Loading	2- log ₁₀ reduction (hrs)	3- log ₁₀ reduction (hrs)	Experimental Data		Chick Watson Predicted Data	
				90 min	180 min	90 min	180 min
TPA $\ln\left(\frac{N_t}{N_0}\right) = -0.03C^{1.99}t$	3 mg/g	11.78	17.63	0.34	0.61	0.25 (25.6)	0.51 (17.1)
	4 mg/g	7.55	11.30	0.40	0.67	0.40 (0.8)	0.80 (-17.8)
	6 mg/g	3.42	5.115	0.91	2.16	0.88 (3.3)	1.76 (18.9)
	9 mg/g	1.78	2.66	1.58	3.24	1.69 (-6.8)	3.38 (-3.9)
AgNP $\ln\left(\frac{N_t}{N_0}\right) = -1.18C^{0.58}t$	0.3 mg/g	7.34	10.98	0.49	0.83	0.41 (16.6)	0.82 (1.8)
	0.6 mg/g	4.90	7.34	0.68	1.23	0.61 (10.0)	1.23 (1.1)

Table 3. Comparison of initial and final LRV and the first order rates (incl. percentages) that were observed after storing the amended wood chips in water for 120 days (at 25°C).

Material	<i>LRV₀</i>	<i>LRV_{Final}</i>	<i>k</i>[day⁻¹]	% change
Unmodified red cedar	0.49±0.15	0.41±0.12	0.032	16.33
0.6 mg/g AgNP	1.96±0.23	1.21±0.09	0.022	38.27
6 mg/g TPA	2.23±0.09	1.64±0.05	0.013	26.46
9 mg/g TPA	2.96±0.43	2.04±0.11	0.049	31.08

TOC/ABSTRACT ART



FIGURES

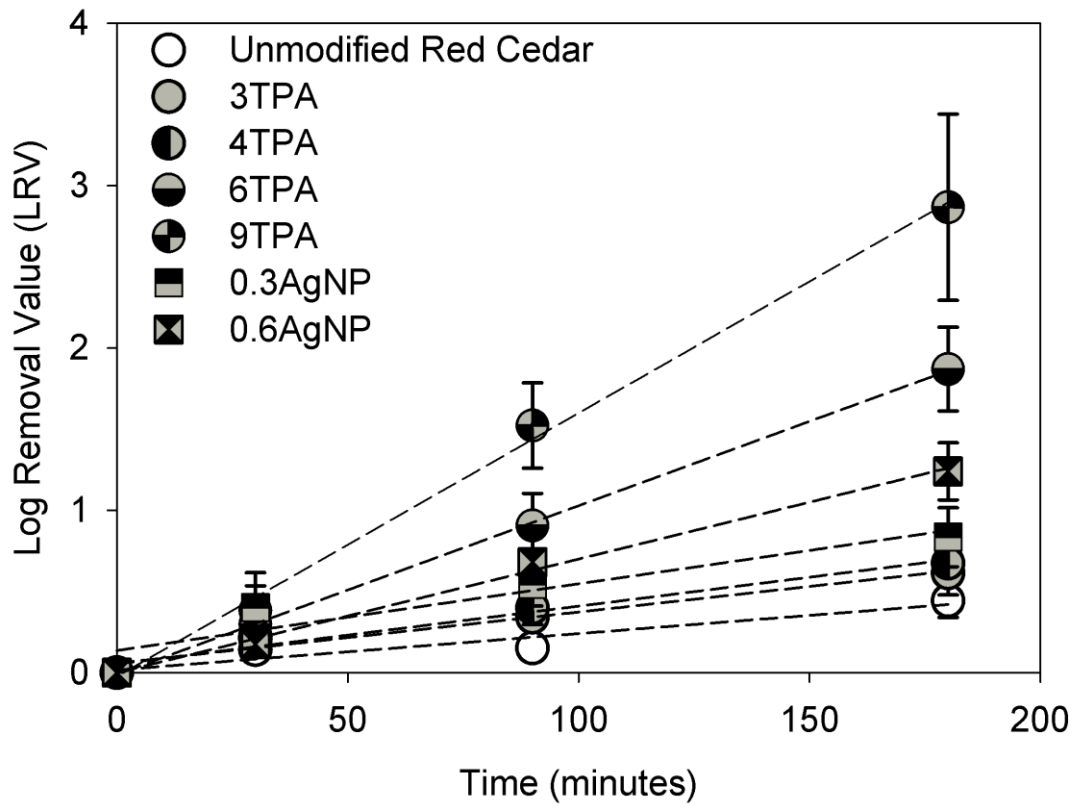


Figure 1. Comparison of (average \pm standard error) LRV to increased exposure times of the six modified materials and the unmodified red cedar. A steeper slope indicates a higher inactivation rate, thus a more effective antimicrobial material.

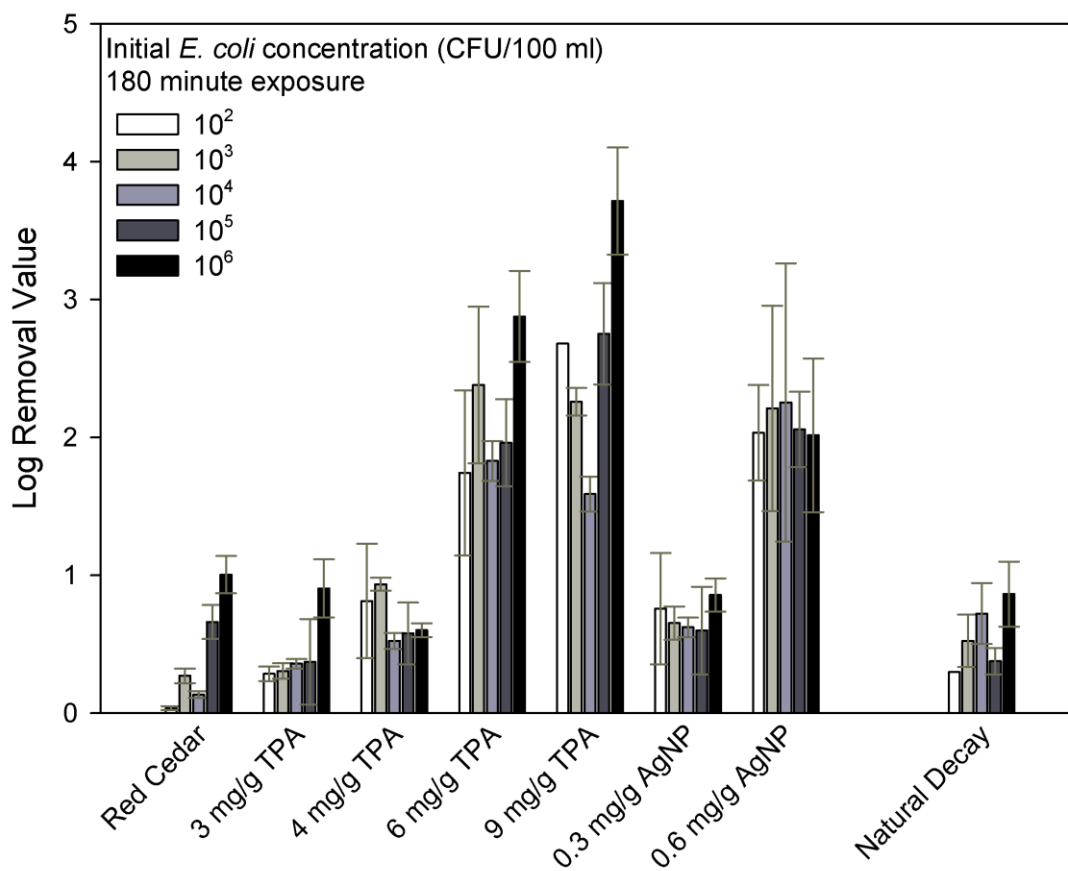


Figure 2. Comparison of \log_{10} removal values (LRV) (average \pm standard error) for the unmodified red cedar wood chips and the six modifications at different *E. coli* concentrations ranging from 10^2 to 10^6 CFU/100ml. All materials were exposed for 180 minutes. Natural decay data shows the fraction of *E. coli* die-off that is not due to antimicrobials or removal by attachment. In order to compare the performance of all the materials data for unmodified red cedar, 6TPA, and 0.6 AgNP was obtained from our previously published work²⁵.

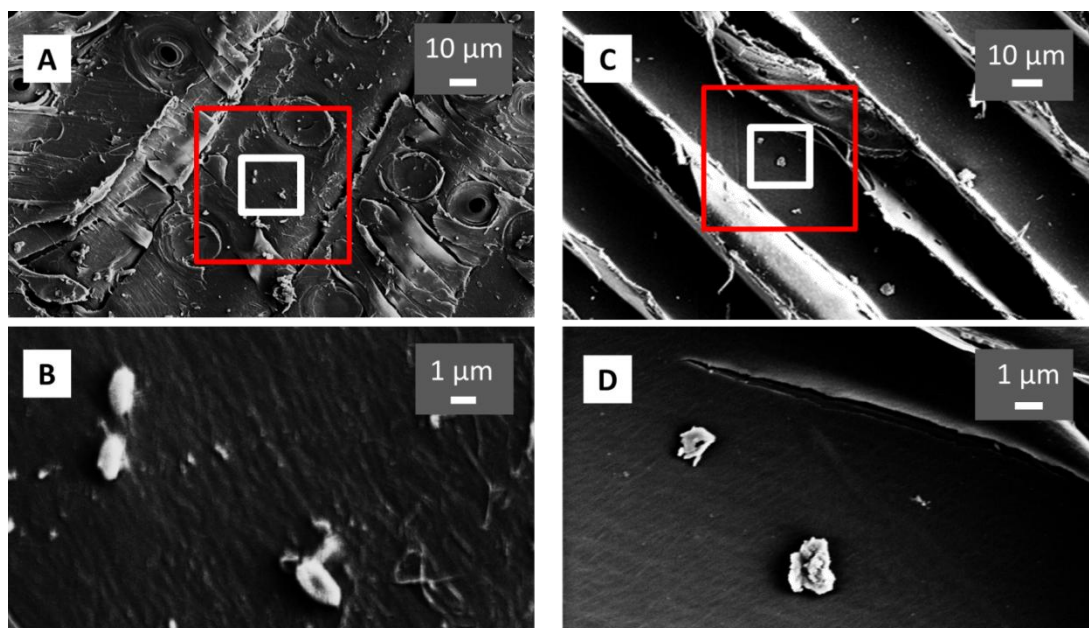


Figure 3. SEM images of unmodified red cedar (A and B) and 6TPA (C and D) with clusters of *E. coli* bacteria attached to the surface. Red squares outline the same size area in both, (A; unmodified red cedar) and (C, 6TPA) for comparison of bacteria cluster densities. White squares indicate what area is represented in figures C and D, which shows unmodified red cedar and red cedar modified with 6 mg/g TPA, respectively. In (D) there are fewer bacteria clusters on the surface of the modified wood and *E. coli* cell walls have been destroyed relative to the well-defined shapes of bacteria in (B). These images were selected after analyzing five different samples for each condition and are therefore representative of the unmodified red cedar and 6mg/g TPA red cedar after being in contact with *E. coli*.

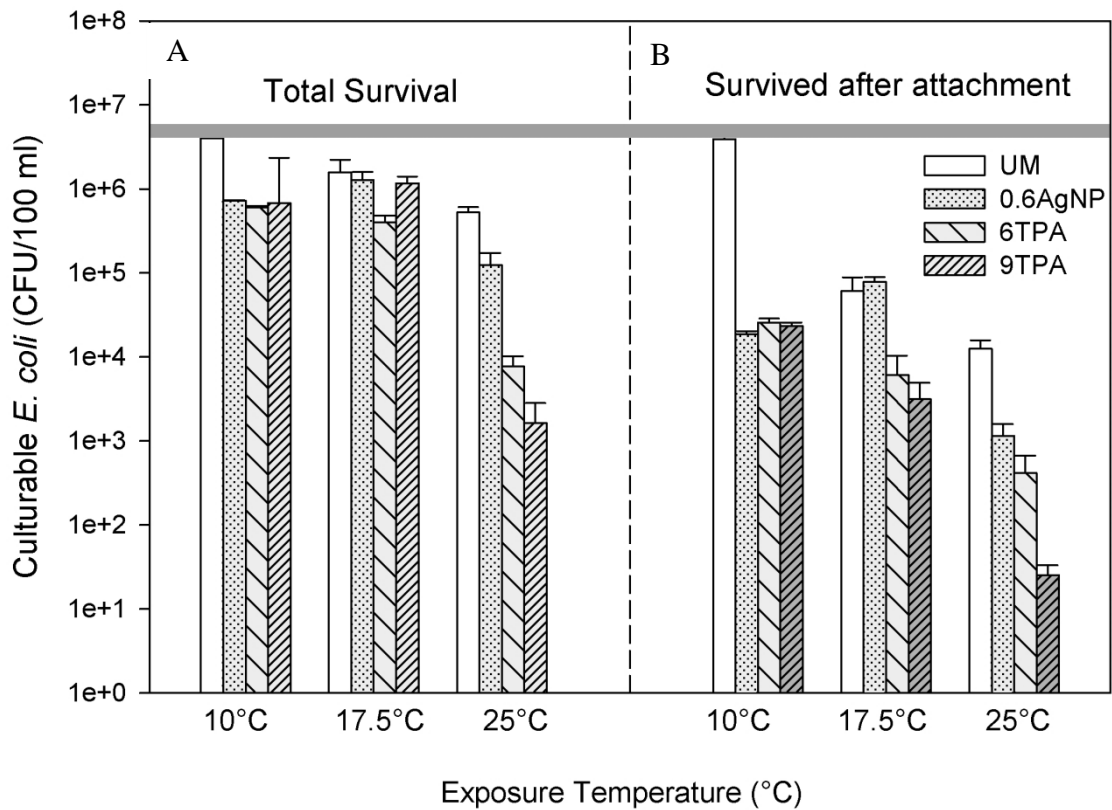


Figure 4. Comparison of the effect of temperature (10°C, 17.5°C, and 25°C) on A) the total number (average \pm standard error) of surviving culturable *E. coli* and B) number of *E. coli* that were cultivated after being attached for 180 minute to 0.6AgNP, 6TPA, and 9TPA. The average initial concentration of *E. coli* was in the order of 10^6 CFU/100ml (horizontal grey bar indicates range of initial concentrations achieved for the experiments).

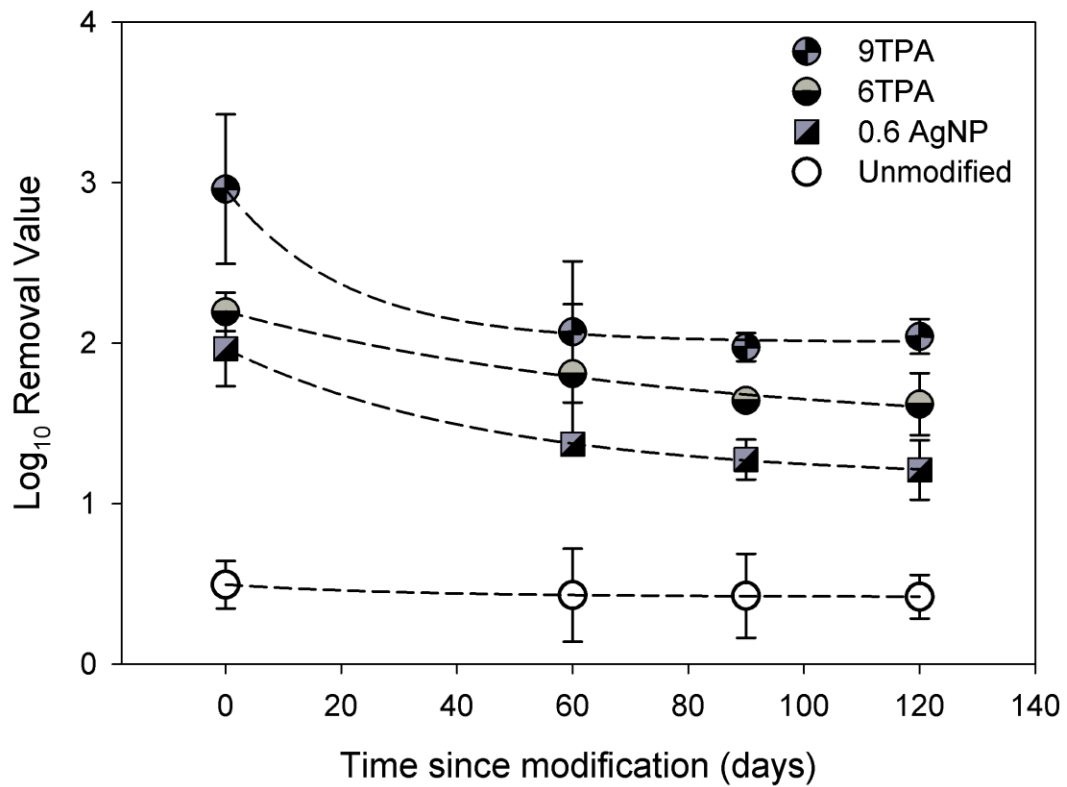


Figure 5. Average \log_{10} removal value \pm standard error for the three most effective materials (6TPA, 9TPA, and 0.6Ag) compared to unmodified red cedar at 25°C. The LRV was determined immediately after modification and at 60, 90, and 120 days after being stored in water. An initial drop in the antimicrobial performance over the first 60 days was followed by a much slower decrease in inactivation performance afterwards.

SUPPORTING INFORMATION

Testing the antimicrobial efficiency of modified cedar wood chips as filter media

Laura A. Schifman 1*, Varun K. Kasaraneni 2, Ryan K. Sullivan 1, Vinka Oyanedel-Craver 2, Thomas B. Boving 1, 2

1 Department of Geosciences, University of Rhode Island, Kingston RI 02881, USA

2 Department of Civil and Environmental Engineering, University of Rhode Island, Kingston RI 02881, USA

Number of pages: 7

Number of Tables: 7

Number of Figures: 2

Supplemental Text

Chick-Watson Model Parameterization

To parameterize the model constants k' and n , a two-step approach is required as described in Tchobanoglous et al. 2003. (Tchobanoglous, Burton and Stensel) Briefly, a linear regression is fitted to a plot of the natural-log normalized ratio $\ln(N_t/N_0)$ versus the experimental exposure time t for each antimicrobial material. The linear regression equation of each data set is utilized to solve for the theoretical time required to achieve a 99% removal of *E. coli*.

Then, the theoretical time to achieve 99% removal of bacteria is plotted against the disinfectant concentration of the material and a linear regression equation for each type of disinfectant system is fitted to the calculated C . The negative inverse of the slope of that linear regression equation equals the coefficient of dilution n . The die-off constant k' , is then calculated using

$$n * \ln(y) = \ln \left[\frac{1}{k'} - \ln \left(\frac{N_t}{N_0} \right) \right] \quad \text{Equation 2}$$

where y is the y -intercept and N_t/N_0 is the desired ratio of *E. coli* concentration at time t relative to the initial *E. coli* concentration, in this example 99%.

Sample Preparation for SEM analysis

Briefly, the samples were fixed in 2.5% glutaraldehyde solution for 30 minutes. After fixation, the samples were washed three times with phosphate buffer and then dehydrated for 20 minutes using sequentially increasing ethanol solutions (increments of 10%) containing 40% to 100% ethanol. The samples were exposed to 100% ethanol three times before being chemically dried using Hexamethyldisilazane (HMDS). The samples were transferred to a 1:2 HMDS:Ethanol solution for 20 minutes, then a 2:1 HMDS:Ethanol solution, and finally into 100% HMDS. The last step was repeated and the HMDS was left to evaporate in the fume hood overnight. The samples were sputter-coated with a thin layer of gold for 90 seconds under vacuum before the imaging was done in a SIGMA VP Field Emission-Scanning Electron Microscope (Zeiss, USA) with an acceleration voltage of 5kV and a SE2 detector.

Supplemental Tables

Table S1a – Performance - ANOVA Table. ANOVA table for one-way comparison of log10 removal values for the six modified red cedar wood chips and unmodified red cedar wood chips using LRV as the response variable and material as the factor.

	Degrees of Freedom	Sum of Squares	Mean Square	F-Value	P-value
Materials	6	132.25	22.042	32.86	<0.001
Residuals	144	96.58	0.671		

Table S1b - Performance - Tukey HSD Summary. The multiple comparison using Tukey’s HSD for the models show differences between the individual materials.

Comparison	Significant?	p-value
Unmodified red cedar vs. 3TPA	N	1.00
Unmodified red cedar vs. 4TPA	N	0.99
Unmodified red cedar vs. 6TPA	Y	<0.001
Unmodified red cedar vs. 9TPA	Y	<0.001
Unmodified red cedar vs. 0.3AgNP	N	0.99
Unmodified red cedar vs. 0.6AgNP	Y	<0.001
4TPA vs. 3TPA	N	0.97
6TPA vs. 3TPA	Y	<0.001
9TPA vs. 03TPA	Y	<0.001
0.3AgNP vs. 3TPA	N	0.97
0.6AgNP vs. 3TPA	Y	<0.001
4TPA vs. 0.3AgNP	N	1.00
6TPA vs. 0.3AgNP	Y	<0.001
9TPA vs. 0.3AgNP	Y	<0.001
0.6AgNP vs. 0.3AgNP	Y	<0.001
6TPA vs. 4TPA	Y	<0.001
9TPA vs. 4TPA	Y	<0.001
0.6AgNP vs. 4TPA	Y	<0.001
9TPA vs. 0.6AgNP	N	0.14
9TPA vs. 6TPA	N	0.14

Table S2a – Attachment - ANOVA Table. ANOVA table for analysis of covariance comparing culturable E. coli after attachment for the three most effective materials (0.6 mg/g AgNP, 6 mg/g TPA, 9 mg/g TPA) compared to unmodified red cedar at three different exposure temperatures (10°C, 17.5°C and 25°C) with the final model being: E. coli removed by attachment ~ Temperature + Material. There is no interaction term in this model as it went through a stepwise regression and the final model as stated above had a lower AIC value compared to the initial model, which was attachment ~ Temperature * Material.

	Degrees of Freedom	Sum of Squares	Mean Square	F-Value	P-value
Temperature	2	49.504	24.7518	49.921	<0.001
Material	3	18.321	6.107	12.317	<0.001
Residuals	22	10.908	0.496		

Table S2b – Attachment – Material - Tukey HSD Summary. The multiple comparison using Tukey’s HSD for the models show differences between the individual materials:

Comparison	Significant?	p-value
------------	--------------	---------

Unmodified red cedar vs. 0.6AgNP	Y	<0.001
Unmodified red cedar vs.6TPA	Y(at $\alpha=0.90$)	0.063
Unmodified red cedar vs.9TPA	Y	<0.001
6TPA vs.0.6AgNP	Y(at $\alpha=0.90$)	0.062
9TPA vs.0.6AgNP	N	N.S.
9TPA vs.6TPA	N	N.S.

Table S2c - Attachment – Temperature - Tukey HSD Summary. The multiple comparison using Tukey's HSD for the models show differences between the individual materials:

Comparison	Significant?	p-value
10°C vs. 17.5 °C	Y	0.046
10°C vs. 25 °C	Y	<0.001
17.5°C vs. 25 °C	Y	<0.001

Table S3 – Inactivation Kinetics. ANOVA table comparing the different models for the inactivation kinetics of the modified red cedar and comparing it to unmodified red cedar.

Model	Estimate	t value	Pr(> t)	Significant?
(Intercept)	0.0158	0.28	0.79	N
Time	0.0022	3.98	<0.05	Y
3TPA	0.0419	0.52	0.61	N
4TPA	0.0366	0.45	0.66	N
6TPA	-0.0270	-0.33	0.74	N
9TPA	-0.0399	-0.49	0.63	N
0.3AgNP	0.1201	1.48	0.16	N
0.6AgNP	-0.0173	-0.21	0.83	N
Time*3TPA	0.0009	1.14	0.27	N
Time*4TPA	0.0013	1.66	0.12	N
Time*6TPA	0.0081	10.21	<0.001	Y
Time*9TPA	0.0140	17.52	<0.001	Y
Time*0.3AgNP	0.0019	2.34	<0.05	Y
Time*0.6AgNP	0.0048	5.97	<0.001	Y

Table S4 – Long-term storage impact on inactivation efficiency. Summary table displaying results from t-tests conducted for each material comparing LRV0 to LRV Final. All amended material showed a significant decrease in inactivation after storage under saturated conditions.

Material	Significant change?	p-value
Unmodified Red Cedar	N	0.24
0.6 mg/g AgNP	Y	<0.01
6 mg/g TPA	Y	<0.01
9 mg/g TPA	Y	<0.05

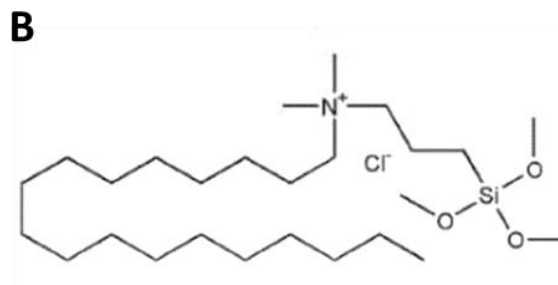
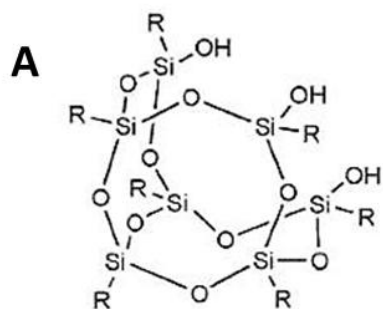


Figure S1. Structure of (A) 3-(trihydroxysilyl) propyldimethyloctadecyl ammonium chloride (TPA) and (B) 3-trimethoxysilyl propyldimethyloctadecyl ammonium chloride.

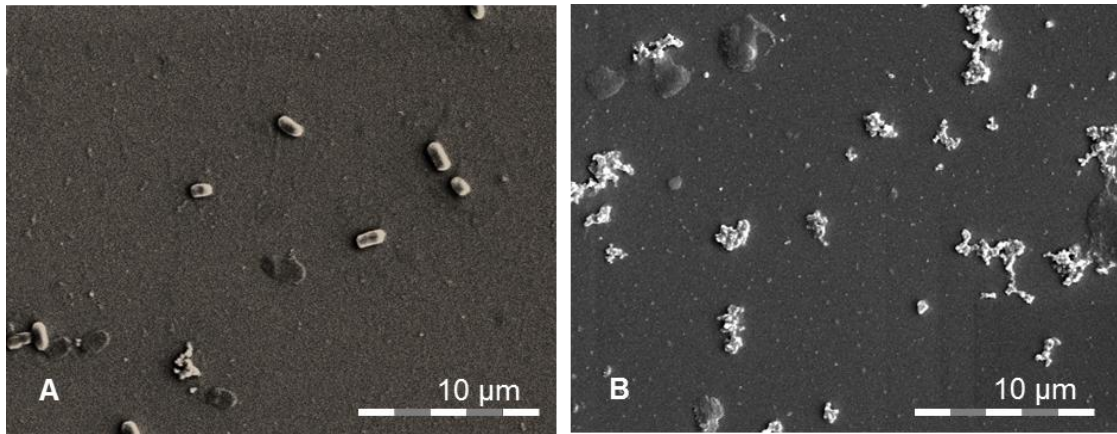


Figure S2. SEM images of *E. coli* on a silicon wafers. In A) the *E. coli* at 10^4 CFU/100 ml were not exposed to TPA and depict live organisms, whereas in B) *E. coli* at 10^6 CFU/100ml were exposed to TPA for three hours before SEM imaging, thus depicting damaged organisms.